MATERIAL SELECTION AND MANUFACTURING METHOD OF BATTERY PACK FOR COMPACT ELECTRIC VEHICLE

NAIYANA LEWCHALERMWONG

A THESIS REPORT SUBMITTED IN PARTIAL FULFILLMENT
OF THE REQUIREMENTS FOR THE DEGREE OF
MASTER OF ENGINEERING IN AUTOMOTIVE ENGINEERING
INTERNATIONAL COLLEGE
KING MONGKUT'S INSTITUTE OF TECHNOLOGY LADKRABANG
ACADEMIC YEAR 2018
KMITL-2018-IC-M-004-006

MATERIAL SELECTION AND MANUFACTURING METHOD OF BATTERY PACK FOR COMPACT ELECTRIC VEHICLE

NAIYANA LEWCHALERMWONG

A THESIS REPORT SUBMITTED IN PARTIAL FULFILLMENT
OF THE REQUIREMENTS FOR THE DEGREE OF
MASTER OF ENGINEERING IN AUTOMOTIVE ENGINEERING
INTERNATIONAL COLLEGE
KING MONGKUT'S INSTITUTE OF TECHNOLOGY LADKRABANG
ACADEMIC YEAR 2018
KMITL-2018-IC-M-004-006

THESIS TITLE	Material Selection and Manufacturing Method of Battery Pack for Compact Electric Vehicle
STUDENT NAME	Miss Naiyana Lewchalermwong
STUDENT ID	59610029
DEGREE	Master of Engineering
PROGRAME	Automotive Engineering
ADVISOR	Asst.Prof.Dr. Chinda Charoenphonphanich
CO-ADVISOR	Dr. Visarn Lilavivat
CO-ADVISOR	Prof.Dr. Takushi Saito

ABSTRACT

Battery packs become the key component in electric vehicles (EVs) the main costs of which are battery cells and assembling processes. The battery cell is indeed priced from battery manufacturers while the assembly cost depends on battery pack designs. Battery pack designers need overall cost of the battery packs as cheap as possible, but they still are high performance and more safety. Material selection and manufacturing technique as well as component design are very important to determine the cost-effectiveness of battery modules and battery packs. Therefore, this thesis presents Decision Matrix Methods, which can aid the decision-making process of component materials and manufacturing techniques for a battery module and a battery pack design. The aim of this study is to take the advantage of incorporating Architecture Analysis Method into Decision Matrix Methods by capturing the best practices for conducting design architecture analysis in full account of key design components critical to ensure efficient and effective development of the designs. The methodology also considers the impacts of choice-alternatives along multiple dimensions. Various alternatives for proper materials and manufacturing techniques of battery packs are evaluated in term of cost, safety and performance for a case study of battery pack design which are presented in this thesis.

ACKNOWLEDGEMENT

Without the contribution of many people, this thesis would not have been existed. It owes the existence to the supports and inspirations from a lot of people.

To my thesis advisor Asst. Prof. Dr. Chinda Charoenphonphanich, co-advisor Dr. Visarn Lilavivat, Dr.-Ing. Manop Masomtob and Prof.Dr. Takushi Saito, I would like to express my deepest gratitude for the encouragement and supervision through all obstacles and challenges since the beginning until the end of my study.

I also want to express my gratitude to all lecturers for your support and guidance to me for the whole two years. Also, I would like to thank all my friends who always be there to support and motivate me as always. Moreover, I also would love to express my gratitude to all respondents who contribute their information and time on this study. And I do believe the study could not been done without their input.

Finally, I must express my very greatest gratitude to my parents and all relatives for providing me with unfailing support and continuous motivation throughout my years of study. This accomplishment would not have been possible without them.

Naiyana Lewchalermwong

TABLE OF CONTENTS

Chapter **Page**

LIST OF TABLES

Table **Page**

LIST OF FIGURES

Figure **Page**

LIST OF SYMBOLS

$\chi 2$	Chi-square test
Q	Rate of heat conduction (Watts)
λ	Thermal conductivity (W/m·K)
A	Cross-sectional area of heat conduction path (m^2)
dT/dL	Temperature gradient at concerned section (K/m)
T	Temperature (K)
L	Length (m)
G	Electrical conductance ($kg^{-1} \cdot m^{-2} \cdot s^3 \cdot A^2$)
σ	Electrical conductivity of the material (S/m)
A	Cross-sectional area of the conductor (m^2)
L	Length of the conductor (m)
V	Voltage (V)
I	Electrical current (A)
R	Resistance (Ω)

LIST OF DEFINITIONS

CNC	Computer Numerical Control
FEM	Finite Element Method
BEV	Battery Electric Vehicle
EV	Electric Vehicle
IACS	International Annealed Copper Standard
NiMH	Nickel–Metal Hydride Battery
NCA	Lithium Nickel Cobalt Aluminium Oxide
LCO	Li-cobalt
OEM	Original Equipment Manufacturer
SOC	State of Charge

CHAPTER 1

INTRODUCTION

1.1 Research background

The battery pack is a crucial component in an electric vehicle (EV) in terms of overall cost and performance. Demand for lithium-Ion batteries is highly variable since the battery electric vehicle market is still developing. The assembly processes for battery packs must be reconfigurable. The high cost of Lithium-ion batteries for electric vehicles is a critical concern. According to the most recent estimates available for batteries used in electric vehicles, the cost of Lithium-ion is four to eight times than which of lead acid and one to four times than which of NiMH (Nishino, 2010). However, the cost of Lithium batteries is expected to decrease significantly because the batteries will be increasingly used for many applications. As the market grows and production scales up, manufacturers will be able to enjoy economies of scale. Additionally, reducing material and component prices of battery cells, representing about 25% of the overall savings opportunity. Component suppliers could reduce their costs dramatically by increasing manufacturing productivity and moving operations to locations where costs are optimal (McKinsey 2012).

The Lithium-ion battery industry has additional significance well beyond its value chain. There are various requirements for battery pack design which are battery performance, durability, vibration, thermal properties, safety and others, as shown in Figure 1.1 with related trade-offs among these requirements. Therefore, the design process involves solving the problem of these trade-offs and determining suitable specifications for the system components to achieve a well-balanced overall system with minimum cost. It is important that battery manufacturing takes place in automotive manufacturing. Battery pack and electric vehicle manufacturing are inherently connected due to sharing in R&D and manufacturing facilities.

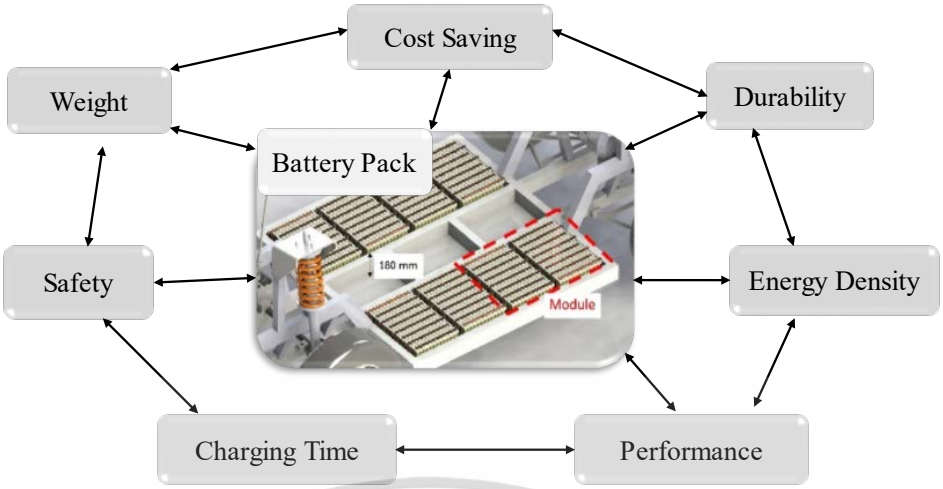

Figure 1.1 Battery performance

1.2 Research objectives

This master thesis is established to enhance the understanding of all component characteristics of the battery pack covering material selection area and manufacturing techniques of battery pack for small electric vehicles using Multiple-Criteria Decision making (MCDM) technique in order to obtain the best choice especially when dealing with multiple conflicting objectives, alternatives, stakeholder conditions and investment cost. Having purpose to distribute knowledge to Thai industries by focusing on battery packs development (see overall scope of battery pack development in Figure 1.2).

- To study materials characteristic of several components in a battery pack in each significant aspect.

- To study manufacturing methods for several components of the battery pack.

- To gather, evaluate, select the optimal choice and provide beneficent information for real production processes of the battery pack.

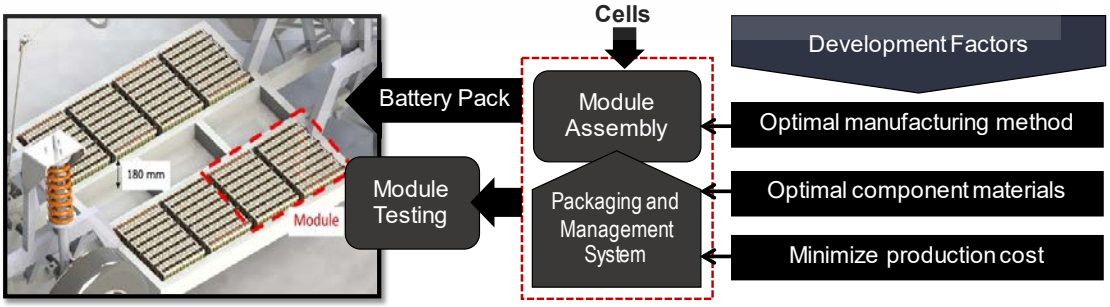

Figure 1.2 Scope of battery pack development

1.3 Scope of work

This thesis used “Battery Pack Development for Compact Electric Vehicle" as a case study, which is cooperation project between National Science and Technology Development Agency (NSTDA) and Thailand Automotive Institute (TAI) by having scope as following details.

- The battery pack in the project uses 18650 battery cells, which accordingly have 18 mm in diameter and 65 mm in length while the number 0 means cylindrical shape. Table 1.1 shows technical information about electrical property of battery pack.

Table 1.1 Technical information of battery pack (Prototype 1) by NSTDA

Electrical Property	Battery Pack Property
Battery pack capacity	≥ 160 Ah and ≤ 420 Ah (3 hrs full charging condition)
Voltage	48-55.2 V
Voltage while working	19.3V – 66 V
Ability to supply normal current	32 A
The ability to supply maximum current	180 A
The ability to supply maximum momentary	at least 225A (2 sec)
Charging performance	Adjustable charging current up to 140A and should be charged within 3 hours
Communication	CAN Bus

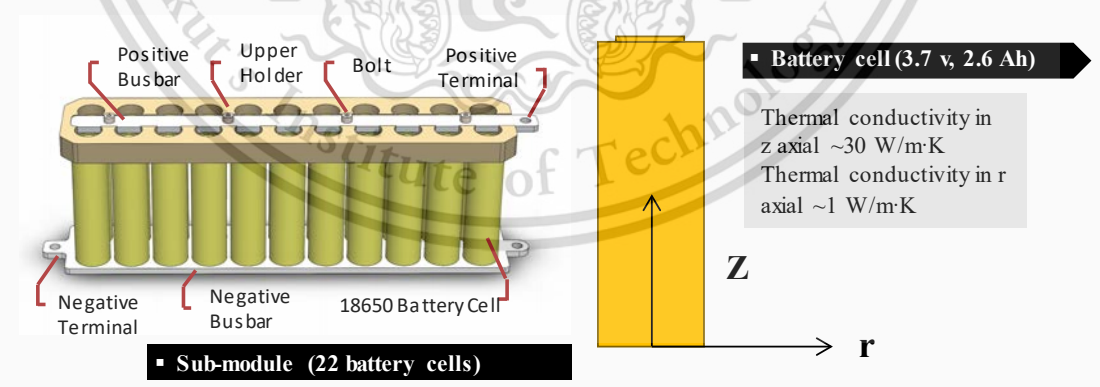

Figure 1.3 Battery Sub-module Sample

Figure 1.3 shows one battery sub-module including 22 Lithium-ion battery cells that are connected in parallel connection to increase capacity. At the positive side, each positive terminal of the battery cells is connected to the Positive Busbar via fuse wire.

At the negative side, each negative terminal of the battery cells is welded with the Negative Busbar by spot welding.

Figure 1.4 shows one half module demonstrates eight battery sub-modules using combination circuit (connect in parallel between battery cells and connect in series between sub-module to up voltage).

- Four components which are Positive Busbar, Negative Busbar, Z bar and Upper Battery Holder are represented in this research (see in Figure 1.5). To select materials such as nickel, copper and aluminium, the decision matrix method is used in decision in term of cost, safety, function, performance and manufacturing. Some components are analysed via the Finite Element Method (FEM) software and experiment to check safety and performance.

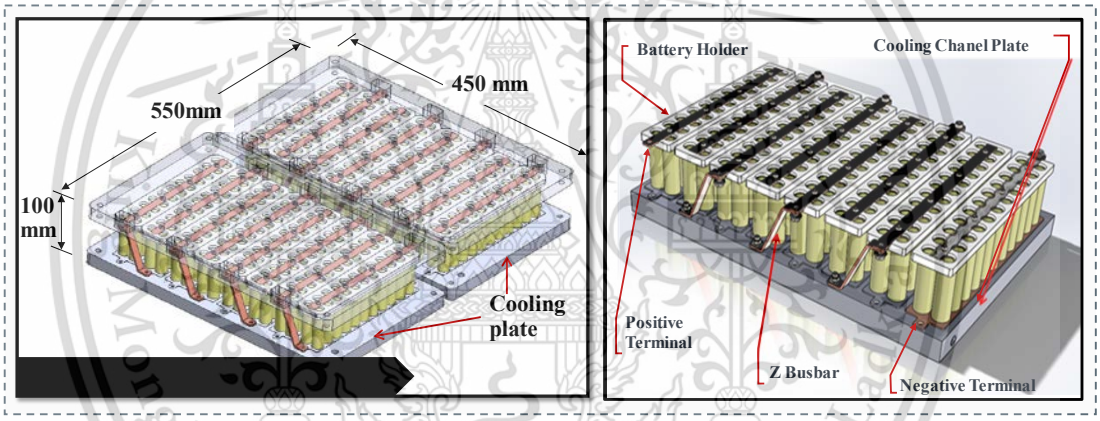

Figure 1.4 Eight battery sub-modules in serial connection for half module

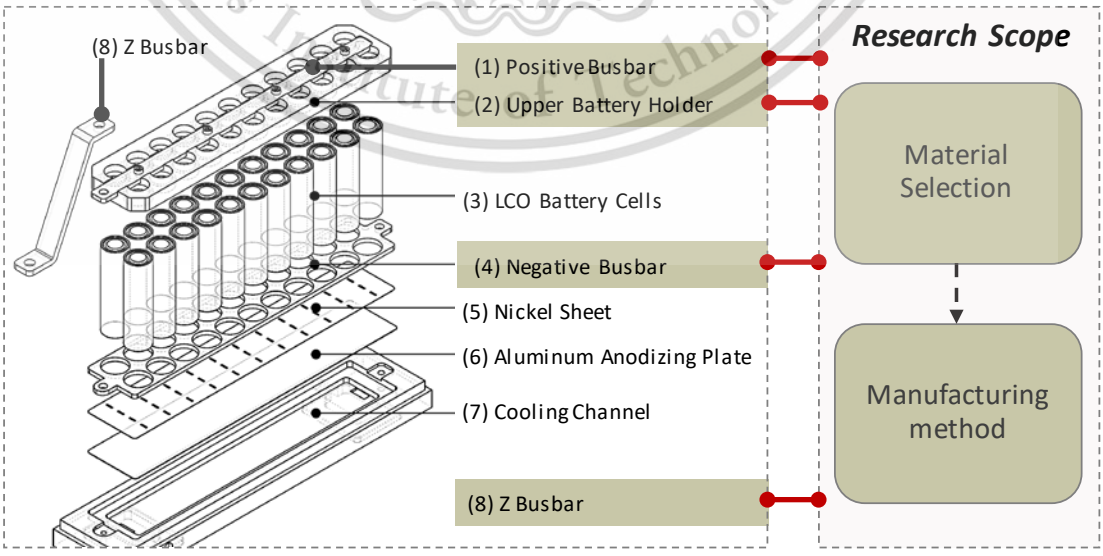

Figure 1.5 Battery pack components

- Use decision matrix as a decision-making tool for selection of material and manufacturing technique for the battery module and the battery pack helping to examine competing alternatives based on multiple criteria that involves various ratings and weights by mathematical model. These are the main factors for producing battery pack to cover efficiency and effectiveness at the lowest production cost.

- By working through a series of decision-process steps, criteria can be established for the assessment and the comparison of different possible alternatives and then compare choices. This method allows us to list and weight various decision criteria deemed important for problem alternatives. The criteria used for the selection are main variables impacts on production consisting of material cost, performance, complexity as well as difficulty in assembling process, time spent and safety.

- The experiments are set up to compare thermal distribution results to that of simulation results with identical conditions.

1.4 Expected benefits

- This research is expected to able evaluate various alternatives for materials and manufacturing techniques of battery pack by applying decision matrix tool based on the gathered information and experiment.

- This research is expected to exhibit simulation results in term of thermal distribution and electrical conductivity from using different materials and manufacturing techniques for battery pack design.

- Moreover, this research is expected to distributed knowledge about material selection for electric vehicle to automotive industry or related manufacturers, for the maximum benefit.

CHAPTER 2

LITERATURE REVIEW

2.1 Challenges and opportunities of batteries for electric vehicles

The automotive industry quests to limit its impact on the environment and transform automotive mobility into a sustainable mode of transportation continues at high intensity, despite the current economic crisis. For current state of battery electric vehicles (BEVs) technology, the value chain of BEVs consists of seven steps: component production (including raw material); cell production; module production; assembly of modules into battery pack (including electronic control unit and cooling system); integration of battery pack into the vehicle; use during the life of vehicle; and reuse and recycling. (see Figure 2.1). This research focuses on the third and fourth step which make up the manufacturer of battery packs for use by OEMs (The Boston Consulting Group (BCG), 2010).

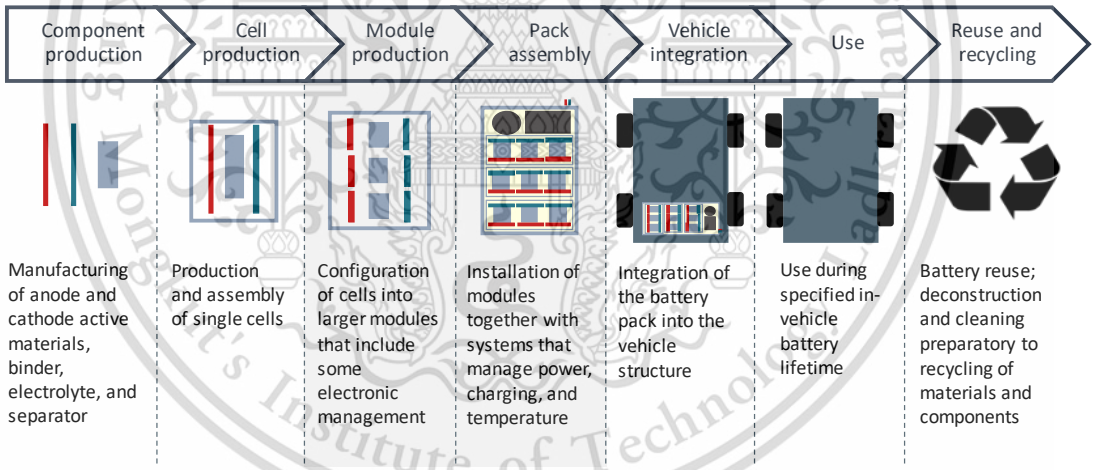

Figure 2.1 Value chain of battery electric vehicles (BEVs)

Figure 2.2 displays batteries cost OEMs about $1,000 per kWh at low volumes. For current costs and forecasting methodologies, most sources estimate the current costs of the automotive lithium-ion battery pack, as sold to OEMs, at between $1,000 and $1,200 per kWh. Citing the current cost of consumer batteries about $250 to $400 per kWh, price tag was further predicted that it will decline to between $250 and $500 per kWh at scaled production. However, consumer batteries must meet significantly fewer demanding requirements, especially regarding safety and life span. Nonetheless, $250 kWh persist as the cost goal for an automotive battery pack. To forecast battery cost, a

line-item model of the individual component cost was constructed under an assumed level of production. The 2009 cost structure includes a complete pack-level bill of materials, direct and indirect plant labor, equipment depreciation, R&D, scrap rates and overhead markup (The Boston Consulting Group (BCG), 2010).

Each component cost was classified as either dependent on battery production volumes or independent of them. These forecast of the evolution of volume-dependent costs assumes the acquisition of industry experience and increasing automation. Volume-independent costs include raw material, labour rates, and general machinery. Estimating that some 70 percent of cell costs and 75 percent of battery pack costs are volume independent, effectively creating a cost "glass floor" for current battery technology that was taken into consideration of various chemistries, various cell-module-pack configurations, and production costs in different countries. For purposes of reference and comparison, a typical supplier of 15 kWh NCA batteries using modestly automated production to make 50,000 cells and highly manual assembly to produce 500 battery packs. These assumptions are the line with currently observe trial production levels. This supplier's 2009 cell costs-$650 to $790 per kWh-account for approximately 65 percent of its total cost for the battery pack. This case focuses on larger batteries, as these are most relevant for cars that are primary electrically driven.

The electric-vehicle and lithium-ion battery businesses hold the promise of large potential profit pools for both incumbents and new players; however, investing in these theologies entails substantial risk. It is unclear whether incumbent OEMs and battery manufacturers or new entrants will emerge as winners as the industry matures. As it stands today, the stage is set for a shakeout among the various battery chemistries, power-train technologies, business models and even regions. OEMs, suppliers, power companies and governments will need to work together to establish the right conditions for a large, viable electric-vehicle market to emerge (The Boston Consulting Group (BCG), 2010).

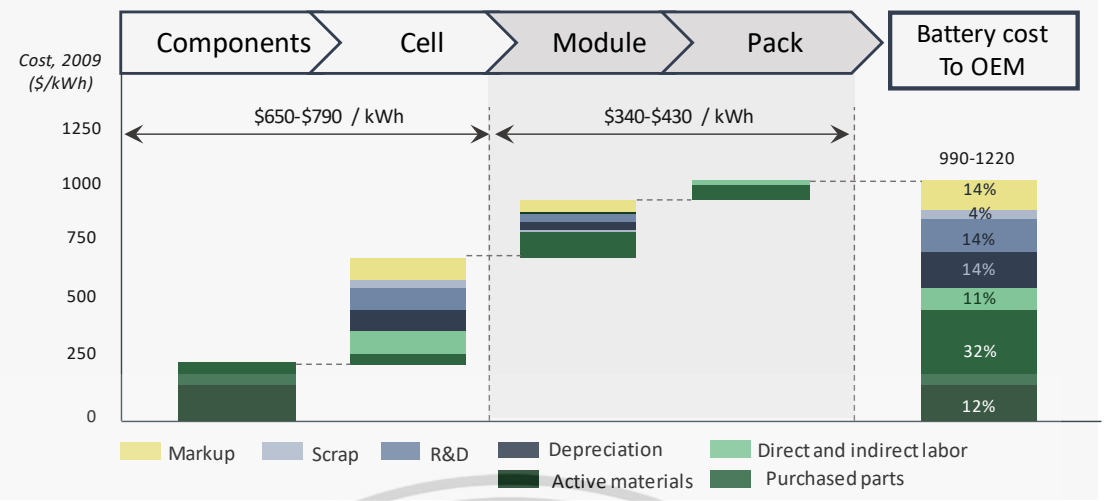

Figure 2.2 Batteries cost OEMs about $1,000 per kWh at Low Volumes

Source: Interviews with component manufacturers, cell producers, tier one suppliers, OEMs and academic experts, Argonne National Laboratory; BCG analysis.

Note: The figure shows the nominal capacity cost of a 15 kWh NCA battery and assumes annual production of 50000 cells and batteries, as well as a 10% scrap rate at the cell level and 2% scrap rate at the module level Numbers are rounded.

Figure 2.3 shows the general structure of the Lithium-ion battery industry as a pyramid. Tier 1 consists of two activities; final pack assembly and cell manufacturing. Tier 2 consists of cell components and electronics including some OEMs that provide their own cell components. Tier 3 comprises key materials

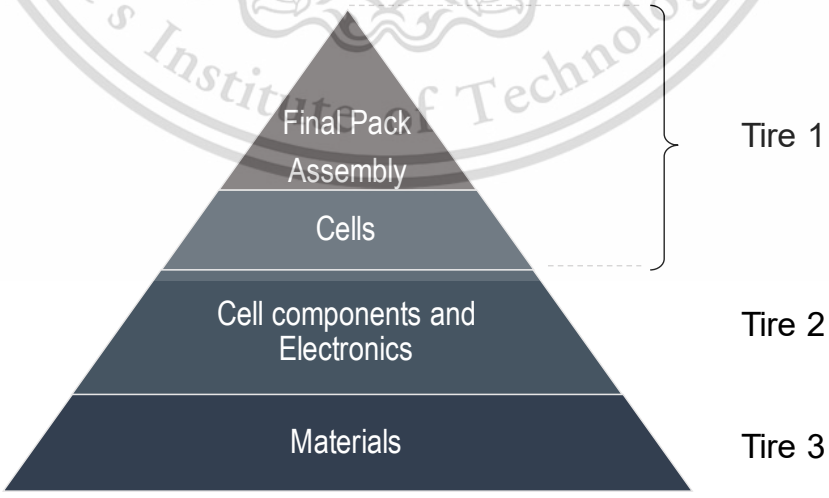

Figure 2.3 Production structure of the Lithium-ion battery industry

Source: CGGC (China Gezhouba Group Company)

2.2 Fundamental of battery

2.2.1 Battery capacity

Capacity indicates the amount of charge or energy contained inside the battery. To refer with the amount of charge, it is always mentioned in Ah which is useful for the usage time estimation. To refer with the amount of energy, it is presented in W·h.

2.2.2 Battery discharge rate

When the battery is applied the load, it discharges the amount of current corresponding the load. This discharging current is usually called “C-rate” which is the amount of current relative to maximum capacity.

A 2.6 Ah battery is discharged with 1.3 A can be called that it is discharged with 0.5C. According to the battery capacity definition, C-rate is used to indicate the operating time for example a 2.6 Ah battery refers that the battery can be operated at 0.5C for two hours or operated at 1.0C for one hour. However, the maximum discharge rate of the battery depends on the specification which is up to the type of the battery chemistry. Not every battery can be operated at the high C-rate.

2.2.3 Battery voltage

The battery voltage is presented by two quantities: Open Circuit Voltage (OCV) and Close Circuit Voltage (CCV). OCV is the battery voltage without operating, it excludes the voltage drop during internal resistance due to the battery material, chemical compound and the transferring ions. On the other hand, CCV is the battery voltage during the operation which includes the effect of internal resistances. CCV is presented by equation (2.1).

$$V_{CCV} = V_{OCV} - i \cdot r_{int} \tag{2.1}$$

Where V_{CCV} = Close circuit voltage (V)
V_{OCV} = Open circuit voltage (V)
i = Electric current (A) (+ discharge, - charge)
r_{int} = Internal resistance (Ω)

The sign of the current is determined by discharge or charge behaviours: positive sign for discharge and negative sign for charge.

2.2.4 Heat generation of battery

Heat generation side the battery is the consequences from the chemical reaction of the electrolyte and the electrodes when release electrons as the product to perform the current transport. The heat generation consists of two sources: joule heating which is caused by Ohmic loss of electric current flowing through the electrodes material and heat generation due to entropy change which is the product from the chemical reaction.

2.2.4.1 Joule heating

The joule heating is one of battery heat sources which is the loss of electric in the form of heat caused by the flow of the current through the electrical resistant material expressed by:

$$\dot{q}_{joule} = i^2 \cdot r_{int} \tag{2.2}$$

Where $\dot{q}_{joule}$ = Joule heating (W)

The internal resistances in equation (2.3) consist of three terms: diffusion resistance caused by the concentration gradient in the electrolyte when the reaction is performed, ion transport resistance caused by the movement of ions and Ohmic resistance which is caused by the electrodes and internal component materials.

$$r_{int} = r_d + r_{ct} + r_{Ohm} \tag{2.3}$$

Where r_d = Diffusion resistance (Ω)
r_{ct} = Charge transfer resistance (Ω)
r_{Ohm} = Ohmic resistance (Ω)

2.3 Battery pack design

2.3.1 Design overview

A battery pack is a system of multiple components, functions and design involves the application of knowledge and practice in the eletrochemical, electrical, mechanical, thermodynamic as well as control fields. The following sections summarize the various stages of a battery pack design. (A123, 2014)

2.3.1.1 Cell configuration

The first step in the design of the pack is to determine the configuration of cells, i.e. how many cells overall, how many are in the series, and how many are in parallel. This is the foundation of the design process since all other design decisions follow from the cell configuration.

2.3.1.2 Structure

The second step is to design a mechanical structure around the cells to support and protect them. This step requires knowledge of electrical, mechanical, thermodynamic, properties of the cells, application and the materials used in the pack. Moreover, this section was focused in this research about component materials and its manufacturing methods.

2.3.1.3 Protection

The third step is to design the protection of the cells, particularly electrical protection. The pack must be protected from inadvertent short circuits internal and external to the pack as well as excessive charging and discharging imposed on its terminals.

2.3.1.4 Control

The fourth step is to design a control system that monitors and manages the cells, keeping them from being damaged and maintaining the pack at peak performance.

2.3.1.5 Use

Finally, a pack performs best when it is used properly. The final section of this chapter describes how to charge and discharge the battery pack to make it perform its best.

Recently lithium-ion batteries have started to be used in a number of electric vehicle applications. Dr. Peter Miller has reviewed these applications and compared the requirements of the applications with the capabilities of the lithium-ion chemistries that are actually being used. The gaps between these requirements and capabilities will be highlighted and future developments that may be able to fill these gaps will be discussed.

Recently prototype battery packs have been developed with significantly higher energy density. For example, the SmartBatt programme Figure 2.4 has recently demonstrated an EV battery pack with 148 $Wh \cdot kg^{-1}$ while meeting all other automotive requirements. This was achieved by combining a lot of high energy lithium-ion cells with innovative materials and state of the art engineering (including a large number of crash test simulations to optimize the design).

Table 2.1 gives the weight breakdown of the SmartBatt pack. The 85% gain in energy per unit weight obtained by the SmartBatt pack far exceeds the long term projections of a 30% improvement in energy per unit weight from lithium-ion chemistry improvements and together they suggest that a 100% gain in energy per unit weight (to around 160 $Wh \cdot kg^{-1}$) may be possible at the pack level for EV packs. (Miller, 2015).

However, it is shown here that, especially for EV battery packs, major weight gains can come from the overall design of the battery pack and these together with better chemistries suggest that a doubling of the energy per unit weight for EV battery packs is possible in the relatively near future. In addition, a lighter weight vehicle is preferred because it can increase the range of vehicle and the life cycle of a battery pack.

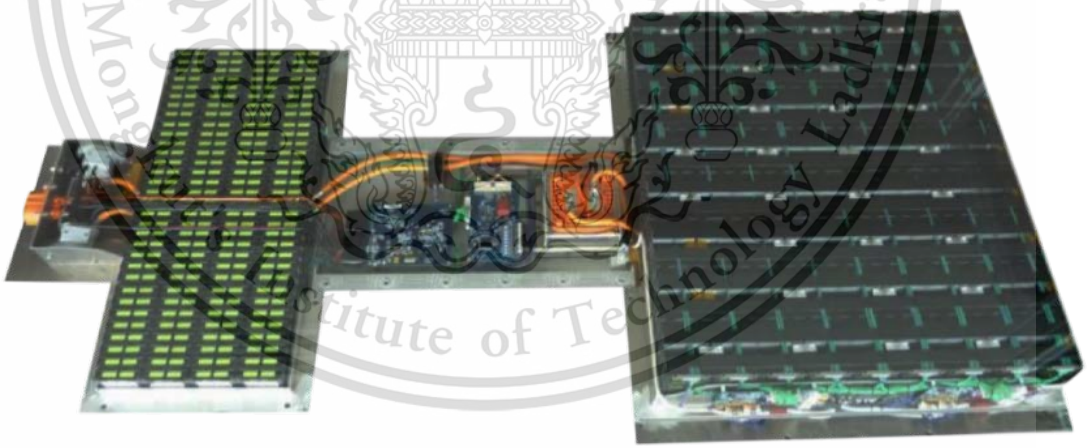

Figure 2.4 SmartBatt battery pack

Table 2.1 SmartBatt Weight Breakdown

Component	Mass, kg	Fraction, %
Housing	8.5	5.5
Module without cells	16.6	10.7
Cells	125.3	80.6
Electrical components	2.1	1.4
Electrical connections	2.9	1.9
Total	155.4	-

2.3.2 Series and parallel battery configurations

Battery arrangement to increase voltage or gain higher capacity. Batteries achieve the desired operating voltage by connecting several cells in series; each cell adds its voltage potential to derive at the total terminal voltage. Parallel connection attains higher capacity by adding up the total ampere-hour (Ah).

Some packs may consist of a combination of series and parallel connections. Laptop batteries commonly have four 3.6 V Li-ion cells in series to achieve a nominal voltage 14.4 V and two in parallel to boost the capacity from 2,400 mAh to 4,800 mAh. Such a configuration is called 4S2P, meaning four cells in series and two in parallel. Insulating foil between the cells prevents the conductive metallic skin from causing an electrical short.

Most battery chemistries lend themselves to series and parallel connection. It is important to use the same battery type with equal voltage and capacity and never to mix different makes and sizes. A weaker cell would cause an imbalance. A weak cell may not fail immediately but will get exhausted more quickly than the strong ones when on a load. On charge, the low cell fills up before the strong ones because there is less to fill, and it remains in over-charge longer than the others. On discharge, the weak cell empties first and gets hammered by the stronger brothers. Cells in multi-packs must be matched, especially when used under heavy loads. (“Serial and Parallel Battery Configurations and Information,” n.d.)

2.3.2.1 Series connection

Portable equipment needing higher voltages use battery packs with two or more cells connected in series. Figure 2.5 shows a battery pack with four 3.6 V Li-ion cells in series, also known as four series (4S), to produce 14.4 V nominal. In comparison, a six-

cell lead acid string with 2 V/cell will generate 12 V, and four alkaline with 1.5 V/cell will give 6 V.

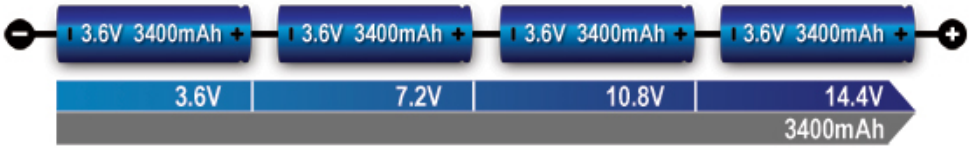

Figure 2.5 Series connection of four cells (4s). (Adding cells in a string increases the voltage; the capacity remains the same.)

Source: Courtesy of Cadex

Some mild hybrid cars run on 48 V Li-ion and use DC-DC conversion to 12 V for the electrical system. Starting the engine is often done by a separate 12V lead acid battery. Early hybrid cars ran on a 148 V battery; electric vehicles are typically 450 - 500 V. Such a battery needs more than 100 Li-ion cells connected in series.

High-voltage batteries require careful cell matching, especially when drawing heavy loads or when operating at cold temperatures. With multiple cells connected in a string, the possibility of one cell failing is real, and this would cause a failure. To prevent this from happening, a solid-state switch in some large packs bypasses the failing cell to allow continued current flow, albeit at a lower string voltage.

High-voltage batteries in electric vehicles, in which a full replacement would be prohibitive, divide the pack into modules, each consisting of a specific number of cells. If one cell fails, only the affected module is replaced. A slight imbalance might occur if the new module is fitted with new cells.

2.3.2.2 Parallel Connection

If higher currents are needed and larger cells are not available or do not fit the design constraint, one or more cells can be connected in parallel. Most battery chemistries allow parallel configurations with little side effect. Figure 2.6 illustrates four cells connected in parallel in a P4 arrangement. The nominal voltage of the illustrated pack remains at 3.60V, but the capacity (Ah) and runtime are increased fourfold.

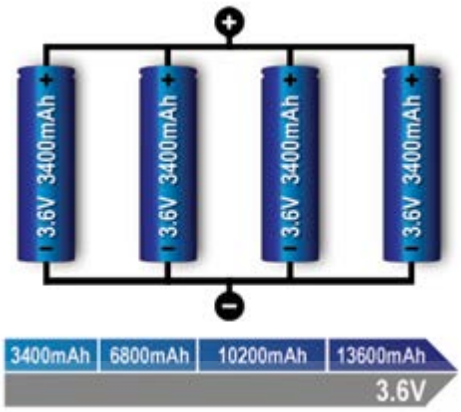

Figure 2.6 Parallel connection of four cells (4P). (With parallel cells, capacity in Ah and runtime increases while the voltage stays the same.)

Source: Courtesy of Cadex

A cell that develops high resistance or opens is less critical in a parallel circuit than in a series configuration, but a failing cell will reduce the total load capability. It looks like an engine only firing on three cylinders instead of on all four. An electrical short, on the other hand, is more serious as the faulty cell drains energy from the other cells, causing a fire hazard. Most so-called electrical shorts are mild and manifest themselves as elevated self-discharge.

A total short can occur through reverse polarization or dendrite growth. Large packs often include a fuse that disconnects the failing cell from the parallel circuit if it were to short. A weak cell will not affect the voltage but provide a low runtime due to reduced capacity. A shorted cell could cause excessive heat and become a fire hazard. On larger packs a fuse prevents high current by isolating the cell.

2.3.2.3 Series/parallel connection

The series/parallel configuration shown in Figure 2.7 enables design flexibility and achieves the desired voltage and current ratings with a standard cell size. The total power is the product of voltage-times-current; four 3.6 V (nominal voltage) cells multiplied by 3,400 mAh produce 12.24 Wh. Four 18650 Energy Cells of 3,400 mAh each can be connected in series and parallel as shown to get 7.2 V nominal and 12.24 Wh. The slim cell allows flexible pack design, but a protection circuit is needed.

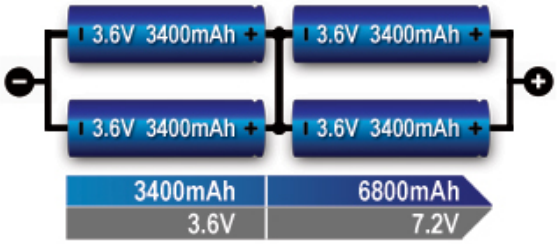

Figure 2.7 Series/parallel connection of four cells (2S2P).

Source: Courtesy of Cadex

Li-ion lends itself well to series/parallel configurations, but the cells need monitoring to stay within voltage and current limits. Integrated circuits (ICs) for various cell combinations are available to supervise up to 13 Li-ion cells. Larger packs need custom circuits, and this applies to e-bike batteries, hybrid cars and the Tesla Model 85 that devours over 7000 18650 cells to make up the 90 kWh pack.

- **Terminology to describe Series and parallel connection**

The battery industry specifies the number of cells in series' first, followed by the cells placed in parallel. An example is 2S2P. With Li-ion, the parallel strings are always made first; the completed parallel units are then placed in series. Li-ion is a voltage-based system that lends itself well for parallel formation. Combining several cells into a parallel and then adding the units serially reduces complexity in terms of voltages control for pack protection.

- **Safety devices in series and parallel connection**

Positive Temperature Coefficient Switches (PTC) and Charge Interrupt Devices (CID) protect the battery from overcurrent and excessive pressure. While recommended for safety in a smaller 2- or 3-cell pack with serial and parallel configuration, these protection devices are often being omitted in larger multi-cell batteries, such as those for a power tool. The PTC and CID work as expected to switch off the cell on excessive current and internal cell pressure; however, the shutdown occurs in cascade format. While some cells may go offline early, the load current causes excess current on the remaining cells. Such an overload condition could lead to a thermal runaway before the remaining safety devices activate.

Some cells have built-in PCT and CID; these protection devices can also be added retroactively. The design engineer must be aware that any safety device is subject to failure. In addition, the PTC induces a small internal resistance that reduces the load current. (“Serial and Parallel Battery Configurations and Information,” n.d.)

2.4 Fundamentals of heat transfer

Heat transfer occurs when there is a different temperature between an object and its surroundings or another object. Heat will be exchanged until both object and surroundings achieve thermal equilibrium. Energy can be transferred from one point to another by common methods which are conduction, convection, radiation or any combination of these (Filip, 2006).

In this study, three forms of heat transfer will always be mentioned to explain the phenomena of the cooling system: heat conduction and heat convection.

2.4.1 Heat conduction

$$\dot{q}_{cond} = -A_c \cdot (k \cdot \nabla T) \tag{2.4}$$

Where $\dot{q}_{cond}$ = Heat conduction (W)
A_c = Conduction area (m^2)
k = Thermal conductivity ($W/m^2 \cdot K$)
T = Absolute temperature (K)

2.4.2 Heat convection

$$\dot{q}_{conv} = h \cdot A_s \cdot (T_s - T_{amb}) \tag{2.5}$$

Where $\dot{q}_{conv}$ = Heat convection (W)
h = Heat transfer coefficient ($W/m^2 \cdot K$)
A_s = Surface area for convection (m^2)
T_s = Surface temperature (K)
T_{amb} = Ambient temperature (K)

2.5 Material properties overview

2.5.1 Thermal conductivity

Conduction is a method of transferring energy directly through molecular communication within a medium. It can also occur between two or more mediums with indirect physical contact. Conduction is greater in solids than in liquids and gases, because the molecules in solids are closer to each other than in liquids and gases. Therefore, there are a lot of opportunities for the molecules to vibrate against each other and exchange thermal energy. Thermal conductivity is used as a parameter to define the ability of a medium to transfer thermal energy. Thermal conductivity depends fundamentally on the molecular bonding type, temperature, density and the phase of the medium. The Fourier equation defines thermal conductivity as in Equation below (Jensen, Tuttle, Stewart, Brechna, & Prodell, 1980).

$$Q = \lambda \cdot A \cdot \frac{dT}{dL} \tag{2.6}$$

Where Q = Rate of heat conduction (Watts)
λ = Thermal conductivity (W/mK)
A = Cross-sectional area of heat conduction path (m^2)
$\frac{dT}{dL}$ = Temperature gradient at concerned section (K/m)
T = Temperature (K)
L = Length (m)

2.5.2 Electrical conductivity

Electrical conductance can be defined as a property of a material which indicates how well an electric charge pass through the material is. Electrical conductance is the reciprocal of electrical resistance. The conductance is varied according to several factors such as chemical composition and the stress state of crystalline structures. The electrical conductance can be used as a measure for categorizing materials and checking for proper heat treatment of materials. A material that has a high electrical conductance is called a conductor, while a material that has a high electrical resistance is called an insulator. If a current pass through the conductor with a length (L) and a cross-sectional area (A), the electrical conductance is proportional to the cross-section area of the conductor, and it is inversely proportional to the length of the connector. These relations are shown in Equation 2.7. In Equation 2.8, an electrical conductivity

(σ) is introduced, and it is defined as the electrical conductance per unit length and per unit of cross-sectional area. Siemens per meter is its SI derived unit, but it is usually reported as percent IACS, which indicates the percentage value comparing to the conductivity of copper. The 100% IACS refers to the electrical conductivity value of the annealed copper, which equals to 5.8001x107 S/m. Figure 2.2 shows a comparison of electrical conductivity values of various pure metals. The conductivities of metals for the same length and cross-sectional area can be compared with the conductivity on a volume basis, while the conductivity on a weight basis is used to compare the conductivities of metals with the same weight. The electrical conductivity values also depend particularly on the temperatures.

Generally, metal is a conductor, but it has a lower conductivity at higher temperatures. Meanwhile, an insulator has a higher conductivity at higher temperatures. (NDT Resource Center, 2015) (Nelson, 2018) (Blue Sea Systems, 2002)

$$G \propto \frac{A}{L}, \tag{2.7}$$

$$G \propto \sigma \cdot \frac{A}{L} \tag{2.8}$$

Where G = Electrical conductance ($kg^{-1} \cdot m^{-2} \cdot s^3 \cdot A^2$)
σ = Electrical conductivity of the material (S/m)
A = Cross-sectional area of the conductor (m^2)
L = Length of the conductor (m)

Table 2.2 Relative conductivities of pure metals (The Aluminium Association, 1989)

Metal	Conductivity (%IACS Volume Basic)	Specific Gravity	Conductivity (%IACS Weight Basic)
Silver	108.4	10.49	91.9
Copper	103.1	8.93	102.6
Aluminium	64.9	2.70	213.7
Titanium	4.1	4.51	8.1
Manganese	38.7	1.74	197.7
Sodium	41.0	0.97	376.2

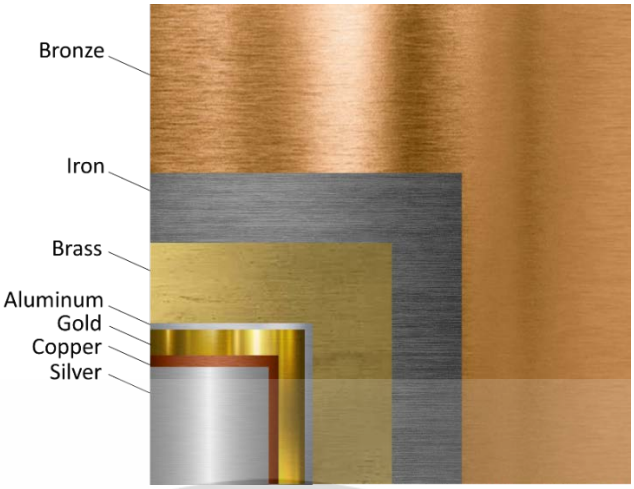

Figure 2.8 Required material sizes for equivalent conductivity

In addition, there is research which has been studied about a comparison of aluminium versus copper as used in electrical equipment in terms of current carrying capacity, connections and terminations, physical properties and cost. The result showed that when the density of Cu is compared to that of Al and taking into consideration the conductivity ratio of Al to Cu of 56%, the result shows that Al has an amperage capability that is approximately 1.85 times that of Cu at the same weight. Most importantly, the designer should be aware that equipment available with aluminium conductors will definitely weigh less than the same equipment with copper and at the current commodity pricing will cost less. (Pryor, Schlobohm, & Brownell, n.d.)

Table 2.3 shows a comparison of some of the properties of Cu and Al are given in the following table. Properties will very depend on the alloy used that need to be discussed are the tensile strength and thermal expansion of the conductors. Of particular concern is the ability of the conductor to withstand the forces resulting from short circuits and the effects of expansion from heat on joints and terminations.

Table 2.3 Physical properties

Characteristics	**Copper**	**Aluminium**
Tensile strength (lb/in2)	50,000	32,000
Tensile strength for some conductivity (lb.)	50,000	50,000
Weight for some conductivity (lb.)	100	54
Cross section for some conductivity	100	156
Specific resistance (ohms-cir/mil ft) (20 °C ref)	10.6	18.52
Coefficient of expansion (per deg. C × 10^{-6}	16.6	23

Reviewing the information in the table above, it can be seen that the aluminium conductor will have a cross sectional area 56% larger than copper for the same current carrying capability. Even though aluminium does have a lower tensile strength than copper it can be seen that the AL has, essentially, the same tensile strength of Cu for the same ampacity (50,000 lb/in2). The main area where this would be of concern as stated previously would be strength to withstand the forces during short circuits. The above table notes that the coefficient of thermal expansion for Al is 42% greater than that of Cu. This characteristic is of concern when the expansion and contraction of conductors in electrical connections during thermal cycling are studied.

One of the important factors in establishing and maintaining a low resistance busbar joint is the use of proper and well-distributed force. To analyse this issue, it is necessary to first understand the potential problem and then look at the methods and techniques manufacturers use to address this issue. Aluminium alloy 6101 is commonly used for busbars and has a tensile strength approaching copper. Alloy 6101T63 has a tensile strength of 27,000 psi and will operate as satisfactorily as copper.

Conductors consist of materials that conduct electric current, or the flow of electrons. Nonmagnetic metals are typically considered to be ideal conductors of electricity. The two most common are copper and aluminium. Conductors have different properties such as conductivity, tensile strength, weight and environmental exposure.

Both Aluminium and Copper have been being effectively used as high current conductors. By many Copper is considered to be a superior conductor material to Aluminium. And despite being significantly more expensive, its usage is wide spread and hardly challenged.

Nonetheless, Aluminium is widely spread and successfully used as a conductor material in busbar. The advantages of Aluminium over Copper for these applications are obvious:

- Significantly lower material costs (up to six times lower than Copper per Ampere),

- About half the weight of Copper per Ampere.

With the exception of silver, copper is the most common conductive metal and has become the international standard. The International Annealed Copper Standard (IACS) was adopted in 1913 to compare the conductivity of other metals to copper. According to this standard, commercially pure annealed copper has a conductivity of 100 percent IACS.

Aluminium has 61 percent of the conductivity of copper but has only 30 percent of the weight of copper. Aluminium is generally more inexpensive when compared to copper conductors.

As a raw material, Al is approximately 70% lighter than Cu. For wires, Al can be up to 60% lighter than the comparable current carrying copper wires the weight is not a direct relation as more Al is necessary to match the capacity of Cu. Al carries about half the capacity of Cu (56% in Al6101). The difference in the weight to electrical capacity ratio means generally, one pound of Al has the electrical conductivity equal to 1.85 lb. of Cu. For example, a Cu busbar could weight around 550 lb., whereas the same busbar in Al would be about 300 lb. Reducing weight may help shipping or even labour cost.

2.6 Manufacturing methods overview

2.6.1 Cutting process

2.6.1.1 Laser cutting

At the beginning of laser cutting process, a laser beam is generated by the laser source. Then it is reflected by the mirrors in order that the beam could be directed to the cutting head. The beam is concentrated by the lens in the cutting headso that it can be used to heat up and melt the material. Meanwhile, the cutting gas is supplied at the cutting head to cool the lens and remove the molten material. Generally, the cutting process depends on the type of cutting gas.

Cutting with oxygen – The laser beam heats up the material to its ignition temperature until it is burned and vaporized. The reaction between the metal and the oxygen provides additional heat energy which promotes the cutting process. As a result, it increases the cutting capability to penetrate thick and reflective metals.

Cutting with inert gases – Cutting with non-reactive or inert gases, such as nitrogen or argon, is also known as clean cutting or high-pressure cutting. Since there is not any

reaction between non-reactive gases and the molten metal, the additional heat energy is not produced. Therefore, cutting with inert gases generally requires higher laser power than cutting with the oxygen of the same workpiece thickness.

There are also other cutting processes such as vaporization cutting and cold cutting. In vaporization cutting, the material is directly converted from the solid phase to vapor phase, which does not pass through the liquid phase. The gases can be used to remove the vapor and protect the cutting lens. In cold cutting, the chemical bonds of the material are cut off by the laser energy, and it often does not require the cutting gas.

Table 2.4 Advantages and disadvantages of laser cutting

Advantages	**Disadvantages**
▪ High speed in comparison with other methods. ▪ Workpiece cleaning after cutting is not required. ▪ High detailed work can be accomplished. ▪ Can be completely operated by CNC control. ▪ Heat affected areas on the material are small. ▪ Requires only light clamping of workpiece. ▪ The running cost of machine is relatively low. ▪ Waste of material can be minimized.	▪ The inside of the tubes should be coated with anti-spatter fluid. ▪ The systems are expensive. ▪ Not efficient for a simple cutting profile.

Generally, laser cutting properties are also influenced by laser power and laser intensity. Laser power describes total emitting energy per second in the form of laser light, while laser intensity equals to laser power divided by the concentrated area. The high intensity laser beam can offer excellent cutting quality and high cutting rates. In addition, high intensity laser provides better ability to cut thick material. Regarding the cutting speed, it relies on the average power level. With higher average power level, cutting speed can be increased. (Berkmanns & Faerber, 2008)

The information of laser cutting ability for different materials is provided following:

Aluminium and aluminium alloys – Since aluminium has high thermal conductivity and high reflectivity, it is difficult to cut aluminium with CO_2 laser. However, it is easier to cut aluminium alloys and anodised aluminium comparing with pure aluminium. The cutting of aluminium ability can be improved using high laser power,

with more than 2 kW power, and an appropriate cutting mode. Both oxygen and nitrogen can be used as the cutting gas.

Copper alloys – It is also difficult to cut copper with CO_2 laser due to its high thermal conductivity and high reflectivity. Brass is easier to cut due to its lower thermal conductivity and reflectivity comparing with copper. It is better to use high laser power, short focal length lens and oxygen cutting for brass and copper alloys.

2.6.1.2 Punching process

Punching is a cutting process in which material is removed from a piece of sheet metal by applying a great enough shearing force. Punching is very similar to blanking except that the removed material, called the slug, is scrap and leaves behind the desired internal feature in the sheet, such as a hole or slot. Punching can be used to produce holes and cut-outs of various shapes and sizes. The most common punched holes are simple geometric shapes (circle, square, rectangle, etc.) or combinations thereof. The edges of these punched features will have some burrs from being sheared but are of fairly good quality. Secondary finishing operations are typically performed to attain smoother edges.(Gupta, n.d.; P. Groover, 2012)

The punching process requires a punch press, sheet metal stock, punch and die. The sheet metal stock is positioned between the punch and die inside the punch press. The die, located underneath the sheet, has a cut-out in the shape of the desired feature. Above the sheet, the press holds the punch, which is a tool in the shape of the desired feature. Punches and dies of standard shapes are typically used, but custom tooling can be made for punching a complex shapes. This tooling, whether standard or custom, is usually made from tool steel or carbide. The punch press drives the punch downward at high speed through the sheet and into the die below. There is a small clearance between the edge of the punch and the die, causing the material to quickly bend and fracture. The slug that is punched out of the sheet falls freely through the tapered opening in the die. This process can be performed on a manual punch press, but today computer numerical controlled (CNC) punch presses are most common. A CNC punch press can be hydraulically, pneumatically, or electrically powered and deliver around 600 punches per minute. Also, many CNC punch presses utilize a turret that can hold up to 100 different punches which are rotated into position when needed.

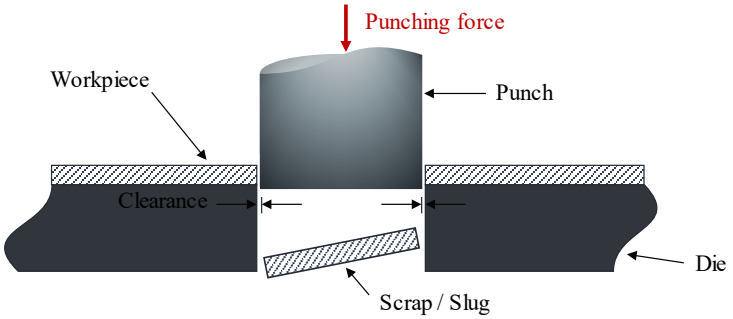

Figure 2.9 A typical punching operation

In Figure 2.9, a typical punching operation is one in which a cylindrical punch tool pierces the sheet metal, forming a single hole. However, a variety of operations are possible to form different features. These operations include the following table:

Table 2.5 Advantages and disadvantages of the punching process

Advantages	Disadvantages
▪ Very fast. ▪ It is often the cheapest for medium to high volume of production. ▪ It can create multiple shaped holes	▪ Fine blanking process is a slow process. ▪ Equipment and tooling costs are high. ▪ Often needs secondary finishing operations

2.6.2 Manufacturing for plastic parts

2.6.2.1 Injection moulding

Injection moulding is the most commonly used manufacturing process for the fabrication of plastic parts. A wide variety of products are manufactured using injection moulding, which vary greatly in their size, complexity, and application. The injection moulding process requires the use of an injection moulding machine, raw plastic material, and a mould. The plastic is melted in the injection moulding machine and then injected into the mould, where it cools and solidifies into the final part. The steps in this process are described in greater detail in the next section.

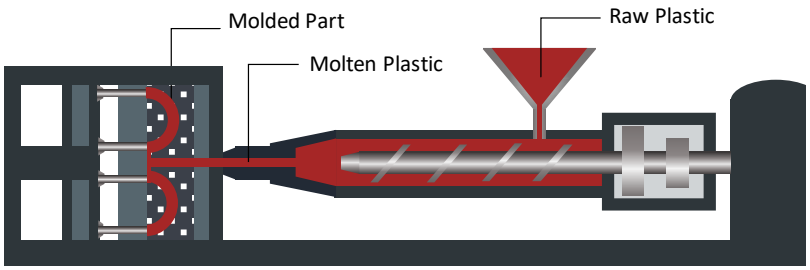

Figure 2.10 Injection moulding overview

Injection moulding is used to produce thin-walled plastic parts for a wide variety of applications, one of the most common being plastic housings. The plastic housing is a thin-walled enclosure, often requiring many ribs and bosses on the interior. These housings are used in a variety of products including household appliances, consumer electronics, power tools and as automotive dashboards. Other common thin-walled products include different types of open containers, such as buckets. Injection moulding is also used to produce several everyday items such as toothbrushes or small plastic toys. Many medical devices including valves and syringes are manufactured using injection moulding as well. ("Injection Molding Process, Defects, Plastic," n.d.; "What is injection moulding?," 2013)

Table 2.6 Advantages and disadvantages of the injection moulding

Advantages	Disadvantages
▪ Can form complex shapes and fine details ▪ Excellent surface finish ▪ Good dimensional accuracy ▪ High production rate ▪ Low labour cost ▪ Scrap can be recycled	▪ Limited to thin walled parts ▪ High tooling and equipment cost ▪ Long lead time possible

2.6.2.2 Milling process

Milling is the most common form of machining, a material removal process, which can create a variety of features on a part by cutting away the unwanted material. The milling process requires a milling machine, workpiece, fixture, and cutter. The workpiece is a piece of pre-shaped material that is secured to the fixture, which itself is attached to a platform inside the milling machine. The cutter is a cutting tool with sharp teeth that is also secured in the milling machine and rotates at high speeds. By feeding the workpiece into the rotating cutter, material is cut away from this workpiece in the form of small chips to create the desired shape.("Milling Process, Defects, Equipment," n.d.)

Milling is typically used to produce parts that are not axially symmetric and have many features, such as holes, slots, pockets, and even three-dimensional surface contours. Parts that are fabricated completely through milling often include components that are used in limited quantities, perhaps for prototypes, such as custom designed fasteners or

brackets. Another application of milling is the fabrication of tooling for other processes. For example, three-dimensional moulds are typically milled. Milling is also commonly used as a secondary process to add or refine features on parts that were manufactured using a different process. Due to the high tolerances and surface finishes that milling can offer, it is ideal for adding precision features to a part whose basic shape has already been formed. (P. Groover, 2012)

Table 2.7 Advantages and disadvantages of the milling process

Advantages	Disadvantages
▪ All materials compatible ▪ Very good tolerances ▪ Short lead times	▪ Limited shape complexity ▪ Part may require several operations and machines ▪ High equipment cost ▪ Significant tool wear ▪ Large amount of scrap

2.6.3 Decision tools

2.6.3.1 Architecture analysis method

This research also applied an application of product architecture design methodology to system design. The application of architecture analysis and core competencies to identify design items and sequence of design through empirical knowledge of experienced engineers. The three underlining techniques in this approach are:

- Clarifying the relationship between performance attributes and specification of the battery pack.

- Extraction of battery pack design items focusing on only four main components.

- Setting an efficient sequence for the process of battery pack design.

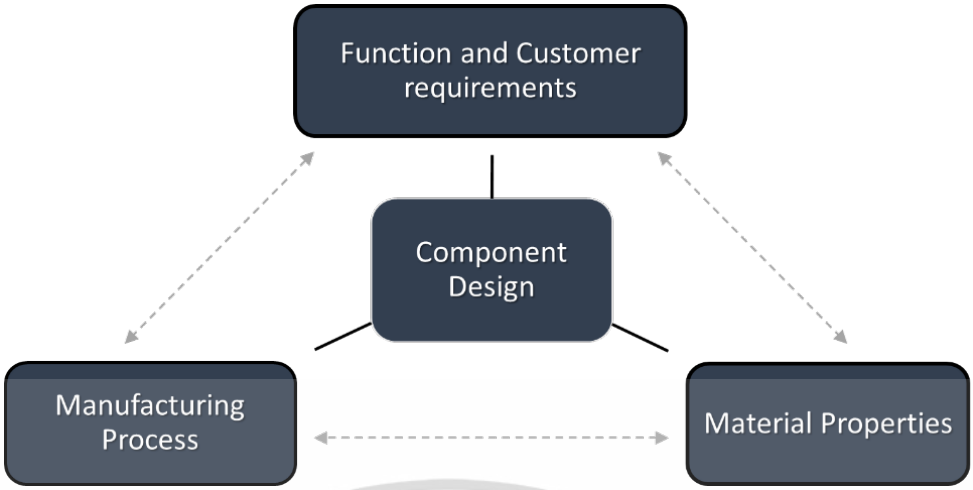

Figure 2.11 Factors that should be considered in the component design

2.6.3.2 Decision matrix

The decision matrix is a decision aid tool that qualitatively evaluates and prioritizes a list of abstract solutions. It also provides a system that relationships between sets of information are identified, analysed and rated. The decision matrix is also known as alternatives evaluation matrix, criteria-based matrix, COWS decision matrix, decision grid, opportunity analysis, problem selection matrix, Pugh matrix, weighted criteria matrix and etc. The decision matrix is frequently used when only one option can be implemented. In addition, it can be used as a method to rank all the alternatives. Moreover, it can also help reduce the number of options in the list by filtering out the unsuitable alternatives. The procedure of the decision matrix is provided following. (Great Britain & Department for Communities and Local Government, 2009; Thokala et al., 2016)

- **Identify alternatives**

The alternatives can be product features, service features, process steps, or potential solutions.

- **Identify selection criteria**

The criteria may result from an affinity diagram or a brainstorming activity in the team. The customer needs are also included if possible. The list of criteria should be discussed and refined within the team.

- **Assign a relative weight to each criterion**

All criteria are weighted depending on the relative importance of each criterion to the concerned situation. The criterion that is more important than others is assigned the higher weight factor. There are several options for weighting scales. For instance, 1 – 10 : 1 = the least priority, 10 = the most important

- **Design scoring system**

There are three options for the scoring system.

Method 1 - A scoring range is established for all criteria. There are also many options for the scoring range. Examples are given following;

1, 2, 3 : 1 = low, 2 = medium, 3 = high
1, 2, 3, 4, 5 : 1 = little to 5 = great
1, 4, 9 : 1 = low, 4 = moderate, 9 = high

Method 2 - Each alternative is ranked according to its performance for the concerned criterion. Number 1 means that it is the least desirable, while the best performance alternative in each criterion gets the highest number.

Method 3 (Pugh matrix) - One alternative is chosen as a baseline. The baseline is given the 0-score in all criteria. Then other alternatives are evaluated by comparing with the baseline. The better performance alternatives get the positive scores such as +1, +2, or +3. Meanwhile the worse alternatives get the minus scores such as -1, -2, or -3. A three-point scale (-1, 0, 1), a five-point scale (-2, -1, 0, 1, 2) or a seven-point scale (-3, -2, -1, 0, 1, 2, 3) can be used.

- **Rate the alternatives**

The scores of all alternatives for each criterion may come from the average values of the scores given by individual team members, or the scores may come from the consensus decision of the team.

- **Total the scores**

All the scores in each criterion are multiplied by their weighting factors. Then the overall score of each alternative can be obtained from the summation of the multiplied scores.

The decision matrix tables are generally formed with the list of all criteria and the list of all alternatives. The list of all criteria is located on the first column, while the list of all alternatives is placed on the first row. The second column usually stores the weighting factors. Therefore, the decision matrix is a L-shaped matrix with 2-dimension variation.

CHAPTER 3

RESEARCH METHODOLOGY

This research studies four components of the new conceptual battery pack for an electric vehicle including Z bar, Positive Busbar, Negative Busbar and battery holder which are highlighted in Figure 3.1. This chapter provides the information regarding the selections of materials and manufacturing methods as shown in Figure 3.1. In each component, the design criteria are specified and discussed with researchers and engineers who are the battery pack designer. For the material selection, the material options are filtered to a small number of alternatives. Then, the decision matrix is used as the decision aid tool to choose the appropriate alternative that is presented in the next chapter. The design criteria of the new concept battery pack are used as the selection criteria in the decision matrix. For the manufacturing method selection, the manufacturing methods that are related to the concerned component are listed and discussed. The brief information of the related manufacturing method is also provided. After that, the selection of the manufacturing method is based on the gathered information from the manufacturers.

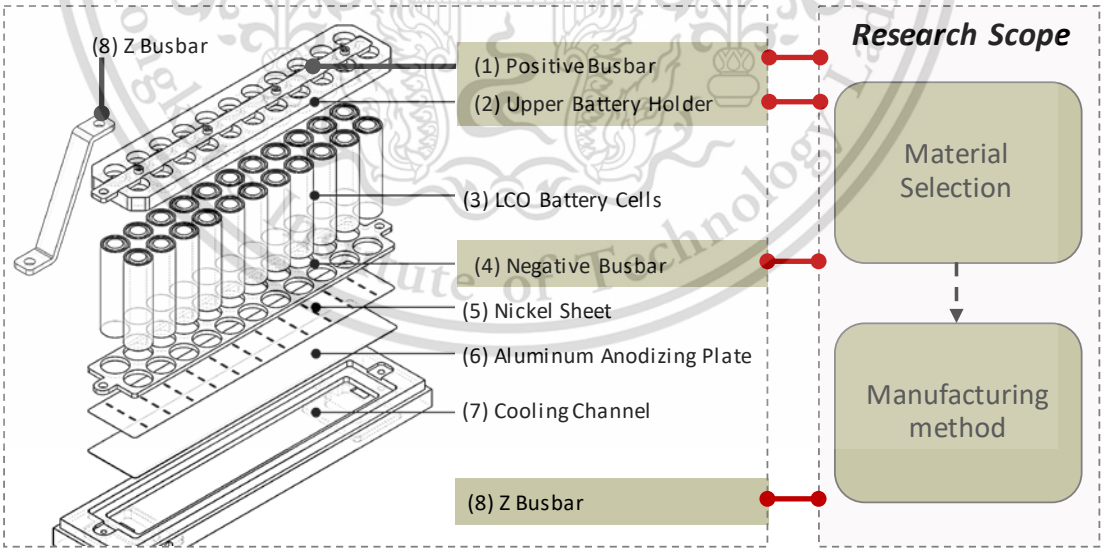

Figure 3.1 18650 lithium-ion battery cells assembled in battery sub-module

3.1 Z bar

The Z bar is used as electrical conductors to make a serial connection between battery sub-modules in order to increase the voltage requirement of the battery pack as shown in Figure 3.2.

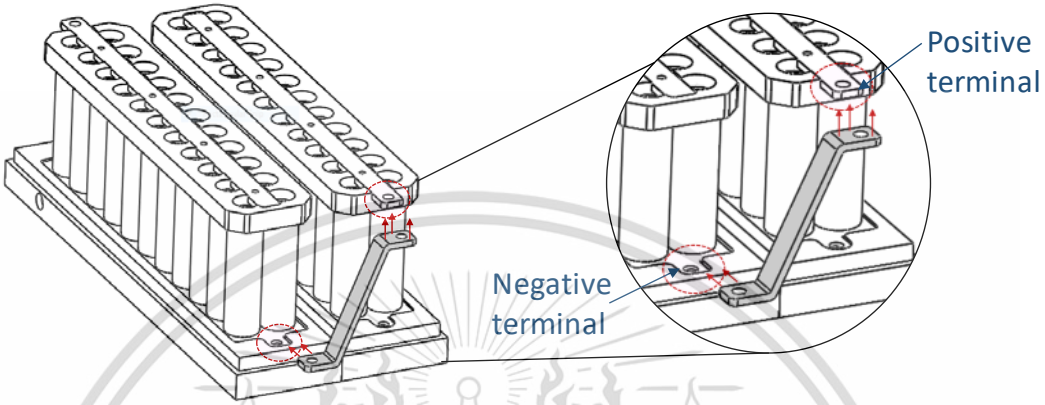

Figure 3.2 Z bar in sub-modules

Figure 3.3 shows two possible designs of the Z bar for battery pack; (a) is the original design and (b) is an improved design. According to the behaviour of electric current, the current always flows in the shortest route. Therefore, the current density is higher in the bending area resulting in high heat generation rate. Moreover, the new design has shorter length than the original design. This can decrease the electrical resistance and reduce the material used for producing the part.

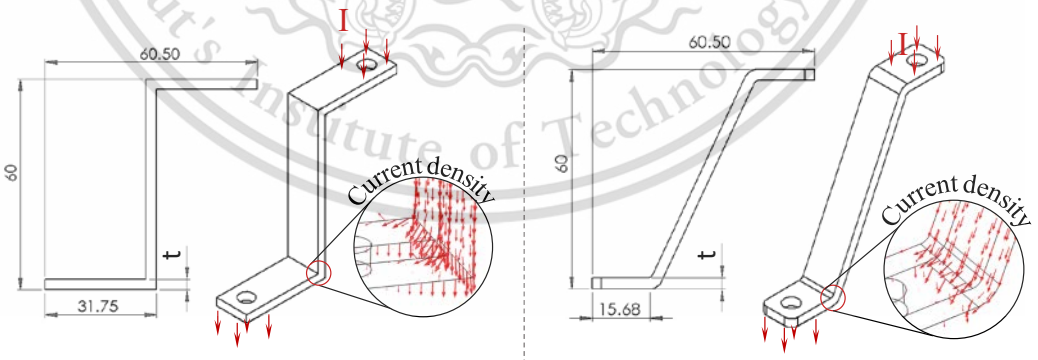

(a) Original design (b) Improved design

Figure 3.3 Comparison of two possible designs

3.1.1 Material alternatives

Regarding Aluminium and Copper have been being effectively used as high current conductors nowadays including busbar application, there are many arguments brought

up against the use of both materials. Hence, this study has selected Aluminium and Copper as material alternatives for Z bar (see in Figure 3.4) by considering four aspects; electrical conductivity, thermal conductivity, density and material cost in order to select the most proper material for Z bar.

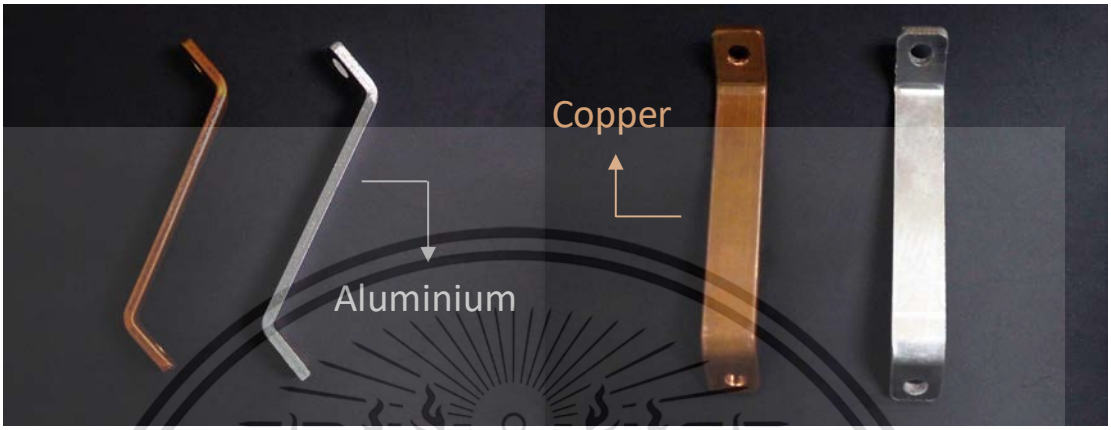

Figure 3.4 Copper and Aluminium Z bar in side and top view

3.1.2 Designing Z bar

After the Z bar shape design is improved and fixed, its thickness (t) shown in Figure 3.3 still needs to be optimized because the electrical resistance is proportional to the cross-section area of the conductor. In order to reduce the cost, design time and unnecessary experiments, a simulation software is mainly used in designing state to obtain the proper thickness in three conditions; two millimetres, three millimetres and four millimetres for those two materials. The reason of setting two millimetres and four millimetres as minimum and maximum thickness is that temperature condition and limited area respectively. However, real experiments are also used to validate with simulation by using only three millimetres of the thickness for Aluminium and Copper.

3.1.2.1 Experiment setup

As far as the simulation is concerned, the material properties from the simulation and the experiment may not be identical because the material grade of the conductor cannot be identified. The comparison with a real experiment is the most reliable and preferred way to validate a simulation model. Consistency tests are used to check that a model produces similar results for input parameter values that have similar effects. Thus, all conditions need to be validated with the real experiment in order to obtain an accuracy

value of temperature, voltage drop, electrical resistance, electric conductivity and heat transfer coefficient under an ambient temperature 45°C as shown in Figure 3.5.

In this research, temperature distribution and electrical resistance are the main parameters used to compare simulation result with the experimental result. The installation of three temperature sensors are also included in the experiment for measuring temperature and reference temperatures calibrating from the thermal camera as shown in Figure 3.6. The voltage probe is also installed to measure the voltage drop for calculating the electrical resistance and real electrical conductivity (see in Figure 3.5)

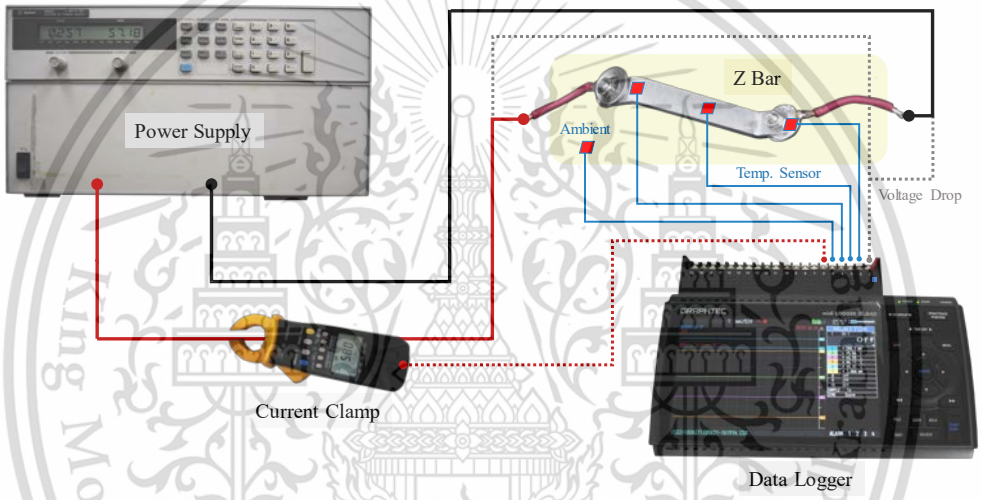

Figure 3.5 Z bar experiment setup for validation measurement

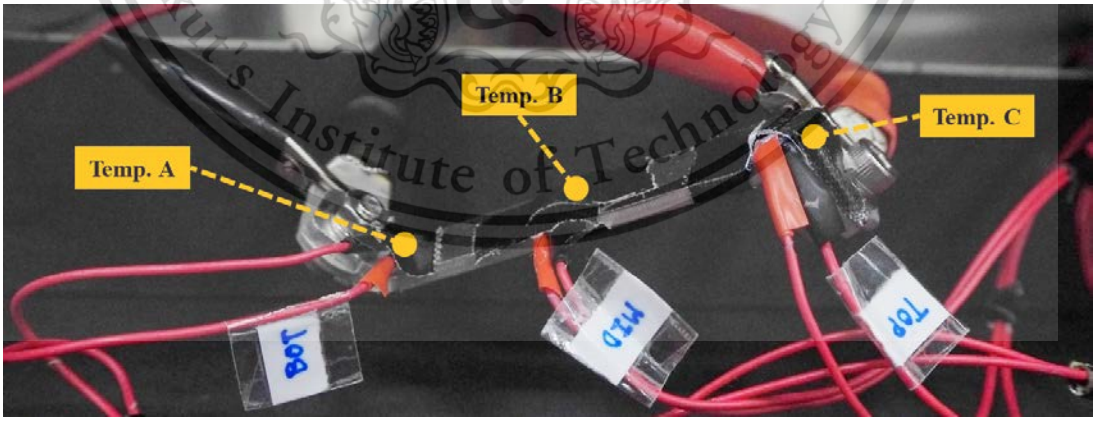

Figure 3.6 Temperature sensor positions for Z bar

Table 3.1 shows the boundary conditions for the experiment including the range of current loads, required outputs and ambient temperature.

Table 3.1 Boundary conditions for the experiment

Boundary conditions		
Current loads	14.3A	(0.25C)
	28.6	(0.5C)
	42.9	(0.75C)
	57.2	(1C)
Output	Voltage drop (V)	
	Temperature changes (°C)	
	Electrical Resistance (Ω)	
	Electric conductivity (S/m)	
Ambient temperature	45 (°C)	

3.1.2.2 Simulation

Since the behaviours of Z bar including current direction, and temperature distribution occur inside work-pieces material cannot be easily observed during experimentation, the effects of following parameters will be also studied through simulation method using the same boundary conditions from the experiment.

CAD modelling

In order to create the 3D geometry for simulations, the Z bar for Li-ion battery pack has been disassembled as shown in Figure 3.7. The dimensions of component parts were measured, and the 3D model of each part was created in SolidWorks program as illustrated in Figure 3.8.

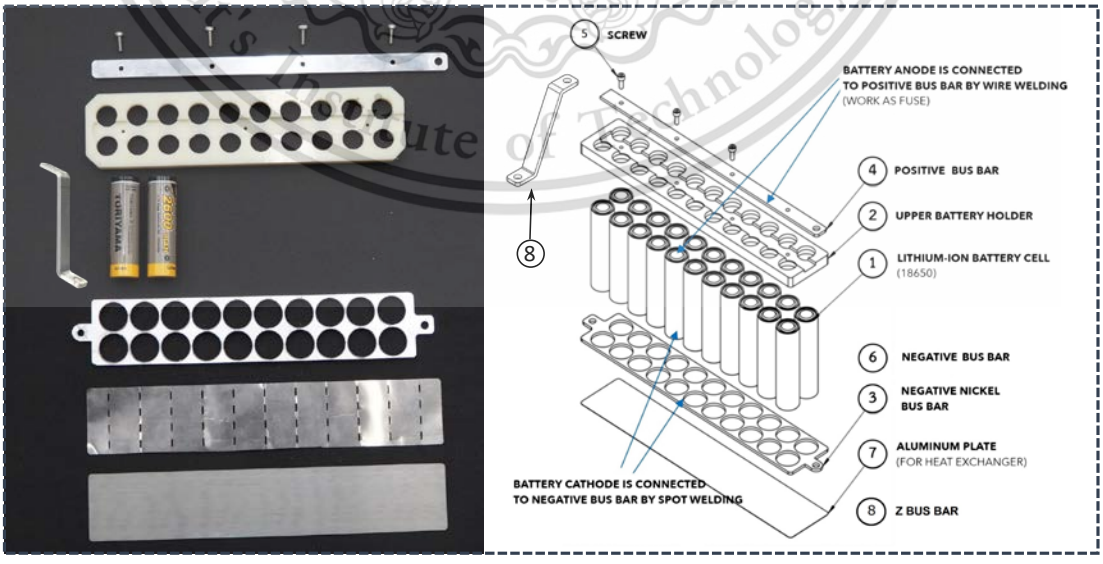

Figure 3.7 Component parts disassembled from a battery sub-module

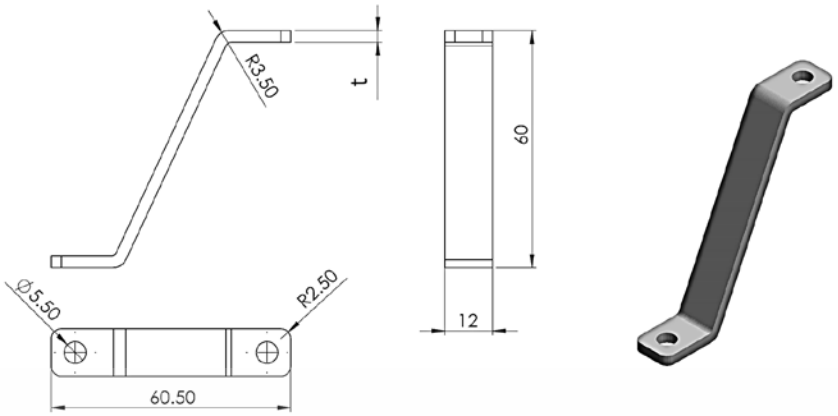

Figure 3.8 Sample of Z bar drawing by CAD model

Simulation method

All simulations in this project were carried out with FEM software as a simulation software and run on a computer using Windows 64-Bit operating system with Intel(R) Core (TM) i7-3610QM CPU @ 2.30GHz 2.30 GHz processor and 8 GB of RAM.

In Figure 3.9, regarding the limit of performance of the computer, the model of the battery pack is divided to two steps including Electrical model and Thermal model. In the first step, the electrical model can calculate current distribution inside and voltage distribution (voltage drop) of each element of the work-pieces when the current flows from the inlet terminal to the outlet terminal. In the second step, both current and voltage distribution from the first step are used to calculate the heat generation from Ohmic lose ($Q = U \cdot V, Q = I^2 \cdot R$). This heat generation, heat convection around the Z bar as well as ambient temperature and initial temperature are set up in the thermal model to calculate the temperature of the Z bar which depends on electric current and time. This method is also used to study the different thicknesses and materials of the Z bar.

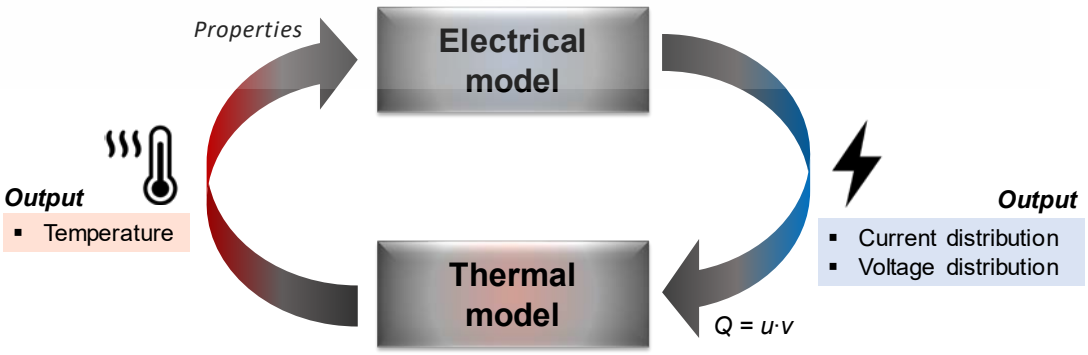

Figure 3.9 Simulation running steps

Simulation Setup

- **Geometry import**

The 3D geometries were created from SolidWorks. The CAD files in (.SAT) file type which is recommended from FEM software was imported in a union form.

- **Material setting**

Copper [solid Copper] and Aluminium [solid Aluminium] from FEM software's material are used**.** and the properties is presented in Table 3.2.

Table 3.2 Material properties of Z bar.

Property	Property	Unit	Copper	Aluminium
Electrical	Resistivity at 20°C	$\Omega \cdot mm^2 / m$	0.02	0.03
	Electrical conductivity at 20°C	$m / \Omega \cdot mm^2$	57.10	35.40
	Electrical conductivity	(%IACS Volume Basis)	103.10	64.90
	Electrical conductivity	(%IACS Weight Basis)	102.60	213.70
Thermal	Thermal conductivity	W / m°C	393.00	203.00
	Specific heat	W·sec / kg·°C	385.00	920.00
	Melting point	°C	1084.00	658.00
	Boiling point	°C	2595.00	2060.00
Mechanical	Specific weight	kg / m^3	8900.00	2700.00
	Tensile strength	kgf / mm^2	24.00	10.00
	Elastic limit	kgf / mm^2	6 – 8	2 – 5

- **Physics setting and boundary conditions**

Electromagnetic module for FEM program is used in the simulation. The Electromagnetic Heating branch includes the Joule Heating interface using boundary conditions as shown in Table 3.3.

The Joule Heating Multiphysics interface is used to model resistive heating and, dielectric heating in devices where inductive effects are negligible. This Multiphysics interface adds an Electric Currents interface and a Heat Transfer in Solids interface. The Multiphysics couplings add the electromagnetic power dissipation as a heat source.

The Electric Currents interface computes electric field, current, and potential distributions by setting cross-sectional area and ground area as shown in Figure 3.10. Time-domain and frequency-domain formulations are also provided. The Electric

Currents interface solves a current conservation equation based on Ohm's law using the scalar electric potential as the dependent variable.

The Heat Transfer in Solids interface provides features for modelling heat transfer by conduction, convection, and radiation. The temperature equation defined in solid domains corresponds to the differential form of the Fourier's law that may contain additional contributions like heat sources. For temperature measurement, this study uses the technique of Domain Point Probe to measure the temperature distribution for three points; top area, middle area and bottom area as shown in Figure 3.6. In addition, the temperature distribution is calculated by two conditions for validation; (1) including air domain and (2) including air domain and copper cable heat loss (see in Figure 3.11). The electrical conductivity for simulation can be calculated from the relationship between voltage drop and electric current in the experiment.

Table 3.3 Boundary conditions for Z bar simulation

Boundary Conditions	**Thickness**		
	2 mm	3 mm	4 mm
Normal Current Density (Jn) @ 1C	57.2/154.12 [A] [mm^2]	57.2/161.74 [A][mm^2]	57.2/169.39 [A] [mm^2]
Normal Current Density (Jn) @ 0.75C	42.9/154.12 [A] [mm^2]	42.9/161.74 [A] [mm^2]	42.9/169.39 [A] [mm^2]
Normal Current Density (Jn) @ 0.5C	28.6/154.12 [A] [mm^2]	28.6/161.74 [A] [mm^2]	28.6/169.39 [A] [mm^2]
Normal Current Density (Jn) @ 0.25C	14.3/154.12 [A] [mm^2]	14.3/161.74 [A] [mm^2]	14.3/169.39 [A] [mm^2]
Initial Value: Temperature		40°C	
Heat Flux: Heat Transfer Coefficient (h)		10 $W/m^2 \cdot K$	
Heat Flux: External Temperature		40°C	

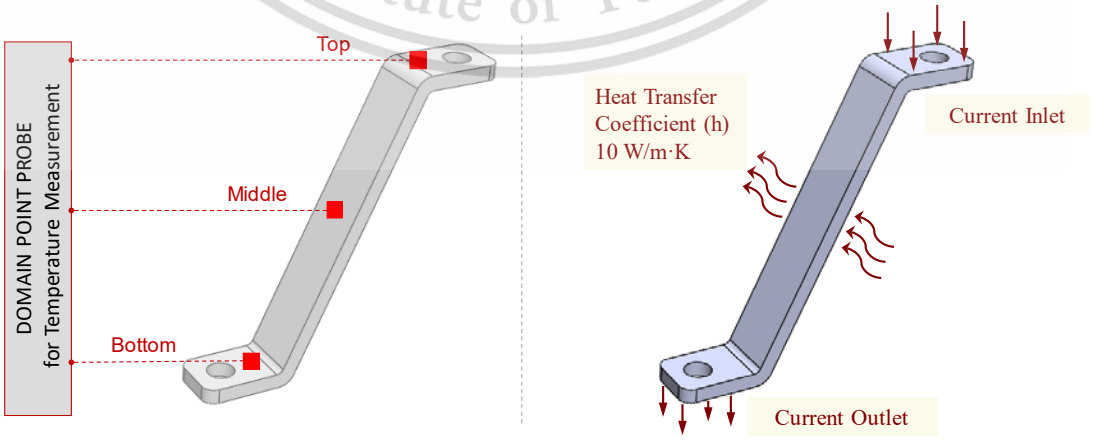

Figure 3.10 Temperature measurement points current inlet and outlet

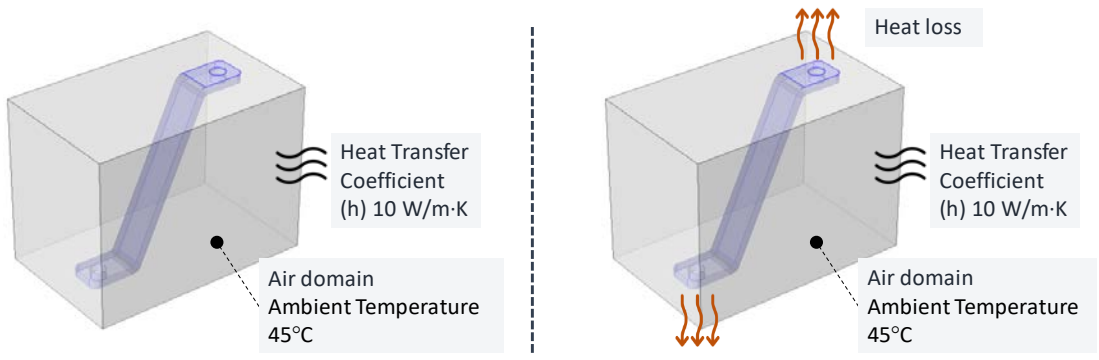

Case study 1 : Computation with air domain

Case study 2 : Computation with air domain and copper cable heat loss

Figure 3.11 Two computation conditions for validation

- **Mesh setting**

To generate mesh using automation function of the software as shown in Figure 3.12. It can be seen that mesh at the bending area is finer than other zones. The complete mesh of the Z bar model consists of 3801 elements, 1782 boundary elements, and 337 edge elements. For other component parts, the number of elements depends on geometry complexity.

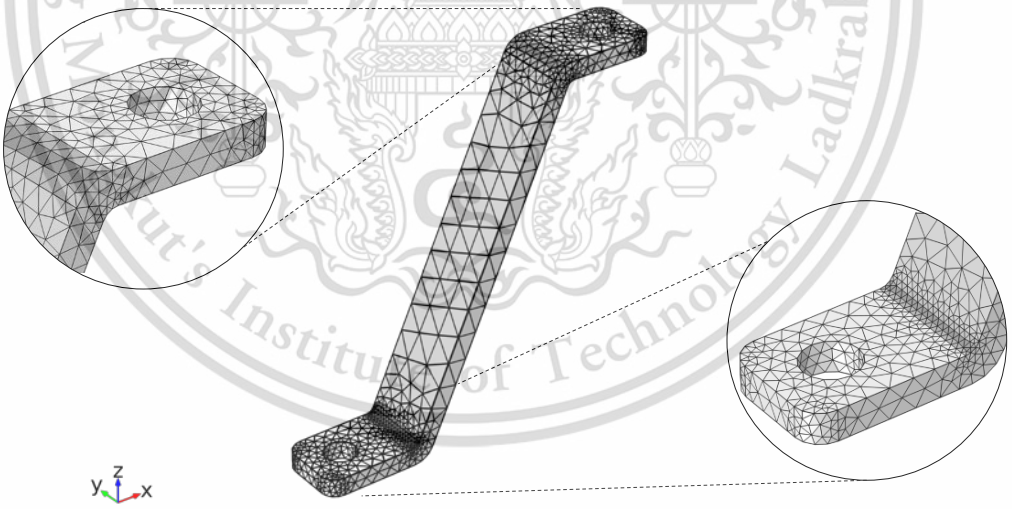

Figure 3.12 Mesh setting of Z bar

- **Solver setting**

The Time Dependent study is used when field variables change over time. In electromagnetics module, it is used to compute transient electromagnetic fields, including electromagnetic wave propagation in the time domain. In heat transfer, it is used to compute temperature changes over time.

3.1.2.3 Experiment and simulation results

This experiment uses a Z bar which is made of Aluminium and Copper for studying its behaviour. For instance, regarding the experiment, the temperature changes under current loads 70 A and 100 A from the initial temperature 25°C for an Aluminium and Copper Z bar with identical thickness (3 mm) as shown in

Figure 3.13. It can be seen that the temperature of both material substantial rises at the beginning and then remains stable. However, the temperature of the Copper Z bar is lower than Aluminium Z bar because of higher electrical and thermal conductivity properties which substantiate with the theory.

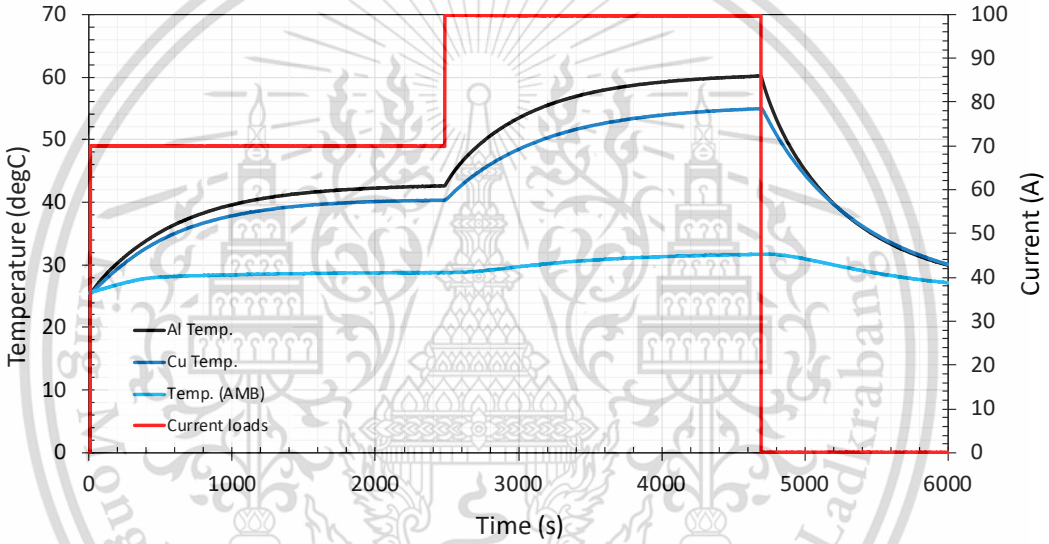

Figure 3.13 Comparison of temperature changes under current loads 70 A and 100 A between an Aluminium and Copper

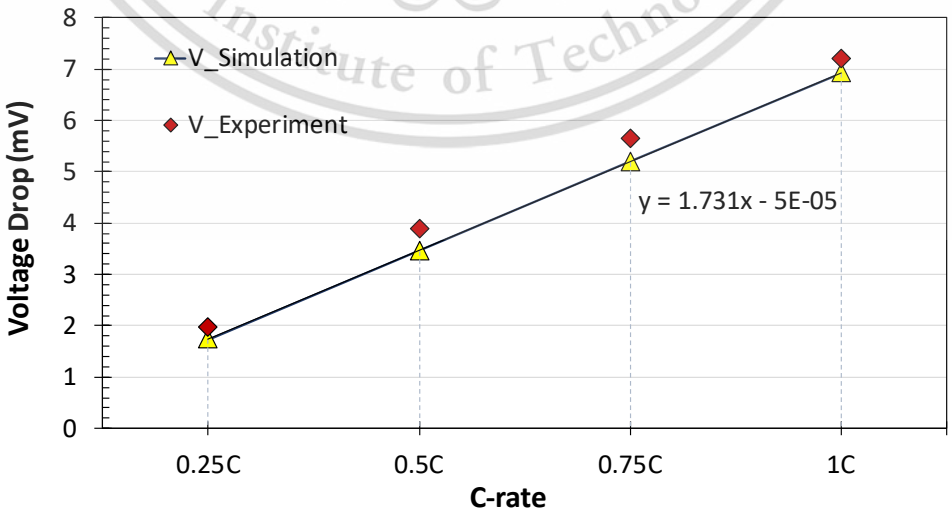

Figure 3.14 Relationship between voltage drop and C-rate of the simulation comparing with the experiment

Figure 3.14 presents the relationship between the voltage drop and the electric current of the model plotted as a line and the experiment result plotted as points. The slope represents an electric resistance. The electrical conductivity can be calculated from the slope of electric resistance from the plot, cross section and length of the specimen in order to be input into the simulation as a boundary condition. The slope was fitted with a least square to calculate the electric resistance. Form linear question $y = a + bx$, b is the electrical resistance of the specimen.

$$\begin{bmatrix} n & \sum x \\ \sum x & \sum x^2 \end{bmatrix} \begin{Bmatrix} a \\ b \end{Bmatrix} = \begin{bmatrix} \sum y \\ \sum xy \end{bmatrix} \tag{3.1}$$

Table 3.4 Data generated from the relationship between voltage drop (y) and electric current (x) of the model at 45°C

	x	**y**	**x^2**	**xy**
1	14.30	0.0020	204.49	0.028041
2	28.60	0.0039	817.96	0.110985
3	42.90	0.0056	1840.41	0.241866
4	57.20	0.0072	3271.84	0.411840
∑	143.00	0.0187	6134.70	0.792700

Where a = 0.3012 and b = 1.7475, the electric resistance of the specimen is 0.0001281 Ω.

Equation (3.2, the electrical conductivity was calculated from this equation.

$$\sigma = \frac{1}{\rho} = \frac{L}{AR} \tag{3.2}$$

Where L = 0.07948 m, A = 0.000036 m^2, R_{Al}= 12.81×10^{-5} Ω and R_{Cu} = 5.42×10^{-5} Ω

$$\sigma_{Al} = \frac{1}{\rho} = \frac{0.07948}{(0.000036)(0.0001281)} = 1.87 \times 10^7 \frac{S}{m} \tag{3.3}$$

$$\sigma_{Cu} = \frac{1}{\rho} = \frac{0.07948}{(0.000036)(0.0000542)} = 4.07 \times 10^7 \frac{S}{m} \tag{3.4}$$

Thus, the electrical conductivity of Aluminium for Z bar is 1.87×10^7 S/m.

And the electrical conductivity of Copper for Z bar is 4.07×10^7 S/m.

Figure 3.15 shows a comparison of experiment and simulation results in temperature changes under different current loads including air domain as a case study 1. Looking at the figure in greater detail, the temperature of simulation is higher than that of the experiment. The reason is that there is heat loss occurred during an experiment between Z bar and copper cable. Hence, copper heat loss need to be added in the simulation to obtain an accurate result as a case study 2. According to the high thermal conductivity of Aluminium and Copper, the temperature distribution on Z bar is quite difficult to observe because heat can easily distribute and transfer between their materials or between the Z bar and the air. Therefore, the simulation is used for observing those behaviour of Z bar materials in this study that its results can explain several behaviours that cannot be investigated by an experiment such as the electric current direction as shown in Figure 3.17 for example.

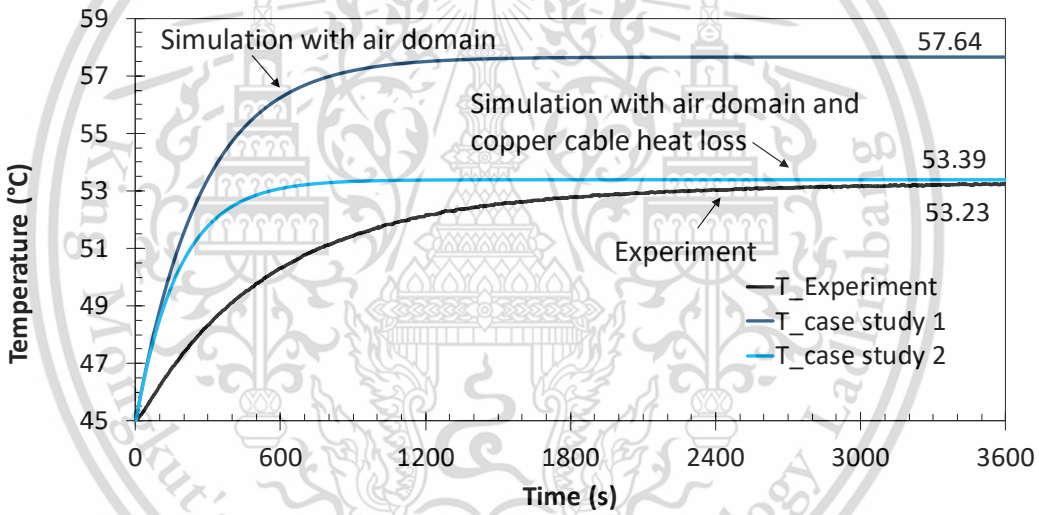

Figure 3.15 Comparison of temperature changes under different current loads between experiments and simulations

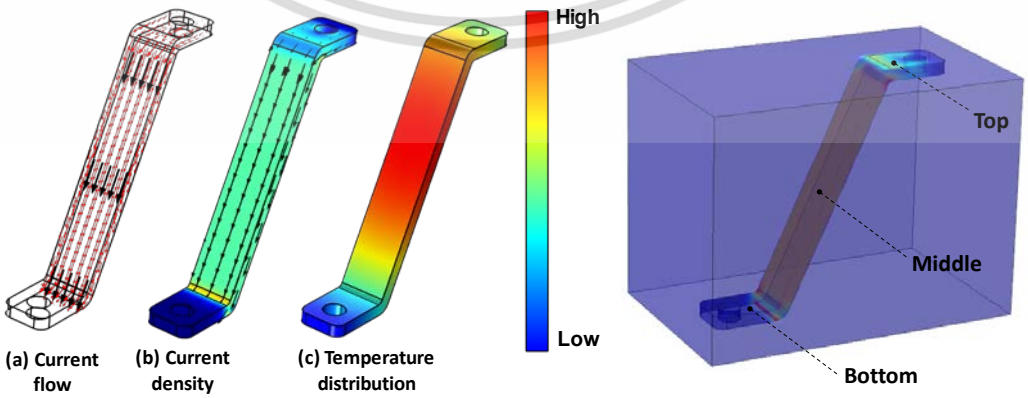

Figure 3.16 Electrical behaviour of Z bar

3.1.3 Manufacturing method

Regarding the manufacturing method of Z bar, the possible alternatives are Laser cutting process (Laser CNC) and bending process or only the punching process. According to the gathered information from manufacturers, only the pouching process is a faster technique compared to Laser cutting process and bending process. In contrast, cost of the punching process is very high due to mold cost. However, the punching process will be cheaper than the Laser cutting process and bending process for high volume production as shown in Table 3.5.

Table 3.5 Production cost of Z Bar

Material	Thickness (mm)	Production Technique	Price per piece (THB)	
			Lot size = 640 pcs	Lot size = 6400 pcs
Aluminium	2	Laser Cutting and Bending	83.67	83.56
Aluminium	3	Laser Cutting and Bending	94.92	94.80
Aluminium	4	Laser Cutting and Bending	116.19	116.03
Aluminium	2	Punching process	138.05	36.80
Aluminium	3	Punching process	155.91	40.59
Aluminium	4	Punching process	173.77	44.39
Copper	2	Laser Cutting and Bending	116.50	116.36
Copper	3	Laser Cutting and Bending	144.16	143.99
Copper	4	Laser Cutting and Bending	181.84	181.63
Copper	2	Punching process	150.84	49.59
Copper	3	Punching process	175.10	59.79
Copper	4	Punching process	199.35	69.98

From Figure 3.17, The cost of punching technique in high volume is much cheaper than that in small volume while the cost of CNC technique is unchanged by lot size. In addition, the cost appraisal of Copper is not too dissimilar to that of Aluminium. This can be concluded that CNC technique is a better choice for small lot size and punching technique is more suitable for big lot size.

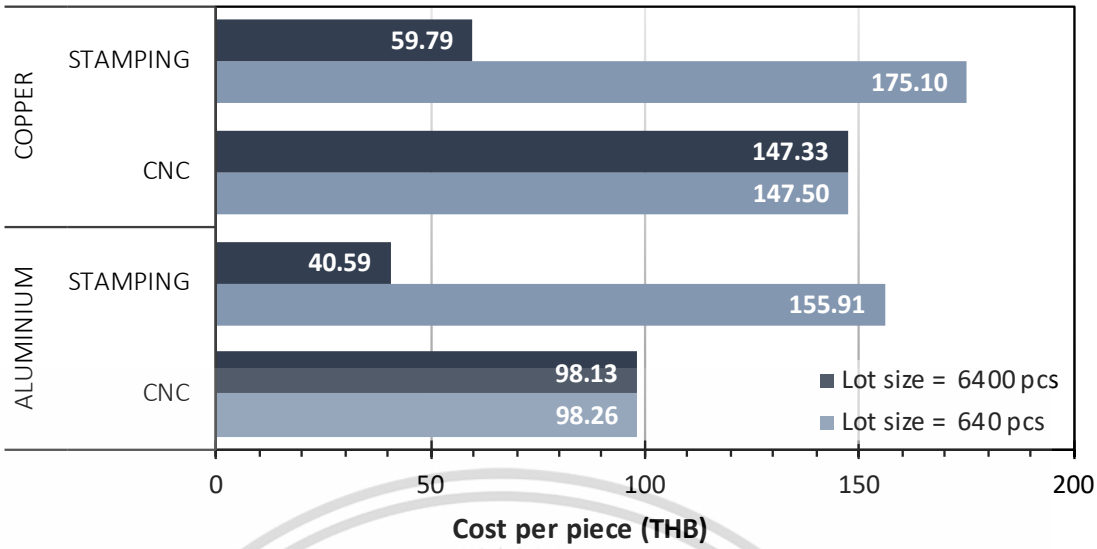

Figure 3.17 Comparison of production cost between punching and CNC technique of Copper and Aluminium Z bar

3.2 Positive Busbar

The Positive Busbar is used as electrical conductors to make a parallel connection between battery cells of battery sub-module by wire bonding welding technique as shown in Figure 3.18.

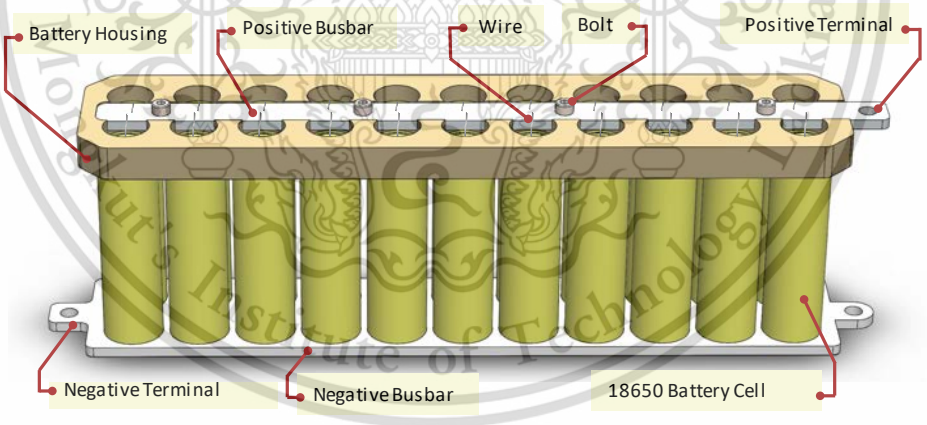

Figure 3.18 Sub-module (22 battery cells)

3.2.1 Material alternatives

Regarding the original design, Copper is only one material which is selected for producing the Positive Busbar. In this study, both Copper and Aluminium are chosen as material alternatives (see in Figure 3.19) by considering the same four aspects as Z bar.

Figure 3.19 Copper and Aluminium positive busbar in top view

3.2.2 Designing Positive Busbar

In term of design, the designing process of a Positive Busbar is not too dissimilar to that of the Z bar. The thickness is optimized by simulation software after validation with the real experiment of three-millimetre Positive Busbar.

3.2.2.1 Experiment setup

The experiment setup of Positive Busbar is different from Z bar experiment because there are 22 current input points instead of one point like Z bar. Therefore, the experiment setup must use the real sub-module battery in order that the electricity can be drawn from 22 battery cells. This experiment study material behaviours of Positive Busbar in the sub-module battery during discharging under an ambient temperature of 45°C as shown in Figure 3.20. In addition, the thermal camera is used for studying temperature distribution of this Positive Busbar. Before the Positive Busbar is observed by the thermal camera, it must be painted by black colour to reduce the reflection of materials. Moreover, three temperature sensors are also installed on the Positive Busbar in order to use them as reference temperatures for calibrating the temperatures from the thermal camera (see in Figure 3.21).

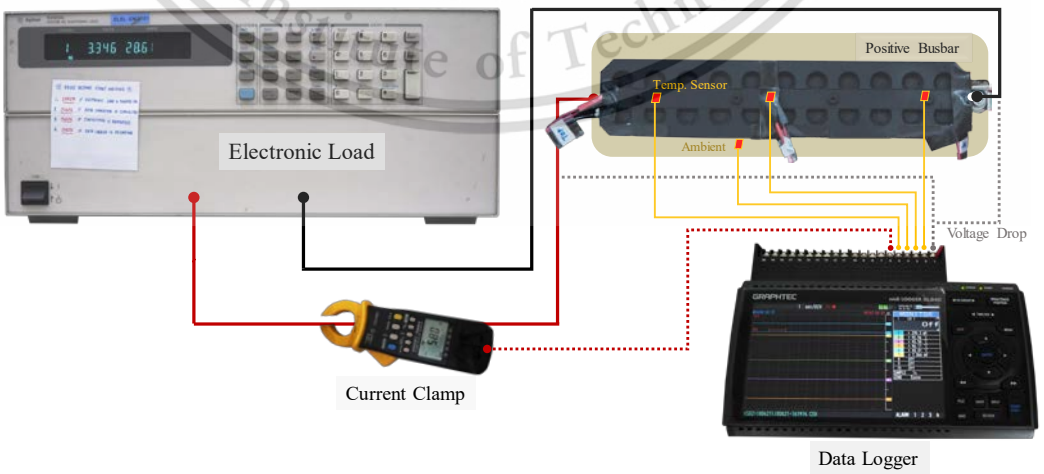

Figure 3.20 Experiment setup for validation measurement of Positive Busbar

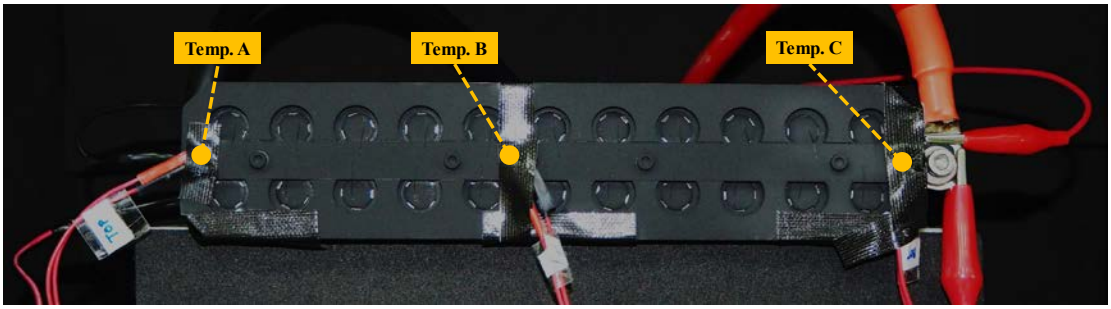

Figure 3.21 Temperature sensor positions for Positive Busbar

Table 3.6 shows the boundary conditions for the experiment including the range of current loads, interesting outputs and ambient temperature.

Table 3.6 Boundary conditions for the experiment

Boundary conditions	
Current loads	28.6 A (0.5C)
Output	Voltage drop (V)
	Electrical Resistance (Ω)
	Temperature changes (°C)
Ambient temperature	45°C
Discharging time	3600 Sec.

3.2.2.2 Simulation

CAD Modelling

In order to create the 3D geometry for simulations, the Positive Busbar has been disassembled from a sub-module battery and the dimensions of component parts were measured to create a 3D model part in SolidWorks program as illustrated in Figure 3.22.

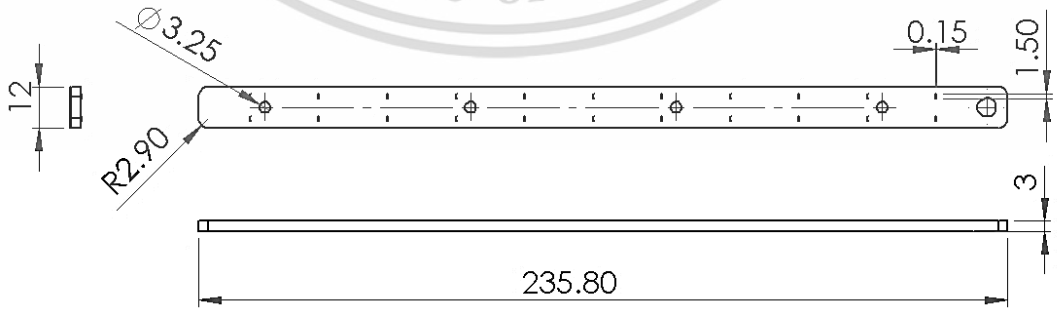

Figure 3.22 Sample of Positive Busbar drawing by CAD model

Simulation Setup

- **Geometry import**

The 3D geometries were created and exported from SolidWorks. The CAD files in (.SAT) file type which is recommend from the FEM software was imported in a union form.

- **Material setting**

Copper [solid Copper] and Aluminium [solid Aluminium] from FEM software's material are applied and modified some material properties using data from an experiment such as electrical conductivity and density to ensure that they are as accurate as the exact values from the real materials.

- **Physics setting and boundary conditions**

Electromagnetic modules for FEM program are also used in the simulation. The Electromagnetic Heating branch includes the Joule Heating interface using boundary conditions as shown in Table 3.7. The current inlet area and current outlet area are set as shown in Figure 3.23. For temperature measurement, this study uses the technique of Domain Point Probe to measure the temperature for three points; point (A), point (B) and point (C), middle area and bottom area as shown in Figure 3.24.

Table 3.7 Boundary conditions for Positive Busbar simulation

Boundary Conditions	**Thickness**		
	2 mm	3 mm	4 mm
Normal Current Density (Jn) @ 1C	57.2/5.06 [A] [mm^2]	57.2/5.06 [A] [mm^2]	57.2/5.06 [A] [mm^2]
Normal Current Density (Jn) @ 0.75C	42.9/5.06 [A] [mm^2]	42.9/5.06 [A] [mm^2]	42.9/5.06 [A] [mm^2]
Normal Current Density (Jn) @ 0.5C	28.6/ 5.06 [A] [mm^2]	28.6/5.06 [A] [mm^2]	28.6/5.06 [A] [mm^2]
Normal Current Density (Jn) @ 0.25C	14.3/5.06 [A] [mm^2]	14.3/5.06 [A] [mm^2]	14.3/5.06 [A] [mm^2]
Initial Value: Temperature	40°C		
Heat Flux: Heat Transfer Coefficient (h)	10 W/m2·K		
Heat Flux: External Temperature	40°C		
Operation Time	3600 Sec.		

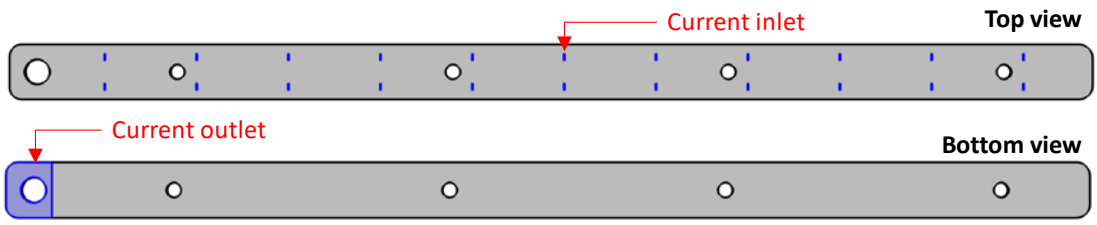

Figure 3.23 Boundary condition for current inlet and outlet

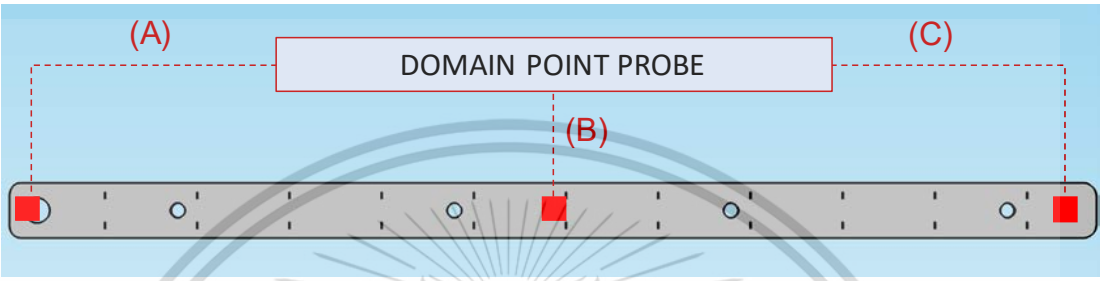

Figure 3.24 Three domain point probes for temperature measurement

- **Mesh setting**

To generate mesh as shown in Figure 3.25. It can be seen that mesh at the wire fuse contact areas is finer than other zones. The total mesh of the Positive Busbar model consists of 64222 elements, 12644 boundary elements, and 1512 edge elements.

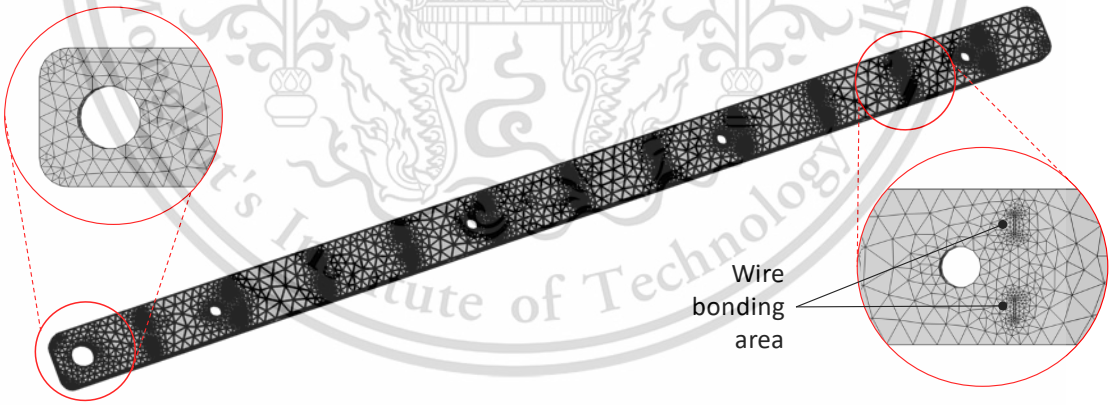

Figure 3.25 Mesh setting of Positive Busbar

- **Solver setting**

The Time Dependent study is also used to compute temperature changes over time same as a solver setting of Z bar.

3.2.2.3 Experiment and simulation results

This experiment uses three-millimetre-thickness Positive Busbar which is made of Aluminium for studying its behaviour. For instance, the temperature distribution under current load 0.5C (28.6 A) which separately flows form 22 the wire fuse contact areas, is captured by the thermal camera. It can be seen that the temperature slightly increased from the left area to the positive terminal (right area) as shown in Figure 3.26.

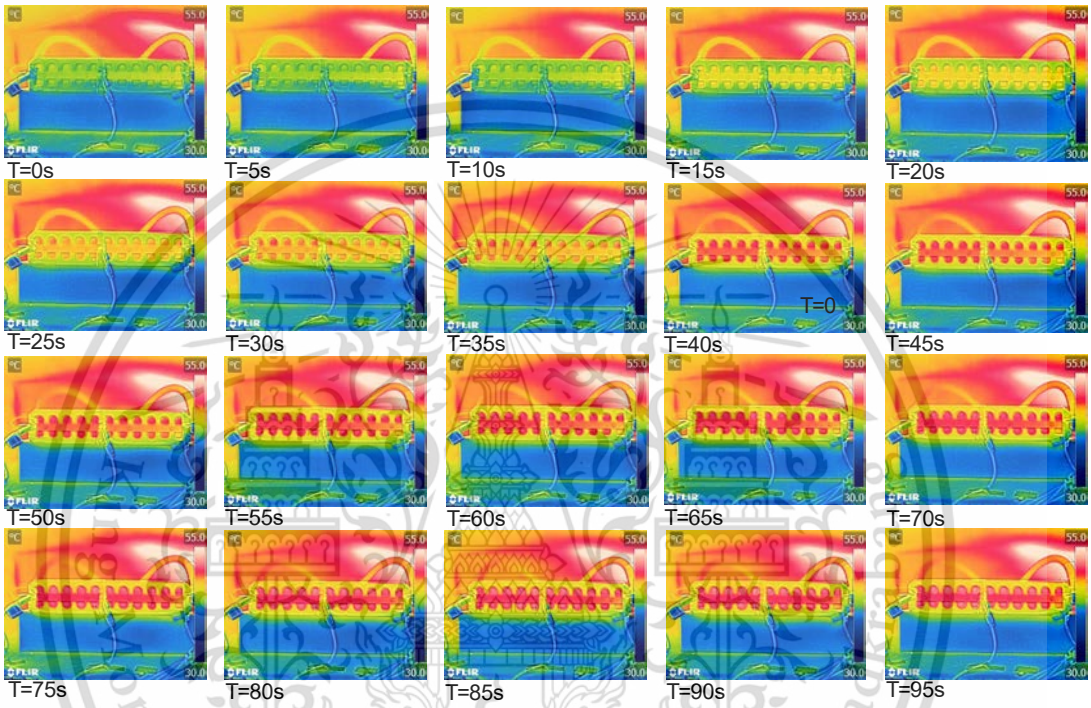

Figure 3.26 Temperature changes under current load (28.6 A) of Positive Busbar

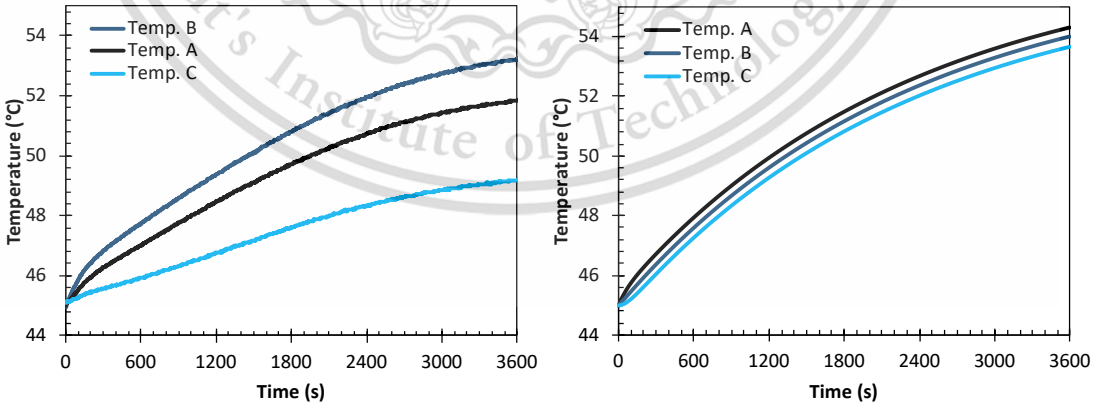

(a) Temperature changes under current load 0.5C of 3 points by *experiment*

(b) Temperature changes under current load 0.5C of 3 points by *simulation*

Figure 3.27 Comparison of temperature changes under current loads between an experiment and simulation of three domain points

Figure 3.27 shows a comparison between an experiment and simulation result in the trend of temperature changes under current load 0.5C in three different temperature measuring points. For simulation result, according to high current density in positive terminal area (A), the temperature of this area becomes the highest, whereas the lowest temperature area is an inside area (C) where density is the lowest. In contrast, for the experiment result, the highest temperature is the middle area (B) because of copper cable heat loss in positive terminal area (A) conducting heat from the part to copper cable. The temperature distribution captured by the thermal camera agrees well with the above explanation that the temperature in the area (A) is lower than the middle area (B) as shown in Figure 3.28.

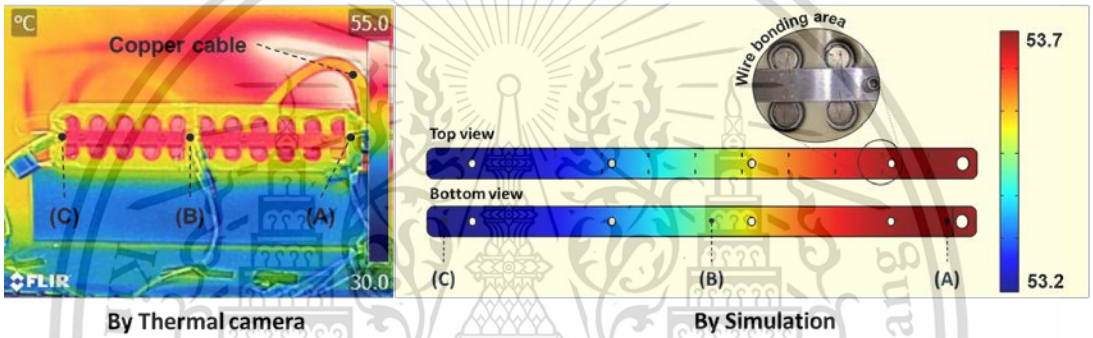

Figure 3.28 Comparison of temperature distribution between thermal camera and simulation

In addition, others behaviours of Positive Busbar materials are also observed by simulation which cannot be investigated by an experiment such as the electric current direction and current decsity as shown in Figure 3.29 and Figure 3.30 for an example.

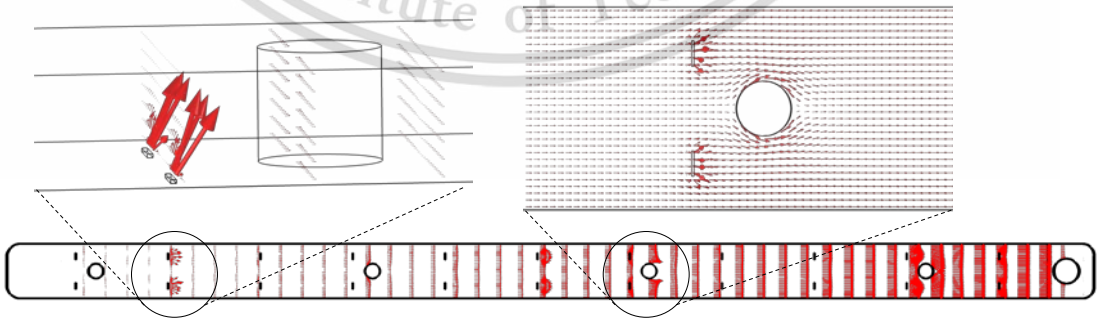

Figure 3.29 Current direction of Positive Busbar

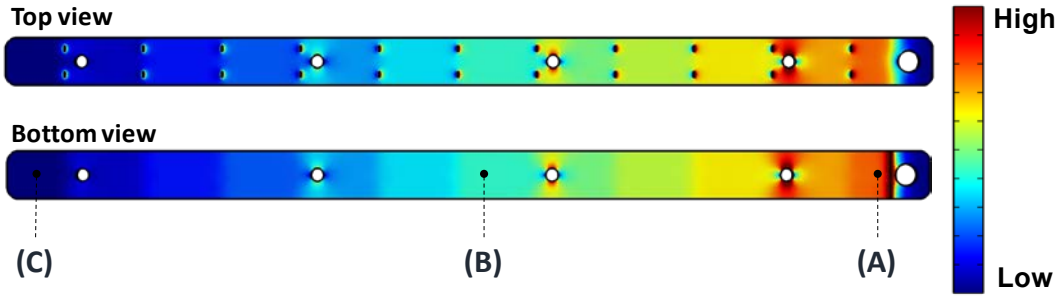

Figure 3.30 Current density of Positive Busbar

3.2.3 Manufacturing method

Regarding the manufacturing method of Positive Busbar, the possible alternatives are the same method as Z bar, but bending process is not necessary after Laser cutting process (Laser CNC) because of the flat shape of the Positive Busbar. For the punching process, it can also product the Positive Busbar; however, the holes on the Positive Busbar are very small. The drilling process may be required that is not concerned in this thesis. Therefore, the comparison of process price in this work considers Laser CNC and Punching process as shown in Table 3.8. The materials used in consideration are Aluminium and Copper.

Table 3.8 Production cost of Positive Busbar

Material	Thickness (mm)	Production Technique	Price per piece (THB)	
			Lot size = 640 pcs	Lot size = 6400 pcs
Aluminium	2	Laser CNC	134.92	99.76
Aluminium	3	Laser CNC	151.28	116.13
Aluminium	4	Laser CNC	177.65	142.49
Aluminium	2	Punching process	129.61	45.23
Aluminium	3	Punching process	140.66	52.07
Aluminium	4	Punching process	150.15	58.74
Copper	2	Laser CNC	200.89	165.73
Copper	3	Laser CNC	250.24	215.09
Copper	4	Laser CNC	309.59	274.44
Copper	2	Punching process	195.58	111.20
Copper	3	Punching process	239.62	151.02
Copper	4	Punching process	282.09	190.69

From Figure 3.31, in term of order quantity, the total cost of high volume (6400 pcs) is much cheaper than that of small volume (640 pcs) in both of CNC technique and

punching technique. In term of the manufacturing method, punching is the cheapest technique for producing a Positive Busbar in both lot size. As far as material is concerned, the total price of Aluminium Positive Busbar is greater than that of Copper especially in punching method.

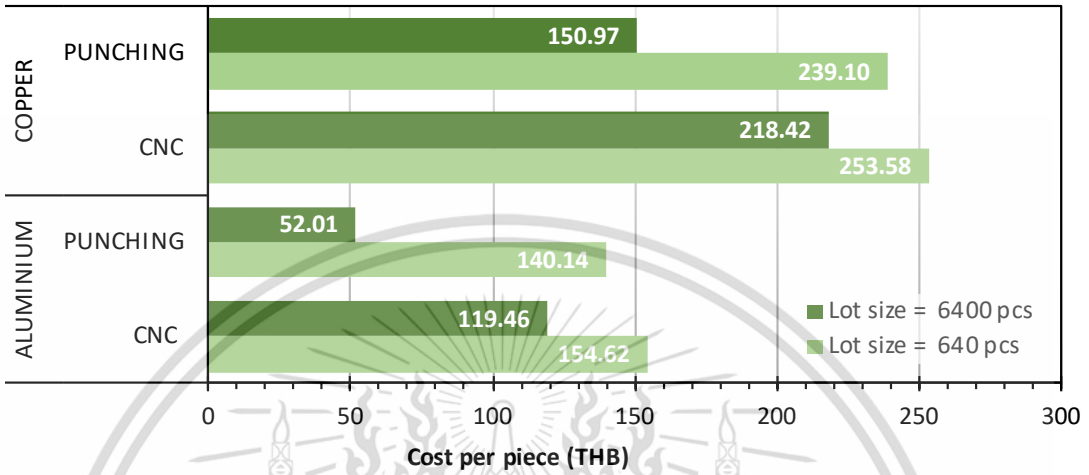

Figure 3.31 Comparison of production cost between punching and Laser CNC technique of Copper and Aluminium Positive Busbar

3.3 Negative Busbar

The Negative Busbar is used as battery lower holder and electrical conductors for negative terminals to make the parallel connection between battery cells of battery sub-modules in order to increase electrical capacity from 2.6 Ah to 57.2 Ah. The Negative Busbar is composed of the lower battery holder and Nickel plate attached with the bottom of battery cells by spot welding as shown in Figure 3.33.

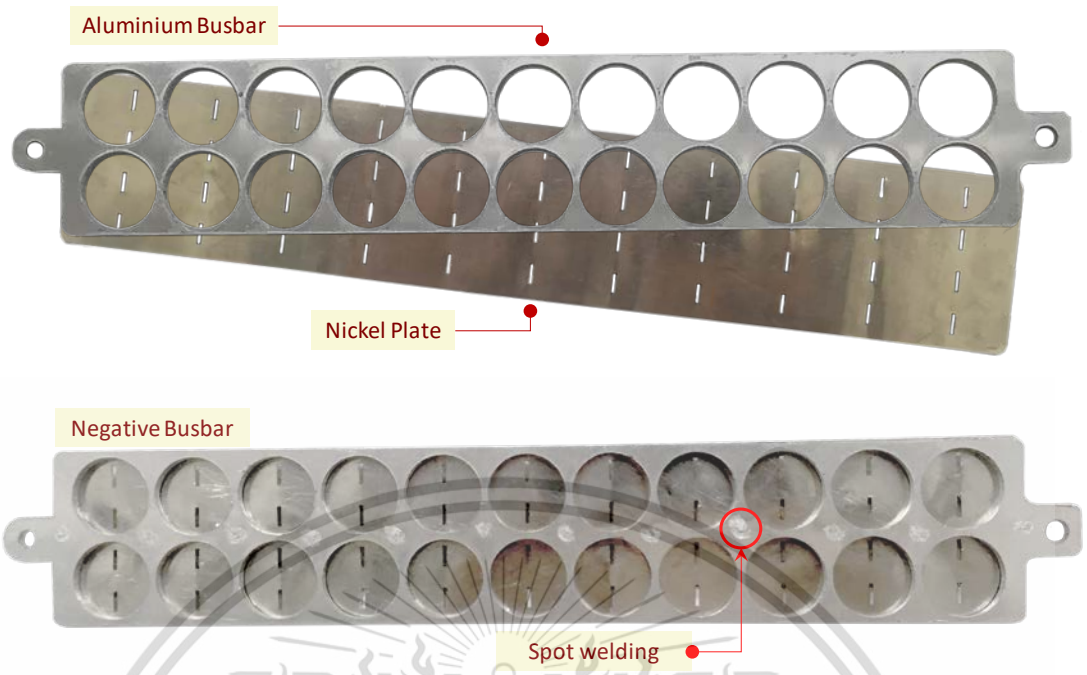

Figure 3.32 Negative Busbar

3.3.1 Material alternatives

Regarding to the negative terminal of the battery cell is Nickel based material which has to be attached with Negative Busbar. In this case, the compatibility issue is the main parameters that need to be considered. Consequently, Nickel is the best optional material for producing Negative Busbar. However, nickel cost is very high and nickel processing is quite difficult. In order to reduce production cost, this research study alternative materials that have a familiar property with nickel which are copper and aluminium.

3.3.2 Designing Negative Busbar

This research designs to use 2 components for producing Negative Busbar and nickel plate is fixed material for the first component. Copper and aluminium are chosen as the optional material for the the second component. Therefore, this research uses the selection criteria for second component of negative busbar same as Positive Busbar and Z bar.

3.3.2.1 Experiment setup

The negative busbar uses the same experimental setup as a Positive Busbar which has the objective to study material behaviours during discharging under an external

temperature 45°C as shown in Figure 3.33. A Thermal camera is also used for investigating temperature distribution behaviour of this negative busbar and three temperature sensors are also installed on the negative busbar in order to use them as reference temperatures for calibrating the temperatures from the thermal camera (see in Figure 3.34). The surface of the negative busbar is also it must be painted by black colour to reduce the reflection of materials before observation by the thermal camera.

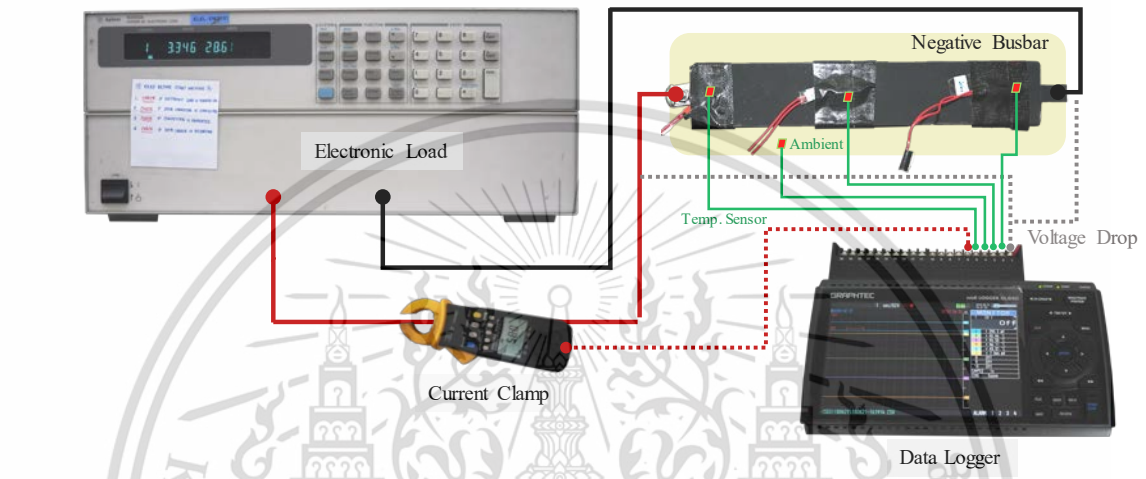

Figure 3.33 Experiment setup for validation measurement of the negative busbar

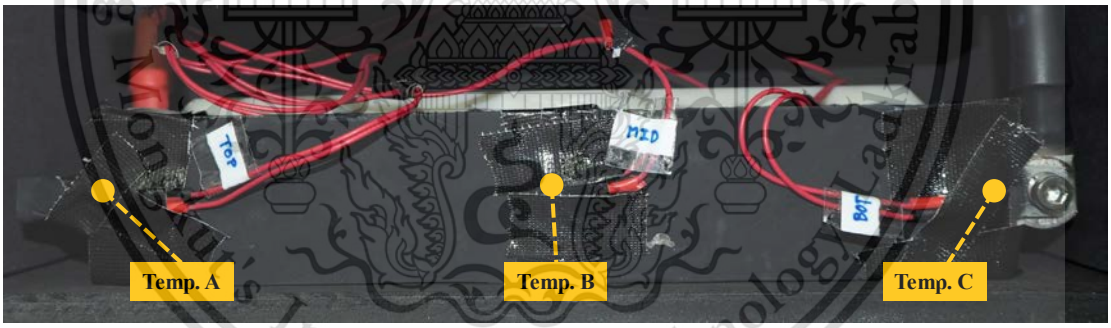

Figure 3.34 Temperature sensor positions for negative busbar

Table 3.9 shows the boundary conditions for the experiment including the range of current loads, interesting outputs and ambient temperature.

Table 3.9 Boundary conditions for the experiment

Boundary conditions	
Current loads	28.6 A (0.5C)
Output	Voltage drop (V)
	Electrical Resistance (Ω)
	Temperature changes (°C)
Ambient temperature	45°C
Discharging time	3600 Sec.

3.3.2.2 Simulation Setup

CAD modelling

In order to create the 3D geometry for simulations, the negative busbar has been disassembled and the dimensions of component parts were measured, and 3D model of each part was created in SolidWorks program as illustrated in Figure 3.35.

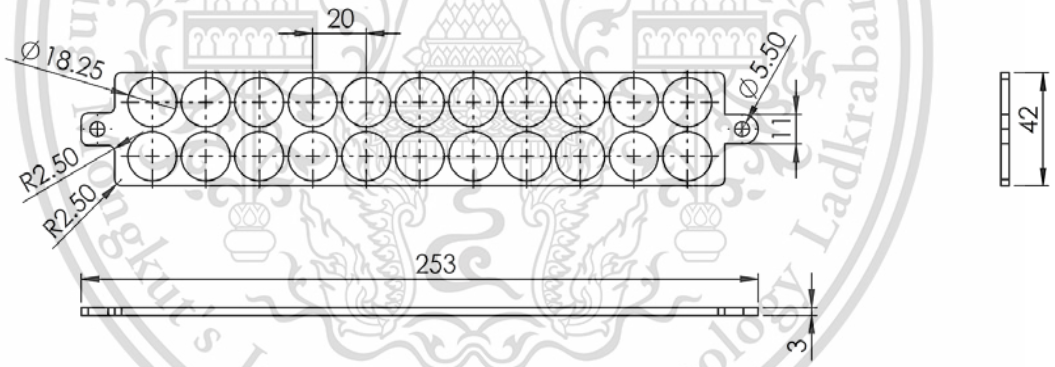

Figure 3.35 Sample of negative busbar drawing by CAD model

Simulation setting

- **Geometry import**

The 3D geometries were created from SolidWorks. The CAD files in (.SAT) file type which is recommended from FEM software was imported in a union form.

- **Material setting**

Copper [solid Copper] with Nickel and Aluminium [solid Aluminium] with Nickel from FEM software's material are applied and modified some material properties by using data from an experiment.

- **Physics setting and boundary conditions**

For negative busbar, Electromagnetic modules for FEM program is also used in the simulation by using boundary conditions as shown in Table 3.10. The current inlet area and outlet area are set as shown in Figure 3.36. For temperature measurement, this study uses the technique of Domain Point Probe to measure the temperature distribution for three points; left area, middle area and right area as shown in Figure 3.37.

Table 3.10 Boundary conditions for negative busbar simulation

Boundary Conditions	Thickness		
	2 mm	3 mm	4 mm
Normal Current Density (Jn) @ 1C	57.2/155.8 [A] [mm^2]	57.2/155.8 [A] [mm^2]	57.2/155.8 [A] [mm^2]
Normal Current Density (Jn) @ 0.75C	42.9/155.8 [A] [mm^2]	42.9/155.8 [A] [mm^2]	42.9/155.8 [A] [mm^2]
Normal Current Density (Jn) @ 0.5C	28.6/155.8 [A] [mm^2]	28.6/155.8 [A] [mm^2]	28.6/155.8 [A] [mm^2]
Normal Current Density (Jn) @ 0.25C	14.3/155.8 [A] [mm^2]	14.3/155.8 [A] [mm^2]	14.3/155.8 [A] [mm^2]
Initial Value: Temperature	40°C		
Heat Flux: Heat Transfer Coefficient (h)	10 W/m2·K		
Heat Flux: External Temperature	40°C		
Operation Time	3600 Sec.		

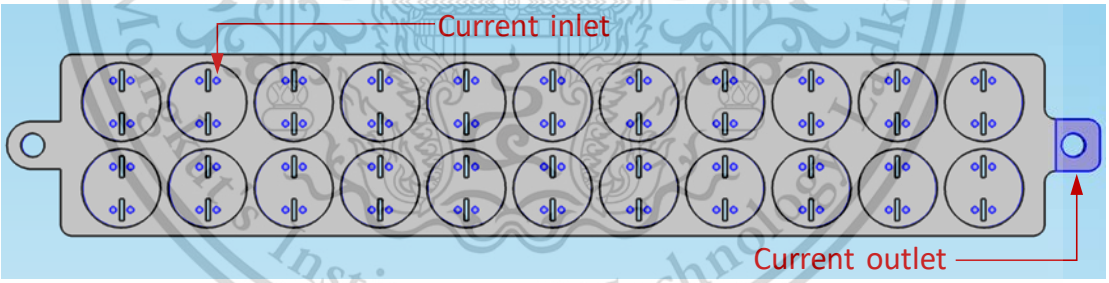

Figure 3.36 Current inlet and Current outlet of negative busbar (top view)

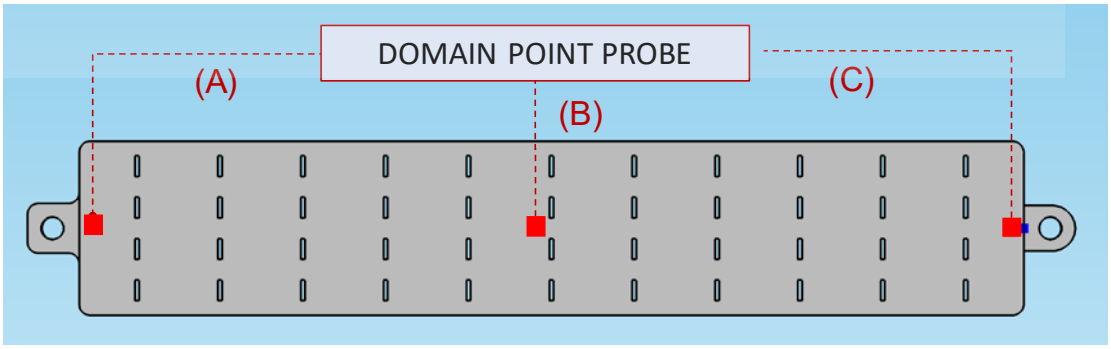

Figure 3.37 Three domain point probes for temperature measurement (bottom view)

- **Mesh setting**

To generate the mesh of negative busbar as shown in Figure 3.38. The complete mesh of the negative busbar model consists of 111179 elements, 67430 boundary elements, and 7307 edge elements.

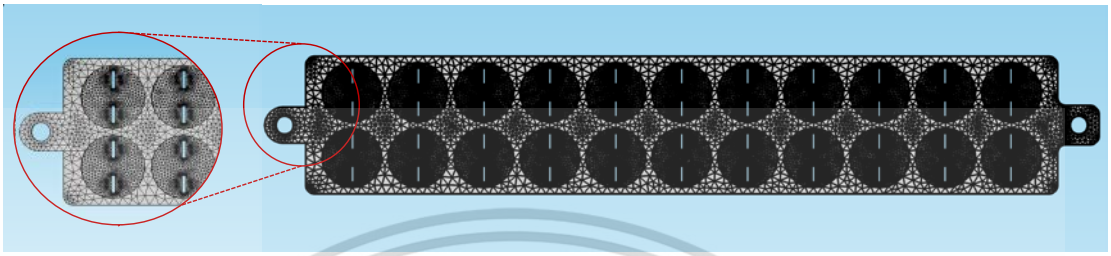

Figure 3.38 Mesh setting of negative busbar

- **Solver setting**

The Time Dependent study is also used to compute temperature changes over time as a solver setting of Z bar and Positive Busbar.

3.3.2.3 Experiment and simulation results

This experiment uses three-millimetre-aluminium negative busbar for studying its behaviour in the temperature distribution under current loads 0.5C (28.6A) captured by the thermal camera. It can be seen that the temperature slightly increased from inside area to negative terminal as shown in Figure 3.39

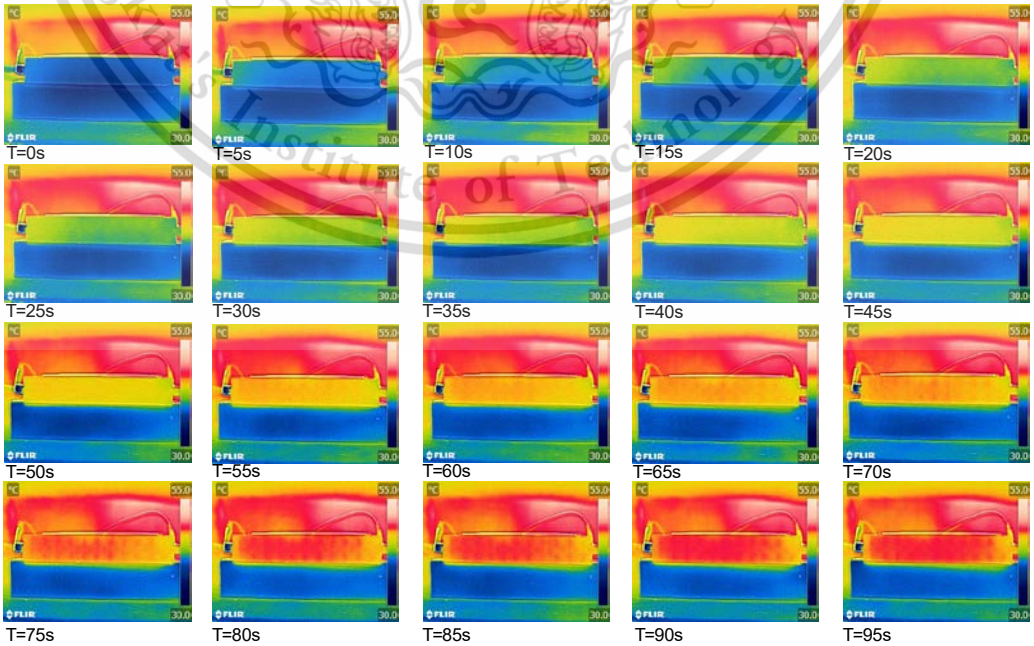

Figure 3.39 Temperature changes under current loads of negative busbar

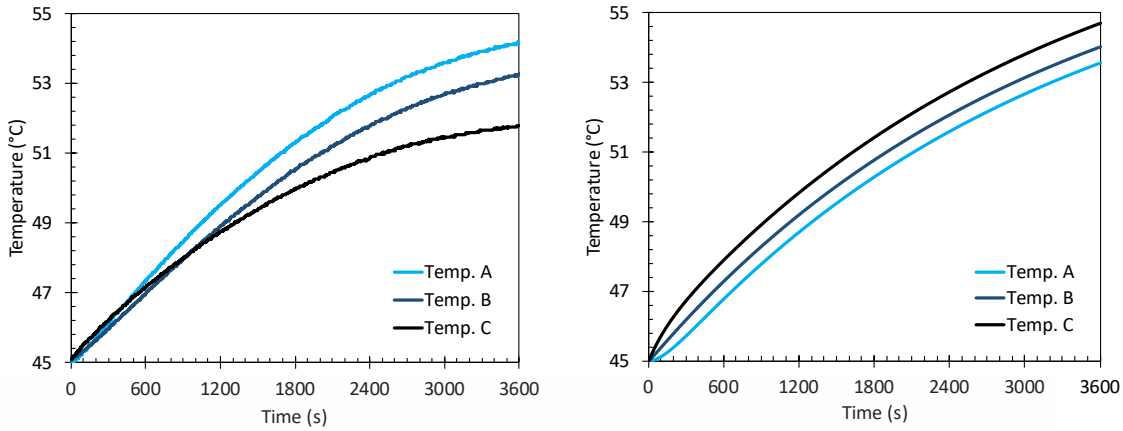

(a) Temperature Changes under current load 0.5C of 3 points by experiment

(b) Temperature Changes under current load 0.5C of 3 points by simulation

Figure 3.40 Comparison of temperature changes under current loads between an experiment and simulation of three domain points

Figure 3.40 shows a comparison between an experiment and simulation result in the trend of temperature changes under current load 0.5C in three different temperature measuring area. For simulation result, according to high current density in negative terminal (C), the temperature of this area become the highest, whereas the lowest temperature area is an inside area (A) where density is the lowest as show in Figure 3.43. In contrast, for the experiment result, the highest temperature turn out to be an area (A) because of copper cable heat loss which connected to the negative terminal area (C) conducting heat from the part to copper cable as shown in Figure 3.41. Another behaviour of negative busbar materials that is observed by simulation is the electric current direction as shown in Figure 3.42.

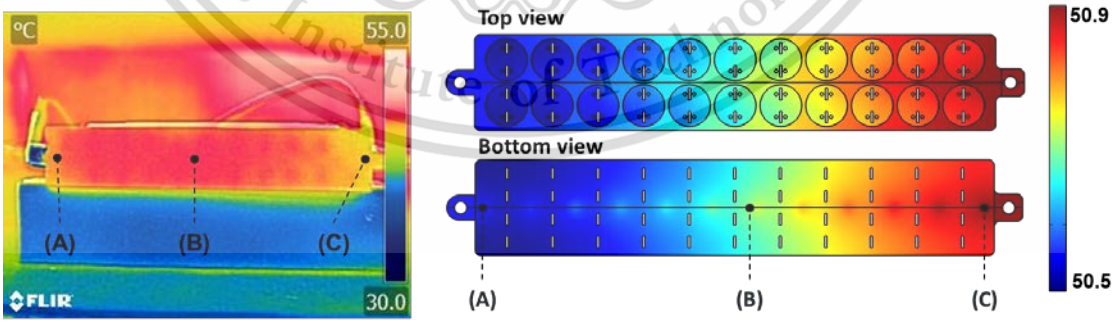

By Thermal camera

By Simulation

Figure 3.41 Comparison of temperature distribution between thermal camera and simulation

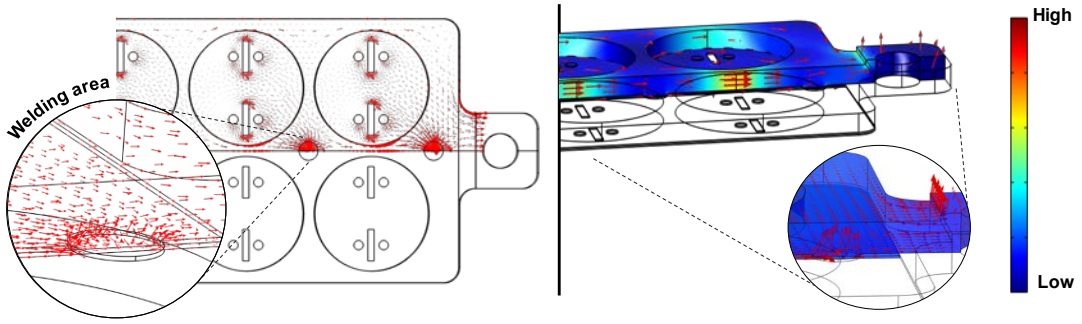

Figure 3.42 Current direction of Negative busbar

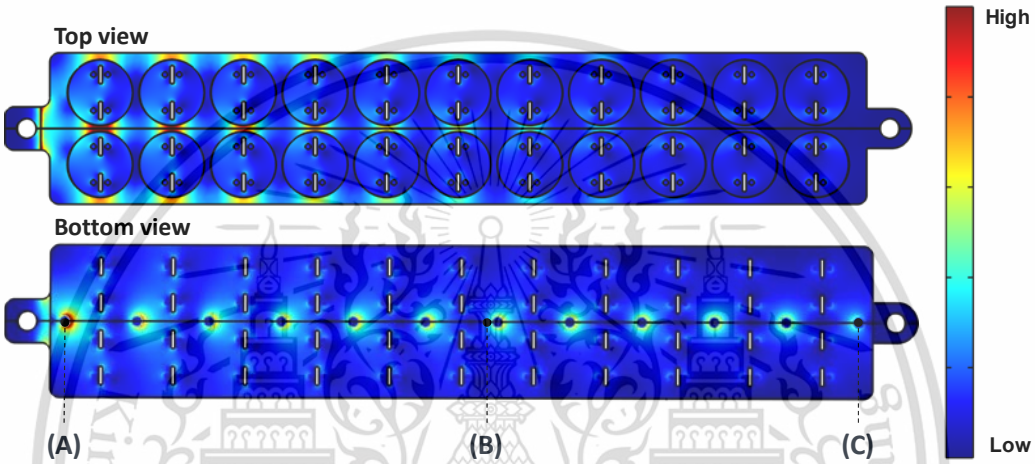

Figure 3.43 Current density of Negative busbar

3.3.3 Manufacturing method

Regarding the manufacturing method of the negative busbar, the possible alternatives are Laser cutting process (Laser CNC) plus milling process and only punching process. The production cost can vary in different manufacturing technique as shown in Table 3.11. Finally, the negative busbar will be attached with a nickel plate by welding methods.

Table 3.11 Production cost of negative busbar

Material	Thickness (mm)	Production Technique	Price per piece (THB)	
			Lot size = 6400 pcs	Lot size = 640 pcs
Aluminium	2	Laser Cutting and milling	83.56	83.67
Aluminium	3	Laser Cutting and milling	94.80	94.92
Aluminium	4	Laser Cutting and milling	116.03	116.19
Aluminium	2	Punching process	75.57	152.91
Aluminium	3	Punching process	80.51	162.07
Aluminium	4	Punching process	85.61	172.79

Material	Thickness (mm)	Production Technique	Price per piece (THB)	
			Lot size = 6400 pcs	Lot size = 640 pcs
Copper	2	Laser Cutting and milling	116.36	116.50
Copper	3	Laser Cutting and milling	143.99	144.16
Copper	4	Laser Cutting and milling	181.63	181.84
Copper	2	Punching process	111.55	188.90
Copper	3	Punching process	134.49	216.05
Copper	4	Punching process	157.58	244.76

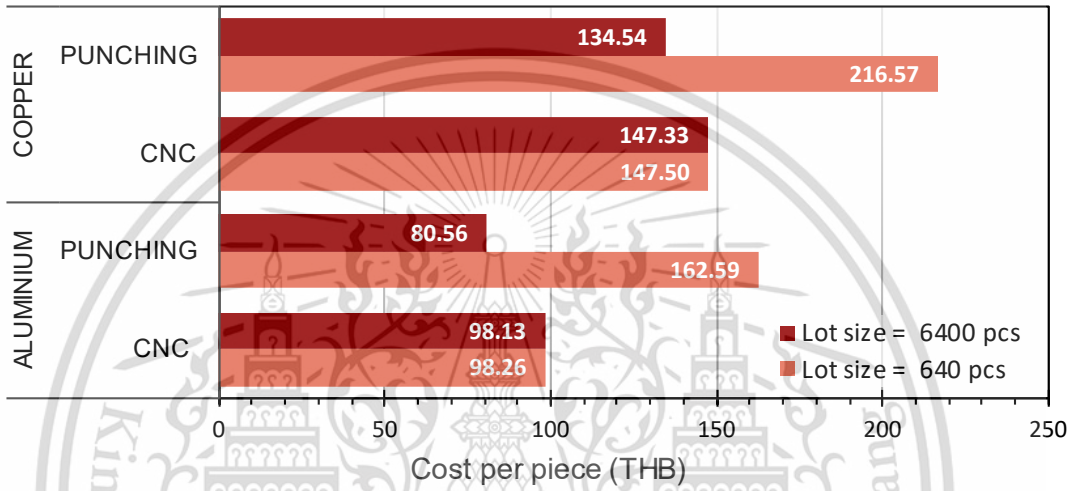

Figure 3.44 Comparison of production cost between punching and CNC technique of Copper and Aluminium negative busbar

From Figure 3.44, the information can be divided into three groups. The first group is the manufacturing method, the punching cost of 640 pcs is more than double that of 6400 pcs while the cost of laser CNC technique is exactly the same for both order volumes. The second group is order quantity, the cost of punching technique is cheaper than CNC technique in high order volume (6400 pcs). In contrast, the punching cost is much higher than the CNC cost for small volume (640 pcs). The last group is material, tern of Copper is not too dissimilar to that of Aluminium. the total price of Aluminium negative busbar is greater than that of Copper.

For lower battery holder and negative busbar, there are 2 possible optional jointing techniques which are spot welding and laser welding technique by seeing in Figure 3.45. This study selects spot welding technique for assembling lower battery holder because of cheaper cost. The spot-welding results between three different material are presented in Table 3.12

Figure 3.45 Spot welding and Laser welding technique

Table 3.12 Welding result for Negative busbar

Material	Cycle time	Voltage	Result	Cost (THB/kg)
(a) Ni+Cu	5 Sec.	6	Attached well	223.95
(b) Al+Cu	5 Sec.	8	Can bear pressure only X and Y	42.7
(c) Ni+Al	5 Sec.	8	Attached well	193.45

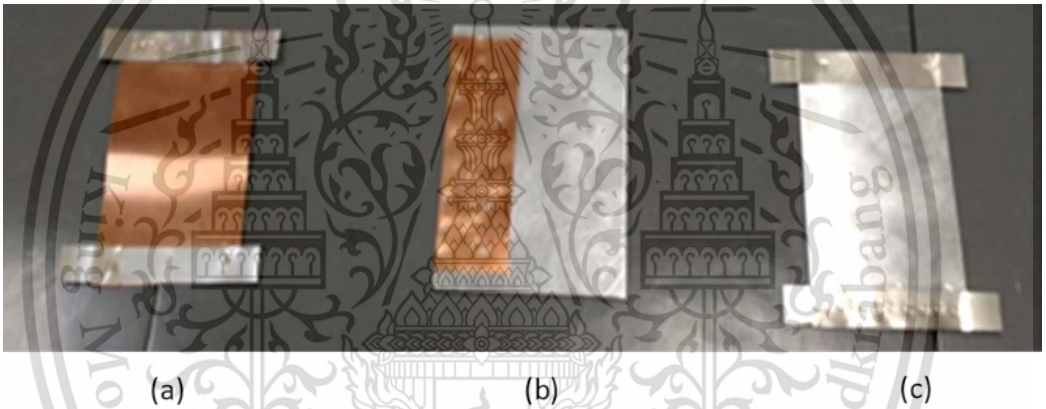

Figure 3.46 Sample result of spot welding for negative bus bar

3.4 Battery holder

The battery holder is used as an Upper Battery Holder protecting the batteries with the shape of the housing moulded as a compartment that accepts batteries in sub-module as shown in Figure 3.19. In this topic, plastic selection guide from Quadrant Engineering Plastic Products is mainly used as a guideline to study material properties of each plastic type for producing the battery holder and its production method.

3.4.1 Material alternatives

Regarding to limit resource material for battery holder prototype in Thailand, there are three possible materials which are Acrylonitrile Butadiene Styrene (ABS), Polyacetals or Polyoxymethylene (POM) and Polypropylene (PP) in this research as presented in

Table 3.13. The guideline provides the information of plastic properties that should be concerned for plastic selection. Additional information of the plastic properties from other resources is also supplied (see in Table 3.14).

Table 3.13 Information of battery holder materials (CustomPartNet, n.d.)

Material name	Abbreviation	Trade names	Description	Applications
Acetal	POM	Celcon, Delrin, Hostaform, Lucel	Strong, rigid, excellent fatigue resistance, excellent creep resistance, chemical resistance, moisture resistance, naturally opaque white, low/medium cost	Bearings, cams, gears, handles, plumbing components, rollers, rotors, slide guides, valves
Polypropylene	PP	Novolen, Appryl, Escorene	Lightweight, heat resistance, high chemical resistance, scratch resistance, natural waxy appearance, tough and stiff, low cost.	Automotive (bumpers, covers, trim), bottles, caps, crates, handles, housings
Acrylonitrile Butadiene Styrene	ABS	Cycolac, Magnum, Novodur, Terluran	Strong, flexible, low mould shrinkage (tight tolerances), chemical resistance, electroplating capability, naturally opaque, low/medium cost	Automotive (consoles, panels, trim, vents), boxes, gauges, housings, inhalors, toys

Table 3.14 Material properties of PP, POM and ABS ("Thermoplastic, Plastic" n.d.)

Property Name	Units	PP	POM	ABS
Tensile Strength, Ultimate	MPa	36.82	57.98	41.51
Density	kg/m^3	938.35	1400.60	1049.07
Deflection Temperature at 1.8 MPa (264 psi)	°C	63.89	110.00	91.67
CTE, linear 20°C	µm/m·°C	120.06	109.98	90.54
Specific Heat Capacity	J/kg·°C	2001.29	1436.07	2001.29
Water Absorption	%	0.08	0.46	0.74
Electrical Resistivity	ohm·m	4.00E+13	6.00E+12	1.70E+13
Max Service Temperature, Air	°C	85.00	110.00	86.67
Thermal Conductivity	W/m·K	1.32	3.01	1.80

3.4.2 Designing Battery holder

Regarding the design of battery holder as illustrated in Figure 3.47, the design criteria are provided following table (Table 3.15):

Table 3.15 The design criteria for battery holder

Design Criteria	Description
Toughness	In the application where the component is subjected to shock loading, toughness is an important criterion when choosing the material. Toughness refers to the amount of impact energy which the material can resist before it breaks.
Thermal expansion	In general, an increase in temperature brings about an expansion of plastic. Meanwhile plastic shrinks when temperature reduces. The coefficient of linear thermal expansion (CLTE) indicates the amount of dimensional expansion or shrinkage of the material due to temperature variation.
Thermal resistance	The maximum temperature in the battery cell is limited at 50°C by the battery design. Hence, both the heat deflection temperature value (HDT 1.8 MPa standard) and the maximum continuous service temperature value must be more than 50°C.
Material price and Material weight	Both material prices and weight of raw plastics can vary according to the different factors such as ingredients, additives, time, manufacturers, and quantities which need to be considered for selecting the battery holder material and its manufacturing technique as shown in Table 3.16.

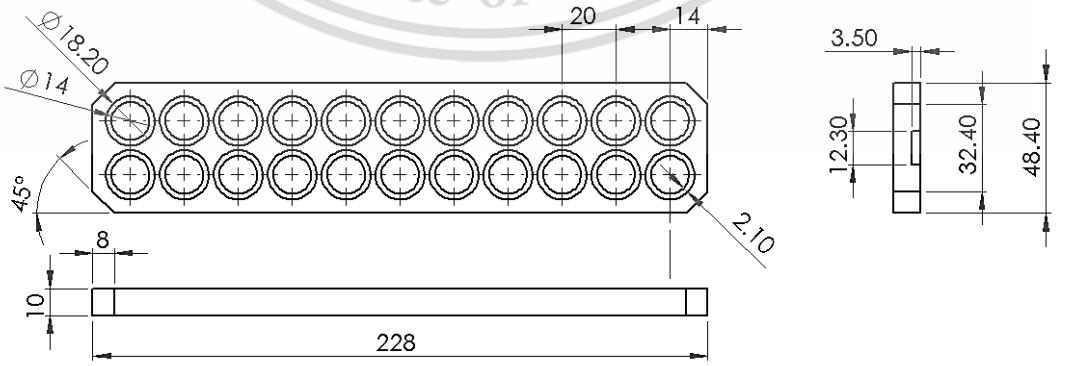

Figure 3.47 Sample of battery holder drawing by CAD model

Table 3.16 Material cost of battery holder

Name	Material	volume (Cm^3)	Density (g/Cm^3)	weight (g)	Baht/kg
Battery holder	ABS	60.83	1.05	63.87	75
	PP	60.83	0.9	54.75	48
	POM	60.83	1.41	85.77	77

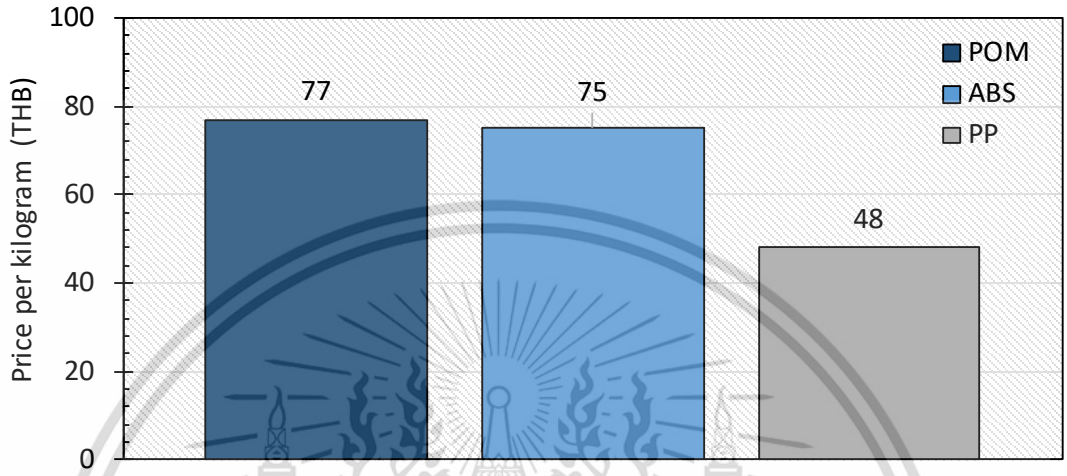

Figure 3.48 Comparison of material cost for battery holder between POM, ABS and PP

Figure 3.48 illustrates the material cost of POM, ABS and PP for the battery holder. In the same volume, POM is the most expensive material whereas the cheapest material is PP. For ABS material, the cost is just lower than that of POM about only one baht.

3.4.3 Manufacturing method

There are two possibilities to produce this battery holder. Firstly, it can be manufactured by plastic injection moulding process. Secondly, battery holder can be manufactured by machining process according to the recommendation from Quadrant EPP plastic manufacturer which is shown in Table 3.17 ("Quadrant Engineering Plastic Products: Engineering Plastics," n.d.).

The plastic injection moulding is concerned as the most popular plastic fabrication method. Plastic components with thin-walled are generally produced by this method. Complex shapes with good dimensional accuracy can be expected from the injection moulding. However, the cost of the tool and equipment is relatively high compared with the machining technique which is the proper choice for small order quantity.

Injection mould cavity in this research divide into two cavities and four cavities as displayed in Figure 3.49. The number of the cavities and mould construction depend on both economic and technical factors, the quantity of parts to be moulded at one cycle, required cycle time, and unit price are related with mould making cost.

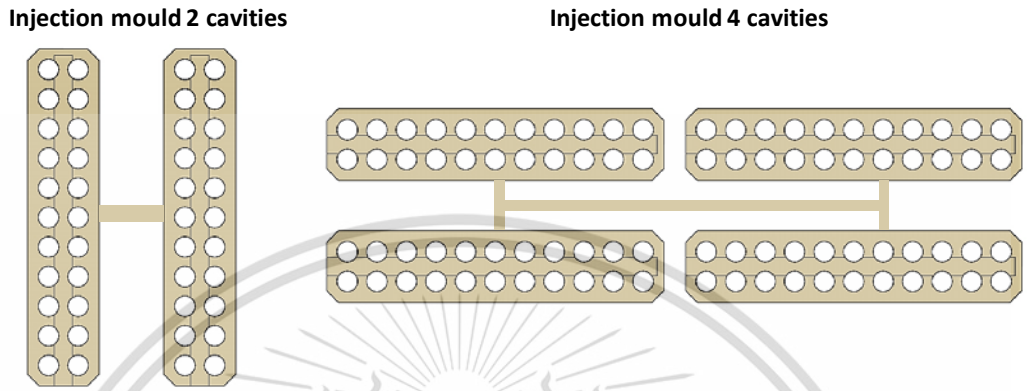

Figure 3.49 Plastic injection mould 2 and 4 cavities for battery holder

Table 3.17 Recommended manufacturing methods for different part shapes by Quadrant Engineering Plastic Products

Plastic shape	Manufacturing method
Long lengths Smaller sections Rod, plate and tube	Extrusion
Large stock shapes (heavy sections) Rod, plate and tube Near net shapes Custom cast parts	Casting
Various shapes in advanced engineering materials Rod, disc, plate and tube	Compression moulding
Plastic shape	Manufacturing method
Small shapes and thin walls in advanced engineering materials High volumes (more than 10000 parts)	Injection moulding

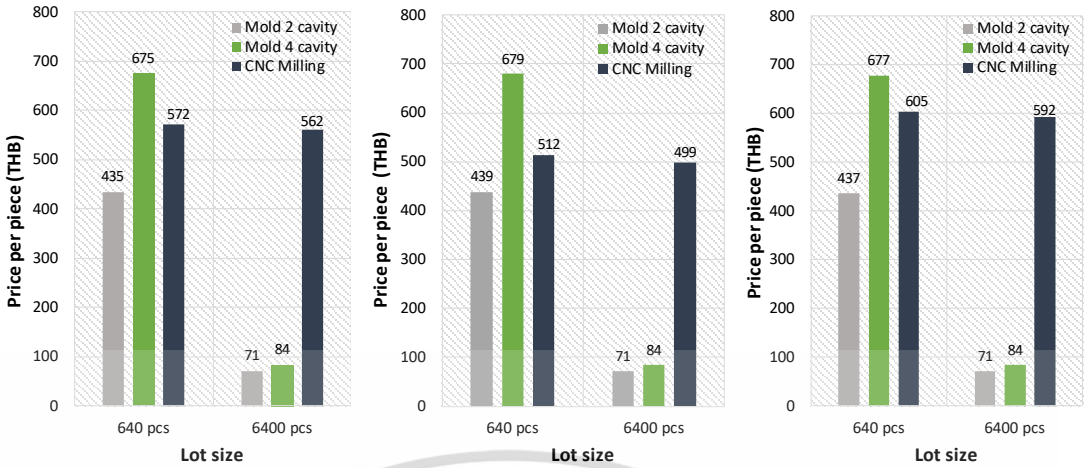

(a) Price per piece (THB) in 3 production methods of **PP**

(b) Price per piece (THB) in 3 production methods of **POM**

(C) Price per piece (THB) in 3 production methods of **ABS**

Figure 3.50 Comparison of production cost between PP, POM and ABS

Figure 3.50 shows the information about the cost of three different production technique for each plastic material. Overall it is noticeable that the production cost of all materials is almost the same in each technique for both production volumes (640 pcs and 6400 pcs). Looking at the data in greater detail in a small volume (640 pcs) as displayed in Figure 3.51, The four-cavity injection moulding is the most expensive technique due to mould cost while the cheapest technique is two-cavity injection moulding and the second expensive technique is CNC milling technique. Turning to production cost in large volume (6400 pcs), the cost of CNC milling becomes highest at 593 baht whereas the lowest production cost is plastic injection moulding at 71 baht as illustrated in Figure 3.52.

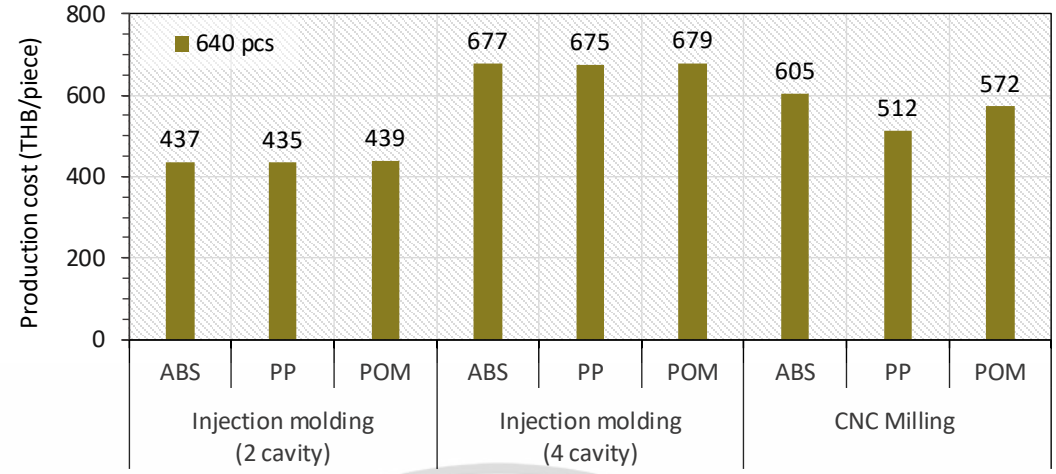

Figure 3.51 A comparison of injection moulding cost between ABS, PP and POM in 2 and 4 cavities in order volume of 640 pcs

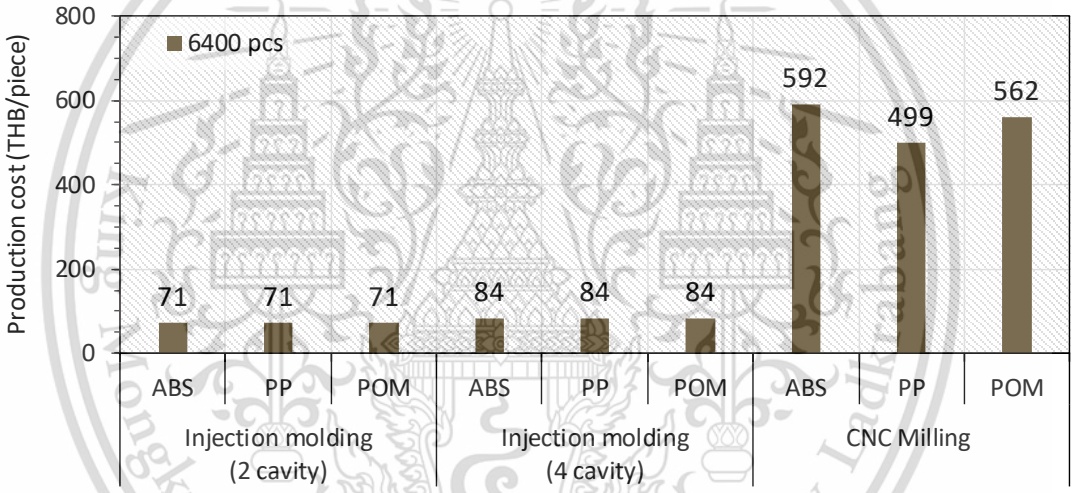

Figure 3.52 A comparison of injection moulding cost between ABS, PP and POM in 2 and 4 cavities in order volume of 6400 pcs

CHAPTER 4

RESULTS AND DISCUSSION

This chapter provides the feasibility study of the developed conceptual battery assembly. This research studies each component of the new conceptuel battery pack, and the information regarding the selection of material as well as the manufacturing method is gathered and provided in this chapter.

Additionally, the decision matrix is utilized as the decision aid tool in order to choose the appropriate material using material information from simulation results. Meanwhile, the selection of the manufacturing method is based on the gathered information including data from real manufacturers in Thailand. The air domain is not calculated for thermal model in the simulation in this chapter in order to reduce the computational time.

4.1 Material selection

4.1.1 Z bar, Positive Busbar and Negative Busbar

Regarding same material alternatives of Z bar, Positive Busbar and Negative Busbar, the material selection processes will be combined in same section. This chapter provides four aspects of consideration which are electrical conductivity aspect, thermal conductivity aspect, weight aspect, and material cost aspect. All four aspects are discussed in the following subsection. Aluminium and Copper in three different thicknesses are used as alternative materials; Aluminium 2 mm, Aluminium 3 mm, Aluminium 4 mm, Copper 2 mm, Copper 3 mm and Copper 4 mm.

4.1.1.1 Electrical conductivity aspect for the material selection

The electrical conductivity aspect is necessary for Z bar, Positive Busbar and Negative Busbar selection due to the electrical conductivity of Aluminium are dissimilar to that of copper in weight basis. Moreover, the resistance of conductors depends on the cross-sectional area that the thinner the diameter, the greater the resistance is as shown in Figure 4.2. Therefore, the thickness of this component needs to be designed and specified in order to obtain the proper electrical conductivity by simulating in the FEM software.

This research tries to specify the proper thickness of Z bar, Positive Busbar and Negative Busbar in range of 2 millimetres, 3 millimetres and 4 millimetres of both Aluminium and Copper. The purpose is not only to compare the resistance in each option, but also to evaluate temperature using FEM software in identical boundary conditions as displayed in Figure 4.1 for example of Z bar which will be used as a reference for Positive Busbar and Negative Busbar.

Every material alternative is evaluated and given scores according to the descriptions provided in Table 4.1, and the evaluation scores for the electrical conductivity aspect are listed in Table 4.2. The best alternative for each property is given the best score which equals to five. Meanwhile, the worst alternative in each material property is given the worst score which equals to one. The gap between the best property value and the worst property value is equally divided into five intervals, so that every section between each score point could have the same difference.

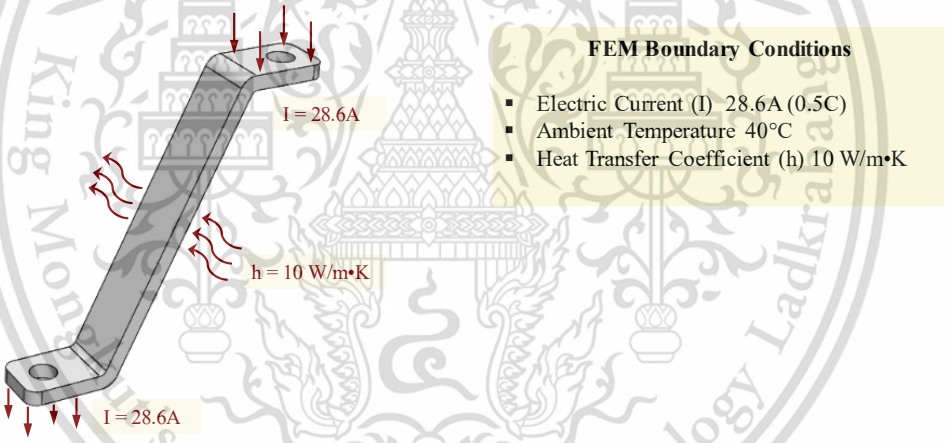

Figure 4.1 Boundary condition for FEM simulation

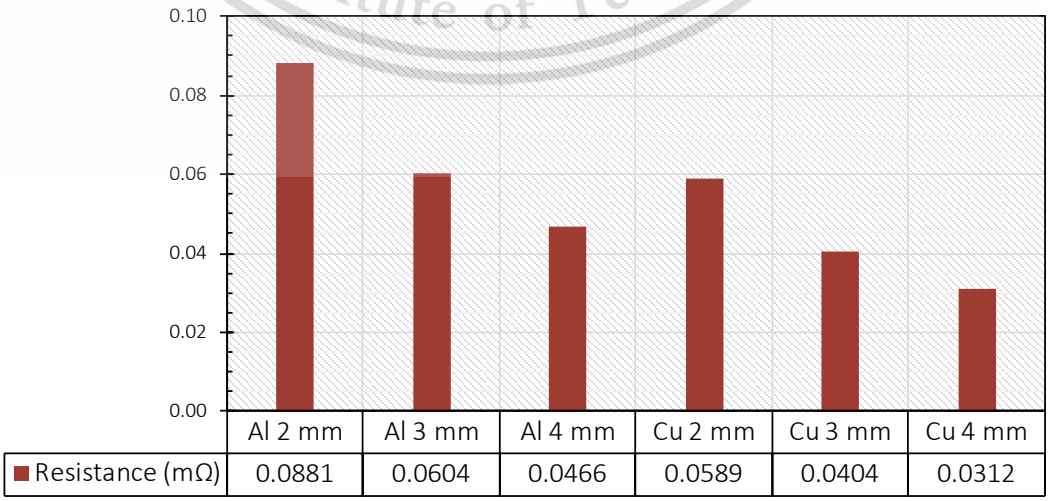

Figure 4.2 The electric resistance of Z bar

Table 4.1 Description of each evaluation score for electrical conductivity aspect

Evaluation score	Description
1	Resistance range is over 0.076 mΩ
2	Resistance range is between 0.065 - 0.075 mΩ
3	Resistance range is between 0.054 - 0.640 mΩ
4	Resistance range is between 0.042 - 0.053 mΩ
5	Resistance range is between 0.030 - 0.041 mΩ

Table 4.2 Evaluation score for electrical conductivity aspect

	Aluminium			Copper		
Material Thickness	Al 2 mm	Al 3 mm	Al 4 mm	Cu 2 mm	Cu 3 mm	Cu 4 mm
Resistance (mΩ)	0.088	0.060	0.0893	0.0808	0.0528	0.0389
Evaluation score	1	3	4	4	5	5

4.1.1.2 Thermal conductivity aspect for the material selection

This aspect is also necessary to be considered for material selection. According to the values providing in Table 3.2. However, the thermal conductivity does not depend on volume basis.

All material alternative is evaluated and given scores according to the descriptions provided in Table 4.3, and the evaluation scores for the thermal conductivity aspect are listed in Table 4.4. The maximum temperature is introduced in order to simplify and score the thermal conductivity values. The best alternative in each property is given the best score which equals to three. Meanwhile, the worst alternative for each material property is given the worst score which equals to one. The gap between the best property value and the worst property value is equally divided into three intervals, so that every section between each score point could have the same difference.

Table 4.3 Description of each evaluation score for Z bar in temperature aspect

Evaluation score	Description
1	Maximum temperature is over 43.30 °C
2	Maximum temperature is between 41.65 – 43.30 °C
3	Maximum temperature is between 40.00 – 41.64 °C

Table 4.4 Evaluation score for Z bar in term of temperature aspect

	Aluminium			Copper		
Material Thickness	Al 2 mm	Al 3 mm	Al 4 mm	Cu 2 mm	Cu 3 mm	Cu 4 mm
Maximum temperature (°C)	44.93	43.30	42.49	43.33	42.22	41.44
Evaluation score	1	2	2	1	2	3

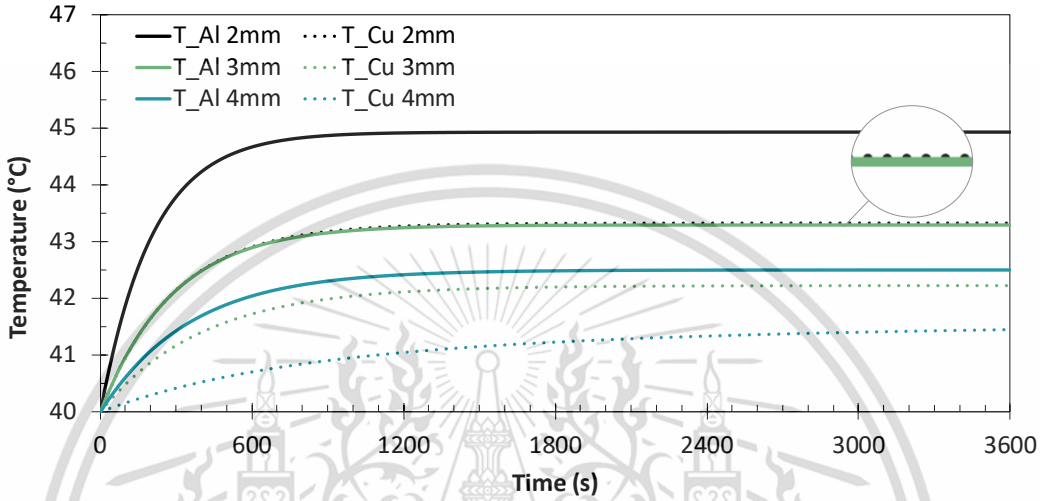

Figure 4.3 Comparison of temperature increasing of Z bar for each material under current load (28.6 A) at 40 °C of ambient temperature by FEM software.

Table 4.5 Description of each evaluation score for Positive Busbar in term of temperature aspect

Evaluation score	Description
1	Maximum temperature is over 51.86 °C
2	Maximum temperature is between 48.44 – 51.86 °C
3	Maximum temperature is between 45.00 – 48.43 °C

Table 4.6 Evaluation score for Positive Busbar in term of temperature aspect

	Aluminium			Copper		
Material Thickness	Al 2 mm	Al 3 mm	Al 4 mm	Cu 2 mm	Cu 3 mm	Cu 4 mm
Maximum temperature (°C)	55.29	48.99	48.99	49.49	45.23	45.23
Evaluation score	1	2	2	2	3	3

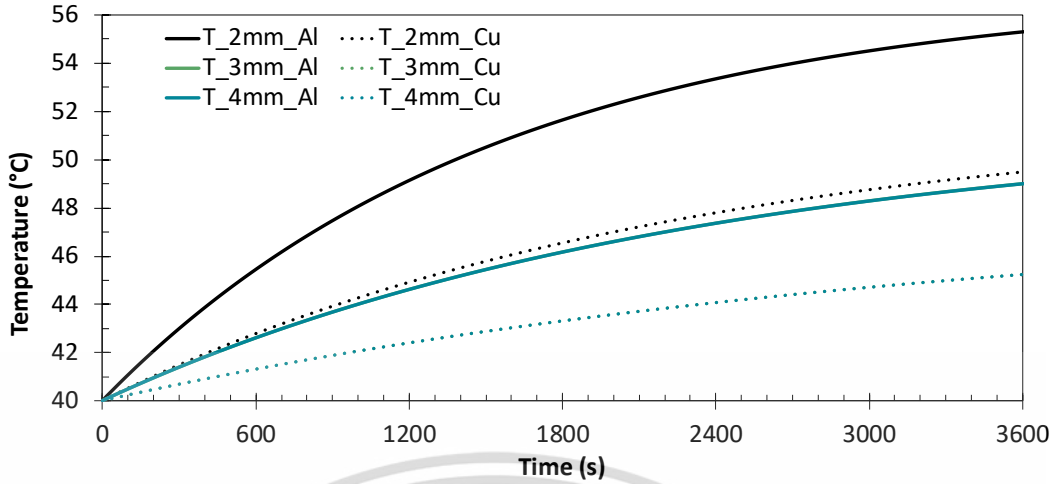

Figure 4.4 Comparison of temperature increasing of Positive Busbar for each material under current load (28.6 A) at 40 °C of ambient temperature by FEM software.

Table 4.7 Description of each evaluation score for Negative Busbar in term of temperature aspect

Evaluation score	Description
1	Maximum temperature is over 50.85 °C
2	Maximum temperature is between 46.94 – 50.85 °C
3	Maximum temperature is between 43.00 – 46.93 °C

Table 4.8 Evaluation score for Negative Busbar in term of temperature aspect

	Aluminium			**Copper**		
Material Thickness	Al 2 mm	Al 3 mm	Al 4 mm	Cu 2 mm	Cu 3 mm	Cu 4 mm
Maximum temperature (°C)	54.78	49.10	46.30	49.69	45.74	43.91
Evaluation score	1	2	3	2	3	3

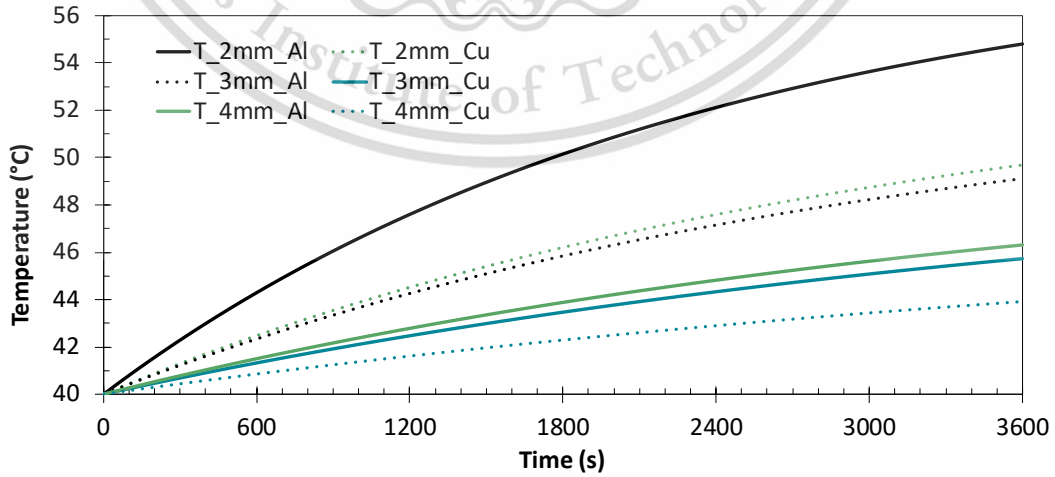

Figure 4.5 Comparison of temperature increasing of Negative Busbar for each material under current load (28.6 A) at 40 °C of ambient temperature by FEM software.

4.1.1.3 Weight aspect

The weight of the conductor; Z bar, Positive Busbar and Negative Busbar can be calculated by multiplying the volume of the part with the density of the material. Therefore, the weight of the material can also be used as a comparison value especially in the different size of the parts. These values are obtained from the Solidworks models of the parts and the weight scale. Table 4.9, Table 4.11 and Table 4.13 list the description of each evaluation score for the parts and Table 4.10, Table 4.12 and Table 4.14 represent the evaluation scores for this aspect. The best alternative for each property is given the best score which equals to five. Meanwhile, the worst alternative in each plastic property is given the worst score which equals to one. The gap between the best property value and the worst property value is equally divided into five intervals, so that every section between each score point has the same difference.

Table 4.9 Description of each evaluation score for Z bar in term of material weight aspect

Evaluation score	Description
1	Weight range is greater than 32.5 g
2	Weight range is between 26 - 32.5 g
3	Weight range is between 19.3 - 25.9 g
4	Weight range is between 12.6 - 19.2 g
5	Weight range is less than 12.6 g

Table 4.10 Evaluation scores for Z bar in term of material weight

Weight aspect	**Aluminium**			**Copper**		
Material Thickness	Al 2 mm	Al 3 mm	Al 4 mm	Cu 2 mm	Cu 3 mm	Cu 4 mm
Weight (g)	5.97	8.94	11.87	19.68	29.46	39.12
Evaluation score	5	5	5	3	2	1

Table 4.11 Description of each evaluation score for Positive Busbar bar in term of material weight aspect

Evaluation score	Description
1	Weight range is greater than 81.9 g
2	Weight range is between 65.2 - 81.9 g
3	Weight range is between 48.5 - 65.1 g
4	Weight range is between 31.7 - 48.4 g
5	Weight range is less than 31.7 g

Table 4.12 Evaluation scores for Positive Busbar bar in term of material weight aspect

Weight aspect	Aluminium			Copper		
Material Thickness	Al 2 mm	Al 3 mm	Al 4 mm	Cu 2 mm	Cu 3 mm	Cu 4 mm
Weight (g)	14.96	22.43	29.91	49.33	73.95	98.59
Evaluation score	5	5	5	3	2	1

Table 4.13 Description of each evaluation score for Negative Busbar in term of material weight aspect

Evaluation score	Description
1	Weight range is greater than 120 g
2	Weight range is between 95.6 - 120 g
3	Weight range is between 71.1 - 95.5 g
4	Weight range is between 46.5 - 71.0 g
5	Weight range is less than 46.5 g

Table 4.14 Evaluation scores for Negative Busbar in term of material weight aspect

Weight aspect	Aluminium			Copper		
Material Thickness	Al 2 mm	Al 3 mm	Al 4 mm	Cu 2 mm	Cu 3 mm	Cu 4 mm
Weight (g)	21.99	32.91	43.82	72.49	108.47	144.45
Evaluation score	5	5	5	3	2	1

4.1.1.4 Cost aspect

The material prices can vary according to the different factors such as lead time, manufacturer and quantity. This section provides only raw material price information of the material alternatives. According to the same material for Z bar, Positive Busbar and Negative Busbar, the material appraisement of Positive Busbar and Negative Busbar are also the same as Z bar. Table 4.15 shows the description of each evaluation score for material cost aspect and Table 4.16 provides wholesale prices of the materials which are obtained from the metal manufacturers in Thailand and also the evaluation scores.

Table 4.15 Description of each evaluation score for Z bar in term of material cost aspect

Evaluation score	Description
1	Range of piece price is over 19.0 Baht
2	Range of piece price is between 14.5 - 19.0 Baht
3	Range of piece price is between 10.0 - 14.5 Baht
4	Range of piece price is between 5.5 - 10.0 Baht
5	Range of piece price is less than 1.0 Baht

Table 4.16 Evaluation scores for Z bar in term of material cost aspect

Thermal conductivity aspect	Aluminium			Copper		
Material Thickness	Al 2 mm	Al 3 mm	Al 4 mm	Cu 2 mm	Cu 3 mm	Cu 4 mm
Material cost (THB)	21.99	32.91	43.82	72.49	108.47	144.45
Evaluation score	5	5	5	3	2	1

4.1.1.5 Weighting parameters and comparison of result

All consideration aspects lead to a comparison of results. The evaluation scores are multiplied by the weighting percentage which are weighted by brainstormimg of 10 specialists who relate in electric vehicle field. For instance, battery pack researcher, battery packer, mechanical engineer, electrical engineer, material scientist and chemical engineer as shown in Table 4.17. Looking at the data in greater detail, the electrical conductivity are concerned as the most important criteria of the Z bar and Negative Busbar material selection; therefore, it is given the highest weighting percentage at 34% and 35% respectively while the most important criteria of the Negative Busbar is Thermal conductivity at 30%. Then, it is followed by material cost at 33%, 29% and 27% weighting percentage for Z bar, Positive Busbar and Negative Busbar respectively because these criteria are not yet constrained by the design criteria whereas other alternatives have already fulfiled the design criteria.

Table 4.18, Table 4.19 and Table 4.20 lists all the evaluation scores of the alternatives regarding each material property. Table 4.21 shows the evaluation scores of Z bar which is multiplied by the weighting percentage, and it also shows the total scores of each material alternative. Table 4.22 and Table 4.23 show the evaluation scores and the total scores in each material alternative of Positive Busbar and Negative Busbar respectively which are multiplied by the weighting percentage.

Table 4.17 Weighting percentage for each criterion

Criteria	Weighting Percentage		
	Z Bar	Positive Busbar	Negative Busbar
Electrical conductivity	35%	36%	27%
Thermal conductivity	13%	20%	30%
Material weight	19%	15%	16%
Material cost	33%	29%	27%
Total scores	100%	100%	100%

Table 4.18 Total evaluation scores for Z bar

Criteria	Aluminium			Copper		
	Al 2 mm	Al 3 mm	Al 4 mm	Cu 2 mm	Cu 3 mm	Cu 4 mm
Thermal conductivity	1	2	2	1	2	3
Electrical conductivity	1	3	4	3	5	5
Material weight	5	5	5	3	2	1
Material cost	5	5	5	3	2	1
Total scores	12	15	16	10	11	10

Table 4.19 Total evaluation scores for Positive Busbar

Criteria	Aluminium			Copper		
	Al 2 mm	Al 3 mm	Al 4 mm	Cu 2 mm	Cu 3 mm	Cu 4 mm
Thermal conductivity	1	2	2	2	3	3
Electrical conductivity	1	3	4	3	5	5
Material weight	5	5	5	3	2	1
Material cost	5	5	5	3	2	1
Total scores	12	15	16	10	11	10

Table 4.20 Total evaluation scores for Negative Busbar

Criteria	Aluminium			Copper		
	Al 2 mm	Al 3 mm	Al 4 mm	Cu 2 mm	Cu 3 mm	Cu 4 mm
Thermal conductivity	1	2	3	2	3	3
Electrical conductivity	1	3	4	3	5	5
Material weight	5	5	5	3	2	1
Material cost	5	5	5	3	2	1
Total scores	12	15	16	10	11	10

Table 4.21 Comparison of evaluation scores with weighting percentage for Z bar

Criteria Weighting	Percentage	Weighting calculation					
		Al 2 mm	Al 3 mm	Al 4 mm	Cu 2 mm	Cu 3 mm	Cu 4 mm
Thermal conductivity	35%	0.35	1.05	1.40	1.05	1.75	1.75
Electrical conductivity	13%	0.13	0.26	0.26	0.13	0.26	0.39
Material weight	19%	0.95	0.95	0.95	0.57	0.38	0.19
Material cost	33%	1.65	1.65	1.65	0.99	0.66	0.33
Total scores	**100%**	**3.08**	**3.91**	**4.26**	**2.74**	**3.05**	**2.66**

Table 4.22 Comparison of evaluation scores with weighting percentage for Positive Busbar

Criteria Weighting	Percentage	Weighting calculation					
		Al 2 mm	Al 3 mm	Al 4 mm	Cu 2 mm	Cu 3 mm	Cu 4 mm
Thermal conductivity	36%	0.36	1.08	1.44	1.08	1.80	1.80
Electrical conductivity	20%	0.20	0.40	0.40	0.40	0.60	0.60
Material weight	15%	0.75	0.75	0.75	0.45	0.30	0.15
Material cost	29%	1.65	1.65	1.65	0.99	0.66	0.33
Total scores	**100%**	**2.96**	**3.88**	**4.24**	**2.92**	**3.36**	**2.88**

Table 4.23 Comparison of evaluation scores with weighting percentage for Negative Busbar

Criteria Weighting	Percentage	Weighting calculation					
		Al 2 mm	Al 3 mm	Al 4 mm	Cu 2 mm	Cu 3 mm	Cu 4 mm
Thermal conductivity	27%	0.27	0.81	1.08	0.81	1.35	1.35
Electrical conductivity	30%	0.30	0.40	0.40	0.40	0.60	0.60
Material weight	16%	0.80	0.80	0.80	0.48	0.32	0.16
Material cost	27%	1.65	1.65	1.65	0.99	0.66	0.33
Total scores	**100%**	**3.02**	**3.66**	**3.93**	**2.68**	**2.93**	**2.44**

4.1.2 Battery Upper Holder

In this section, plastic selection guide from Quadrant Engineering Plastic Products is used as a guideline to select plastic type for the Upper Battery Holder and its production method.

The plastic properties that are used in this evaluation are material price per kilogram, ultimate tensile strength, heat deflection temperature at 1.8 MPa, the coefficient of linear thermal expansion (CTE), and material weight. All the data are obtained from the material database of CustomPartNet ("Thermoplastic, Plastic, Metal Property Data Sheets," n.d.) as shown in Table 4.24. Every plastic alternative is evaluated and given scores. Table 4.25 lists all the evaluation scores of the plastic alternatives regarding each material property. The best alternative in each plastic property is given the best score which equals to three. Meanwhile, the worst alternative in each plastic property is given the worst score which equals to one.

Table 4.24 The plastic properties for evaluation

Property Name	Units	PP	ABS	POM
Ultimate Tensile Strength	MPa	36.82	41.51	57.98
Density	kg/m^3	938.00	1049.00	1401.00
Deflection Temperature at 1.8 MPa (264 psi)	°C	63.89	91.67	110
CTE, linear 20°C	µm/m/°C	120.06	90.54	109.98
Weight	g/piece	54.75	63.87	85.77
Cost	Baht/kg	48	75	77

4.1.2.1 Evaluation score for each aspect

A scoring range is established for all criteria for the plastic material selection that are given following; 1, 2, 3: 1 = Worst, 2 = Medium, 3 = Best.

Table 4.25 Evaluation score for each aspect

Property Name	Units	PP	ABS	POM
Ultimate Tensile Strength	MPa	1	2	3
Deflection Temperature at 1.8 MPa (264 psi)	°C	1	2	3
CTE, linear 20°C	µm/m/°C	3	1	2
Weight	g/piece	3	2	1
Cost	Baht/kg	3	2	1
Total scores		**11.00**	**9.00**	**10.00**

4.1.2.2 Weighting percentage for each criterion

In this thesis, the Ultimate Tensile Strength, material price and material weight are concerned as the most important criteria of the plastic material selection; therefore, it is given the highest weighting percentage at 26%. Then, it is followed by the deflection temperature and the coefficient of linear thermal expansion at 11% weighting percentage as shown in Table 4.26. Table 4.27 shows the evaluation scores which is multiplied by the weighting percentage, and it also shows the total scores of each material alternative.

Table 4.26 Weighting percentage for each criterion

Property Name	Weight
Ultimate Tensile Strength	26%
Deflection Temperature at 1.8 MPa (264 psi)	11%
CTE, linear 20°C	11%
Weight	26%
Cost	26%
Total scores	100%

Table 4.27 Comparison of evaluation scores with weighting percentage

Property Name	Weight	PP	ABS	POM
Ultimate Tensile Strength	**26%**	0.26	0.53	0.79
Deflection Temperature at 1.8 MPa (264 psi)	**11%**	0.11	0.21	0.32
CTE, linear 20°C	**11%**	0.33	0.11	0.22
Weight	**26%**	0.77	0.52	0.26
Cost	**26%**	0.78	0.52	0.26
Total scores	**100%**	**2.26**	**1.89**	**1.85**

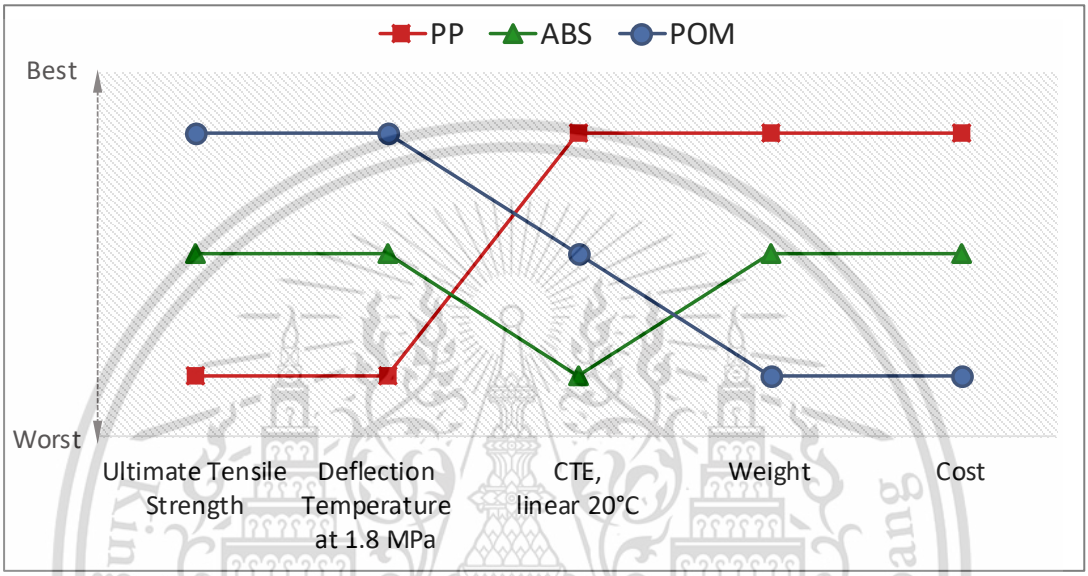

Figure 4.6 A value path diagram for each material

Figure 4.6 displays trade-offs among performance criteria for understanding the relative advantages and disadvantages of the material options. The horizontal axis representing different criteria and the vertical axis representing the rescaled performance for each attribute. In this example, PP option is better than other options for three criteria. Therefore, PP material is the most proper material for battery holder.

4.2 Manufacturing method

4.2.1 Z bar, Positive Busbar and Negative Busbar

Regarding the manufacturing method of Z bar, Positive Busbar and Negative Busbar, the information of Laser Cutting Machine (Laser CNC) and Punching are provided as manufacturing technique alternatives. According to the material selection, four-millimetre-thickness Aluminium is the most proper material for these connectors selected by decision matrix tool in previous section (see in Table 4.21, Table 4.22 and Table 4.23). Manufacturing technique for Aluminium Z bar, Positive Busbar and

Negative Busbar can be divided in two groups by production volume. The first group is production volume of 640 pcs, Laser Cutting Machine (Laser CNC) is chosen to be the appropriate methods for Z bar and Negative Busbar while punching technique is a proper technique for producing Positive Busbar because of its simple shape as shown in Figure 4.7. Turning to the high production volume (6440 pcs), The proper manufacturing method is punching technique for those three components especially Z bar and Positive Busbar (see in Figure 4.8). if the order is placed in bulk quantity, the cost per piece becomes less. This is mainly because the total production cost of this technique depends on the order quantity.

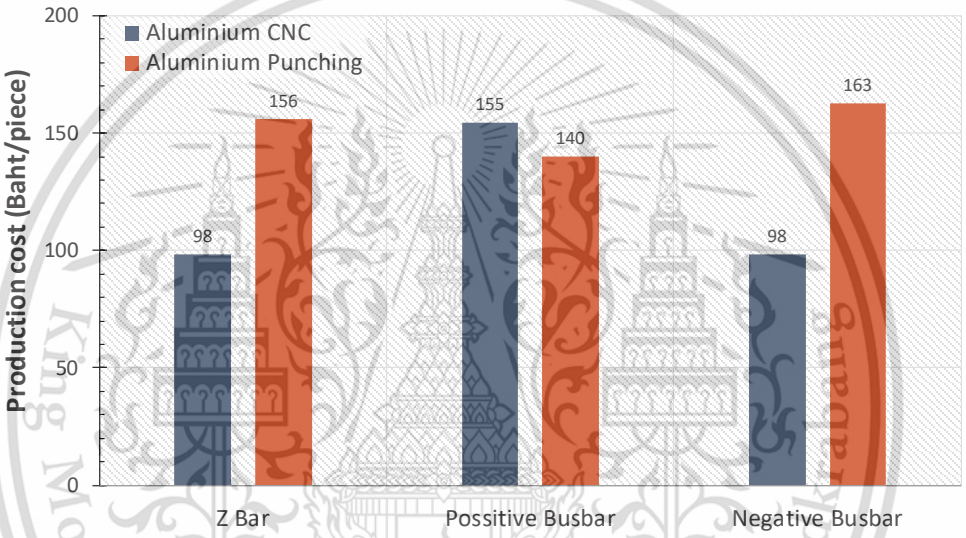

Figure 4.7 Comparison of production cost between punching and Laser CNC technique in order volume of 640 pcs

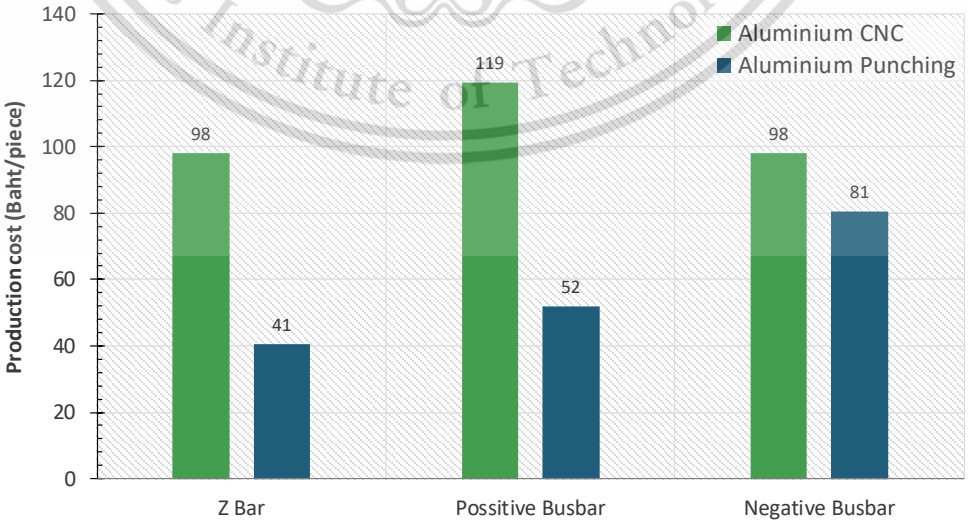

Figure 4.8 Comparison of production cost between punching and Laser CNC technique in order volume of 6400 pcs

4.2.2 Upper Battery Holder

According to PP is the most proper material for battery holder selected by decision matrix tool in previous section, the information of injection moulding and CNC milling technique are provided as manufacturing technique alternatives for battery holder. Regarding the small and simple shapes, two-cavity injection moulding is chosen to be the appropriate methods because of the lowest production cost in both production volume of 640 and 6400 pcs. The next proper manufacturing method is four-cavity injection moulding and CNC milling technique respectively in large production volume. In contrast, the next proper technique in small production volume is CNC milling technique and four-cavity injection moulding respectively as shown in Figure 4.10. Looking at the information in greater detail about cost breakdown of injection moulding process, mould cost is the large majority of the production cost which is just above 90 percent of total cost as shown in Figure 4.9.

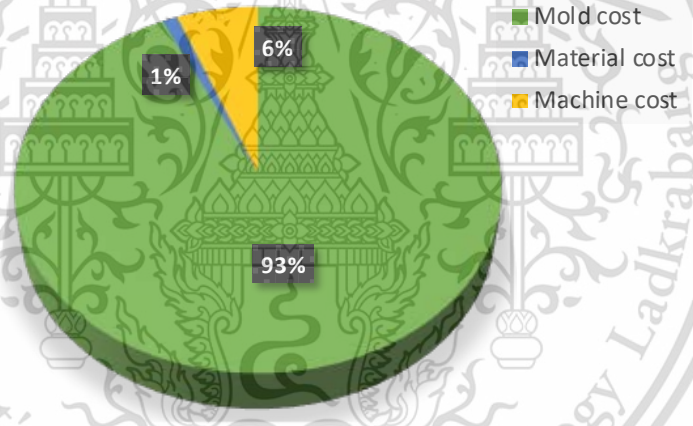

Figure 4.9 Cost breakdown of injection moulding technique

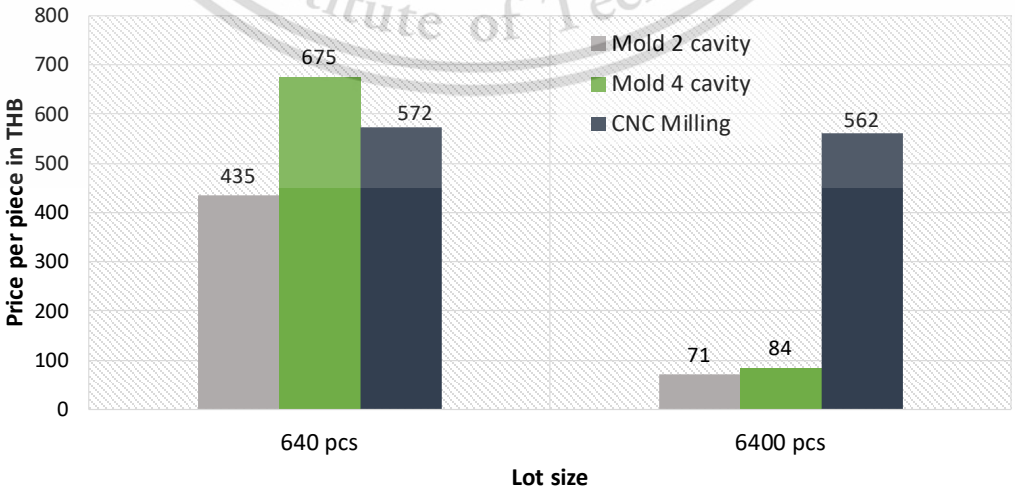

Figure 4.10 PP production cost (THB) in 3 production methods

CHAPTER 5

CONCLUSIONS AND RECOMMENDATIONS

Concerning Z bar, Positive Busbar and Negative Busbar, this research provides four aspects of consideration for the material selection, which are thermal conductivity aspect, electrical conductivity aspect, weight aspect and material cost aspect. The information regarding each aspect is supplied. In addition, the temperature distribution and electrical resistance simulation were also conducted in the FEM software to represent as thermal conductivity and electrical conductivity measurement. Then, each material alternative is evaluated and scored in these four consideration aspects with the decision matrix tool. According to the results, four-millimetre-thickness aluminium receives the best total scores; therefore, it is chosen as the material for Z bar, Positive Busbar and Negative Busbar. Regarding the manufacturing method of positive bus bar and Z bar, this research selects Laser cutting (Laser CNC) to produce the parts due to low production volume.

Concerning the battery holder, the plastic selection guide from Quadrant Engineering Plastic Products is used as a guideline. The information regarding the selection factors is further provided, and the design criteria of battery holder is also discussed. These design criteria are used as the input variable into the plastic material database. Further evaluation is conducted using the decision matrix tool to choose the suitable material alternative. Three different plastic alternatives; PP, POM and ABS with available price and properties information are evaluated further with the decision matrix method. The selection criteria used in this evaluation are material price, material toughness, heat deflection temperature, thermal expansion and weight, which are based on the plastic selection guide. According to the results from the decision matrix tool, Polypropylene (PP) receives the best total score, which is chosen as the material. Regarding the manufacturing method, brief information of injection moulding is provided as the suitable manufacturing method.

To clarify the result of new battery pack design, Figure 5.1 demonstrates the comparison of total material cost (a) and weight (b) between original design and developed design. As far as the material cost is concerned, the total material cost of

developed design is 1.6 million baht based on sale volume at 1,000 car units while the total material cost of the original design is 9.9 million baht, which is six times more than that of the original design. To sum up, the new design can save 8.3 million baht in term of material cost. Turning to material weight per car unit, the figure shows that the developed design can reduce total material weight per car unit from 16.5 kilograms to 8.3 kilograms, which is exactly half that of the original design.

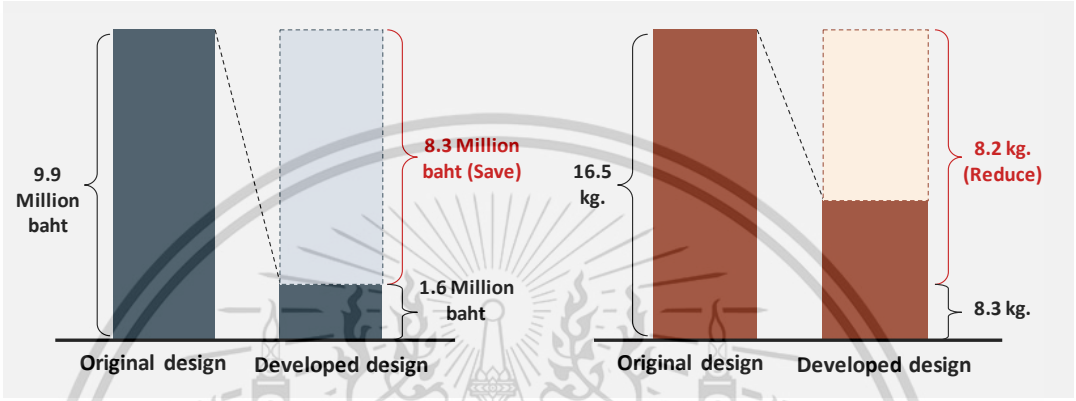

(a) Comparison of material cost per 1,000 car units (b) Comparison of material weight per car unit

Figure 5.1 Comparison of total material cost and weight

Regarding to selected material, Aluminium alloys is restricted by their high chemical activity and potentially poor corrosion resistance and its alloys have excellent resistance to corrosion. It is preferable to avoid corrosion through appropriate alloy choice and geometric design. A variety of protection methods are applied to aluminium and its alloys to enhance their corrosion resistance. Pure aluminum is very electrically conductive, but oxidized aluminum (Al_2O_3) is an excellent electrical insulator. As aluminum starts oxidizing instantly upon exposure to air, its surface electrical resistance can increase rapdily. Protective coatings, particularly chemical films, can be applied to aluminum to prevent oxidation while allowing good surface electrical conductivity. Chemical film has two types which are typically applied to aluminum; type IA when maximum protection and good bonding characteristics are desired, and type III when electrical conductivity through the film is important. Chemical films are relatively easy to apply and strip from a part. Chemical films make a good field repair protective coating; a can of chemical film can be brought into the field to fill in areas of coating that suffered scratches, damage, or repair work which exposed bare aluminum. (The Aluminium Federation (ALFED), 2017; Song, Wang, Zibart, & Koch, 2012; ©AFSA, 2011)

Conclusion

This research is expected to able evaluate various alternatives for materials and assembly techniques of battery pack, and some sample costs are presented. A methodology that choose the most proper alternative on the basis of this analysis is presented. The methodology also considers the impacts of choice-alternatives along multiple dimensions. This research studies each component of the new concept battery, and the information regarding the material selection as well as the manufacturing method selection is gathered and provided in this research. Furthermore, the decision matrix is utilized as the decision aid tool in order to choose the appropriate material. Meanwhile, the selection of the manufacturing method is based on the gathered information from experiment, simulation and real manufacturer in Thailand. Moreover, this research is expected to distribute knowledge of battery pack development for small electric cars leading to increased business opportunities. And it can be used as a guide for automotive industry in familiar field, for the maximum benefit to consumers and manufacturer as well.

REFERENCES

©AFSA. (2011). CORROSION RESISTANCE OF ALUMINIUM AND PROTECTIVE MEASURES WHERE APPROPRIATE. *The Aluminium Federation of South Africa*, *First Edition*, 36.

A123. (2014). Battery Pack Design, Validation and Assembly guide using A123 systems, 71.

Berkmanns, J., & Faerber, M. (2008). *Laser cutting*. LASERLINE Technical. In: BOC, The Linde Group.

Blue Sea Systems. (2002, May 15). Electrical Conductivity of Materials. Retrieved from https://www.bluesea.com/resource/108/Electrical_Conductivity_of_Materials

CustomPartNet. (n.d.). Plastics in Manufacturing. Retrieved July 4, 2018, from http://www.custompartnet.com/wu/plastics

Filip, V. (2006). Thermal conductivity of metals. *University of Bucharest, Faculty of Physics*, Pp. 1-2.

Great Britain, & Department for Communities and Local Government. (2009). *Multi-criteria analysis: a manual.* Wetherby: Communities and Local Government. Retrieved from http://www.communities.gov.uk/documents/corporate/pdf/1132618.pdf

Gupta, H. N. (n.d.). Manufacturing Processes, Second Edition, 195.

Injection Molding Process, Defects, Plastic. (n.d.). Retrieved October 11, 2018, from https://www.custompartnet.com/wu/InjectionMolding

Jensen, J. E., Tuttle, W. A., Stewart, R. B., Brechna, H., & Prodell, A. G. (1980). Selected Cryogenic Data Notebook. *Brookhaven National Laboratory Associated Universities*, Pp. VII-A-1.

Miller, B. P. (2015). Automotive Lithium-Ion Batteries. *Johnson Matthey Technology Review*, *59*(1), 4–13. https://doi.org/10.1595/205651315X685445

Milling Process, Defects, Equipment. (n.d.). Retrieved October 11, 2018, from https://www.custompartnet.com/wu/milling

NDT Resource Center. (2015, July 8). Electrical Conductivity and Resistivity. Retrieved from https://www.ndeed. org/EducationResources/CommunityCollege/Materials/Physical_Chemical/Electrical.htm

Nelson, R. (2018, March 14). What Is Electrical Conductivity? Retrieved from http://www.wisegeek.com/what-is-electrical-conductivity.htm

Nishino, H. (2010). Key Technology for EVs; Lithium-Ion Secondary Battery. Retrieved from http://mitsui.mgssi.com/issues/report/r1005j_nishino.pdf.

P. Groover, M. (2012). *Fundamentals of Modern Manufacturing : Materials, Processes, and Systems, 5E* (5th Revised ed.). New York, United States: John Wiley & Sons Inc.

Pryor, L., Schlobohm, R., & Brownell, B. (n.d.). A Comparison of Aluminum versus Copper. *Sr. Specification Engineer, GE Consumer & Industrial*, 7.

Quadrant Engineering Plastic Products: Engineering Plastics. (n.d.). In *Product Guide for Design Engineers* (Vol. 2011, p. Pp. 6-14). The Quadrant group of companies.

Serial and Parallel Battery Configurations and Information. (n.d.). Retrieved August 12, 2018, from https://batteryuniversity.com/learn/article/serial_and_parallel_battery_configurations

Song, J., Wang, L., Zibart, A., & Koch, C. (2012). Corrosion Protection of Electrically Conductive Surfaces. *Metals*, *2*(4), 450–477. https://doi.org/10.3390/met2040450

The Aluminium Federation (ALFED). (2017). UK Aluminium Industry Fact Sheet 2 : Aluminium and Corrosion. *Aluminium Federation Ltd - UK Company No. 723801*, 6.

The Aluminum Association. (1989). The Aluminum Association: Aluminum Electrical Conductor Handbook (p. Pp. 2.1-2.2). Washington, D.C.

The Boston Consulting Group (BCG). (2010). Batteries for Electric Cars: Challenges, Opportunities, and the Outlook to 2020, 18.

Thermoplastic, Plastic, Metal Property Data Sheets. (n.d.). Retrieved July 8, 2018, from http://www.custompartnet.com/materials/

Thokala, P., Devlin, N., Marsh, K., Baltussen, R., Boysen, M., Kalo, Z., … Ijzerman, M. (2016). Multiple Criteria Decision Analysis for Health Care Decision Making—An Introduction: Report 1 of the ISPOR MCDA Emerging Good Practices Task Force. *Value in Health*, *19*(1), 1–13. https://doi.org/10.1016/j.jval.2015.12.003

What is injection moulding? (2013, May 14). Retrieved October 11, 2018, from http://www.avplastics.co.uk/what-is-injection-moulding

APPENDIX A

Weight measurement

Z bar

Aluminium Positive Busbar

Copper Positive Busbar

Nickel plate

Negative Busbar

ABS battery holder

Aluminium anodizing plate

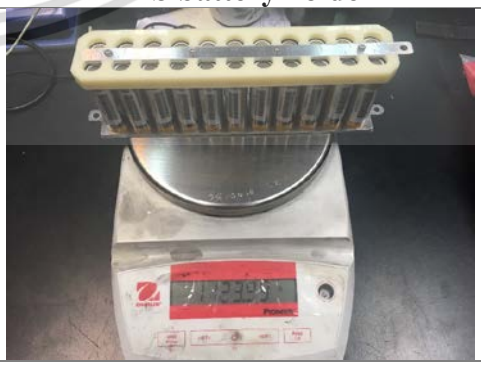

Li-ion battery submodule

Experiment equipments

Electronic loads

Power supply

Data logger

Current clamp

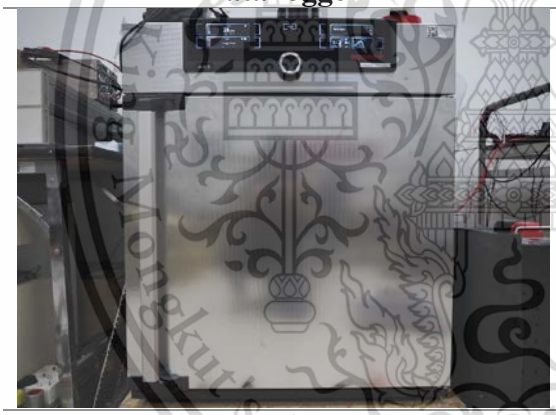

Controlled vacuum oven

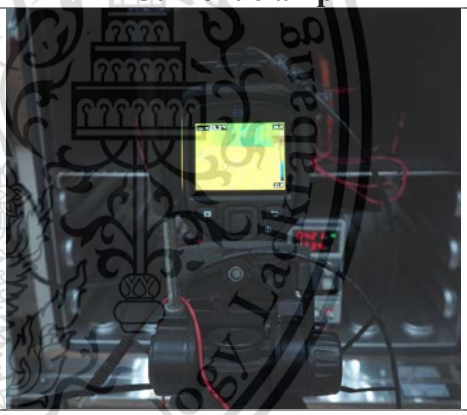

Thermal camera

The 8th TSME International Conference on Mechanical Engineering
12-15 December 2017
Bangkok, Thailand

AMM0020

MATERIAL SELECTION AND ASSEMBLY METHOD OF BATTERY PACK FOR COMPACT ELECTRIC VEHICLE

N. Lewchalermwong[1], M. Masomtob[2,*], V. Lailuck[2] and C. Charoenphonphanich[1]

1 Department of International College, King Mongkut's Institute of Technology Ladkrabang, Bangkok, 10520, Thailand
2 Materials for Energy Research Unit, National Metal and Materials Technology Center (MTEC), National Science and Technology Development Agency (NSTDA), Pathum Thani, 12120, Thailand

* Corresponding Author: manopm@mtec.or.th

Abstract. Battery packs become the key component in electric vehicles (EVs) the main costs of which are battery cells and assembling processes. The battery cell is indeed priced from battery manufacturers while the assembling cost is dependent on battery pack designs. Battery pack designers need overall cost as cheap as possible, but it still is high performance and more safety. Material selection and assembly method as well as component design are very important to determine the cost-effectiveness of battery modules and battery packs. Therefore, this work presents Decision Matrix, which can aid the decision-making process of component materials and assembly methods for a battery module design and a battery pack design. The aim of this study is to take the advantage of incorporating Architecture Analysis method into decision matrix methods by capturing best practices for conducting design architecture analysis in full account of key design components critical to ensure efficient and effective development of the designs. The methodology also considers the impacts of choice-alternatives along multiple dimensions. Various alternatives for materials and assembly techniques of battery pack are evaluated, and some sample costs are presented. Due to many components in the battery pack, only seven components which are positive busbar and Z busbar are represented in this paper for using decision matrix methods.

AUTHOR BIOGRAPHY

Author: Miss Naiyana Lewchalermwong

Degree: Master of Engineering

Date of Graduation: 15th August 2018

Date of Birth: 6th March 1991

Place of Birth: Bangkok, Thailand

Undergraduate and Graduate Education:
Master of Engineering in Automotive Engineering,
King Mongkut's Institute of Technology Ladkrabang, Bangkok, 2018

Bachelor's degree in management engineering and Logistics,
Silpakorn University, Sanamchandra Palace Campus, Nakhon Pathom, 2012

Major: Automotive Engineering

Presentations and Publications:

[1] Naiyana Lewchalermwong, Chinda Charoenphonphanich, Viset Lailuck and Manop Masomtob "Material Selection and Assembly Method of Battery Pack for Compact Electric Vehicle", 2017, The 8th TSME International Conference on Mechanical Engineering, December 12-15, 2017, Arnoma Grand Hotel, Bangkok, Thailand.